Universitat de Lleida

Escola Politècnica Superior

Màster en Ciències Aplicades a l'Enginyeria

Treball de final de màster

Analysis of thermal properties of phase change materials (PCM) using differential scanning calorimeter (DSC)

Autora: Falguni Sheth Karathia
Directors: Cristian Solé
Luisa F. Cabeza
September 2011

INDEX

LIST OF FIGURES

LIST OF TABLES

ABSTRACT

Commercially available phase change materials were studied experimentally in the present work. Experiments were carried out using a heat flux differential scanning calorimeter (hf-DSC). The selected phase change materials were RT 20, RT 27, SP 22 A17 and SP 25 A8 from the company Rubitherm GmbH. These materials were selected because the aim of the work was to analyze and compare thermal properties of two different types of phase change materials using differential scanning calorimetry. The samples were analyzed using dynamic and isostep methods to compare the effect of both methods on the final results. Three sub-samples of each sample were analyzed for the dynamic mode operation and each sub-sample was cycled three times. As a result nine sample cycles were obtained and the overall behaviour was concluded. The experimental results of the RT 20 and RT 27 presented good agreement with the commercial values. Moreover these samples presented good thermal recyclability and repeatability with similar values. Finally it was concluded that the step method is more reliable method compared to the dynamic method due to continuous heating and cooling and thus the effect of thermal equilibrium. On the other hand the salt hydrate samples SP 22 A17 and SP 25 A8 did not show the phase change. Hence, it was concluded that DSC is a suitable method for the analysis of paraffin based phase change materials. Whereas, it was concluded that DSC is not a proper method for salt hydrate samples.

Key-words: Thermal energy storage, PCM, paraffins, salt hydrates, DSC analysis, dynamic mode, isostep mode, repeatability.

OVERVIEW

In the present work, different techniques for the thermal energy storage are discussed using different materials.

Chapter 1 covers the background for the need of alternative energy sources with some statistical reports in the research area.

Chapter 2 includes the objectives of the present study.

In chapter 3, different thermal energy storage techniques are incorporated as a state of the art. Later the latent heat storage technique is discussed in details due to favourable advantages of this technique. Some examples of different materials under the mentioned methods are given.

Chapter 4 focuses on phase change materials (PCM) which are the heart of the work. Content of the chapter is the focused work of the thesis, including requirements and classification of PCM.

Chapter 5 discloses some of the published applications of PCM.

Chapter 6 introduces the context of available techniques for the thermal analysis of phase change materials with advantages and disadvantages.

Chapter 7 is based on the experimental work. The context includes the properties of the selected PCM, their results and discussion.

Chapter 8 points out the conclusions of the present work.

And finally chapter 9 shows the references of the master thesis.

1 Introduction

1.1 Energy requirements

Energy demand and its consumption are essential parts in routine life for every human being. It is consumed through one or the other way and in more or less quantity for almost all basic requirements and applications. It is estimated that the demand of energy in the world has increased dramatically during the last two decades. There are some major factors which are responsible for the increased energy demand such as, continuously increasing population, development of new technologies including human comfort, transportation, etc.

Figure 1 shows a comparison of the energy consumed by various sectors worldwide. It shows that a big fraction of energy (32%) is consumed by industry (such as, agriculture, mining, manufacturing, construction, etc.) followed by transportation purposes (28%), thermal comfort applications for households (22%), and finally in less amount by the commercial sector (19%). In the category of household energy consumption, the dominant energy fraction (almost 50%) is due to domestic building heating, ventilation and air-conditioning (i.e., thermal comfort) and in a smaller ratio to lighting appliances and electrical equipment. Ortiz et al. [3] mentioned that 40-50% of energy is consumed by buildings for thermal conditioning. That can also be seen in

Figure 1 (b). Cold countries need more energy for space heating and hot countries need energy for the air-conditioning. Therefore household energy demand also strongly depends upon the geographical location of the user.

(a)   (b)
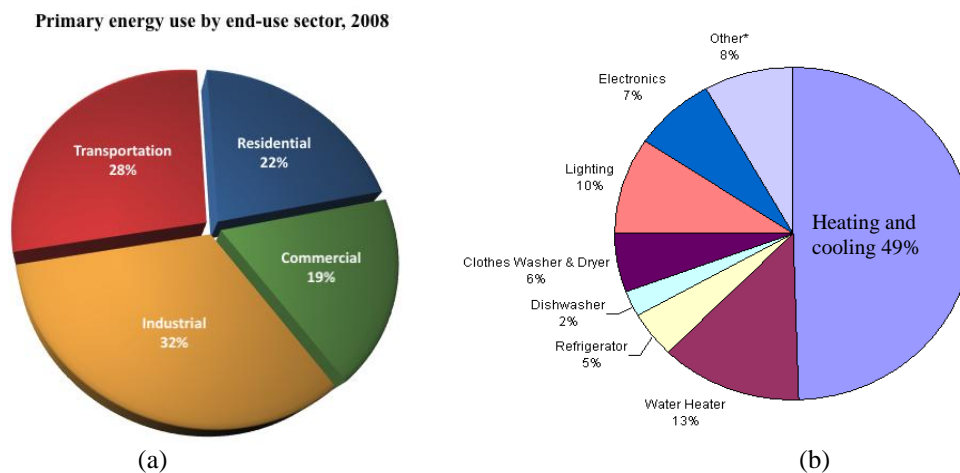
Figure 1. (a) Primary energy use by end-use sector, 2008 1] and (b) Household Energy Usage Breakdown [2]

1.2 Energy sources

There are two types of energy sources: (1) Non-renewable energy sources and (2) Renewable energy sources.

Non-renewable energy sources are natural resources which cannot be produced, grown, generated, or used on a scale which can sustain its consumption rate, once used there is no more remaining. Most of these sources are in limited amount and are consumed much faster than nature can create them again. The non-renewable energy sources include fossil fuels such as coal, petroleum and natural gas, and nuclear power such as uranium [4].

The renewable energy derives from natural processes which are furnished constantly. The renewable energy sources are the natural resources such as sunlight, wind, rain, tides, biomass, hydroelectricity, biofules and geothermal heat which can naturally be replenished [5].

Table 1 shows world energy consumption by power source. It shows that prime source for production of electrical energy is conventional fossil fuels which are non-renewable energy sources. Table 1 shows that most electrical energy is produced by combusting fossil fuels and thus increasing carbon dioxide levels in the atmosphere. Thus it results in continuously increasing greenhouse gas emissions. The sectorwise greenhouse gas emissions breakdown can be seen in the Figure 2. Moreover, excessive use of these energy sources produce harmful gases such as carbon dioxide (CO_2), which leads to the cause of global warming, and many other harmful gases responsible for climate change and atmospheric pollution [7], and consequently unexpected thermal changes.

Table 1. World energy consumption [6]

Energy by power source 2008			Average power in TW		
	TWh	**%**	**1980**	**2004**	**2006**
Oil	48,204	33,5	4.38	5.58	5.74
Coal	38,497	26,8	2.34	3.87	4.27
Gas	30,134	20,9	1.8	3.45	3.61
Nuclear	8,283	5,8	0.25	0.91	0.93
Hydro	3,208	2,2	0.6	0.93	1
Other renewable energy soruces	15,284	10.6	0.02	0.13	0.16
Others	241	0,2			
Total	**1,43,851**	**100**	**9.48**	**15**	**15.8**
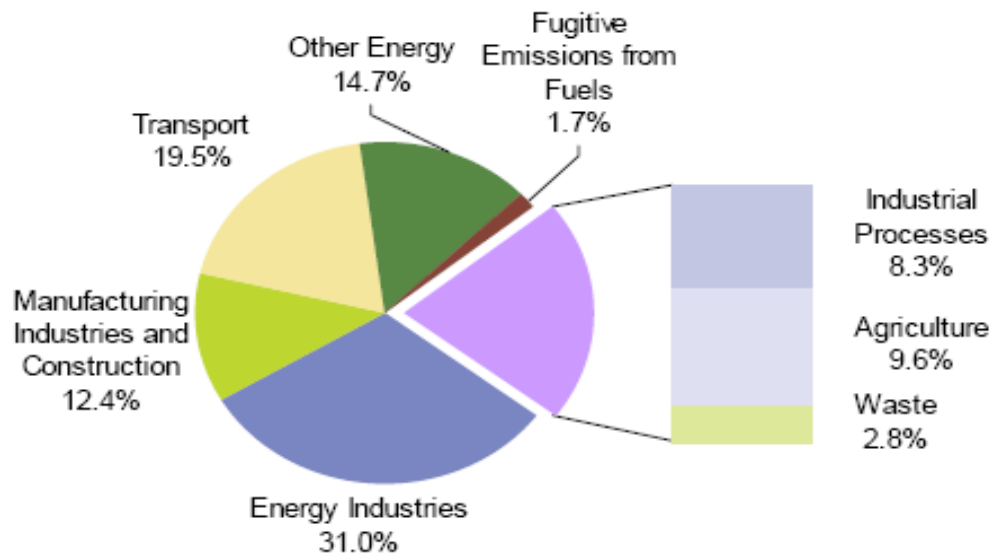
Figure 2. Greenhouse gas emissions by sector, 2008 8]

Due to the limited sources of non-renewable energy, it is in great demand to search other sources of energy using renewable energy sources. Attentively, the scientists all over the world are efficiently searching for renewable energy sources.

2 Objectives

Solid-liquid phase change materials have high energy storage density, smaller volume change during the phase change and constant melting-freezing temperatures independent of pressure change. Hence, the objective of the present work was analysis and comparison of two different types of the solid-liquid phase change materials. The aims of the work were:

- To analyze commercially available phase change materials such as paraffins (RT 20 and RT 27) and salt hydrates (SP 22 A17 and SP 25 A8) with DSC, using dynamic and isostep methods, and to show the accuracy of each method for these samples.

- To indicate which DSC method is proper for the analysis of such materials.

- To check the repeatability of the thermal properties of these samples.

3 State of the art

3.1 Thermal energy storage

Increasing use of non-renewable energy sources for producing electrical energy is the main cause for reduced quantity of non-renewable energy sources which causes increased fuel prices. This is one of the main factors leading to search for more effectively utilize various sources of renewable energy [9]. One of the possible ways is the thermal energy storage technique. It could be accomplished by some physical media that can store the thermal (heat and cold) energy at a time and the stored energy could be extracted at later time. Thermal energy storage (TES) can be achieved by three different methods, such as: (i) sensible heat storage (SHS), (ii) latent heat storage (LHS) and (iii) heat of thermochemical reactions [10], which can be seen in Figure 3. Thermal energy storage in general, and phase change materials (latent heat storage) in particular, have been a main topic in research for the last 20 years [11]. TES allows balancing the supply and demand of energy, shifting the peak-load for reducing the dependency on peak price electricity during the time when the atmospheric temperature is at its extreme, improving performance of energy systems, plays a crucial role in conserving the energy and thus contributing to a more efficient and nature friendly energy use [7, 10].
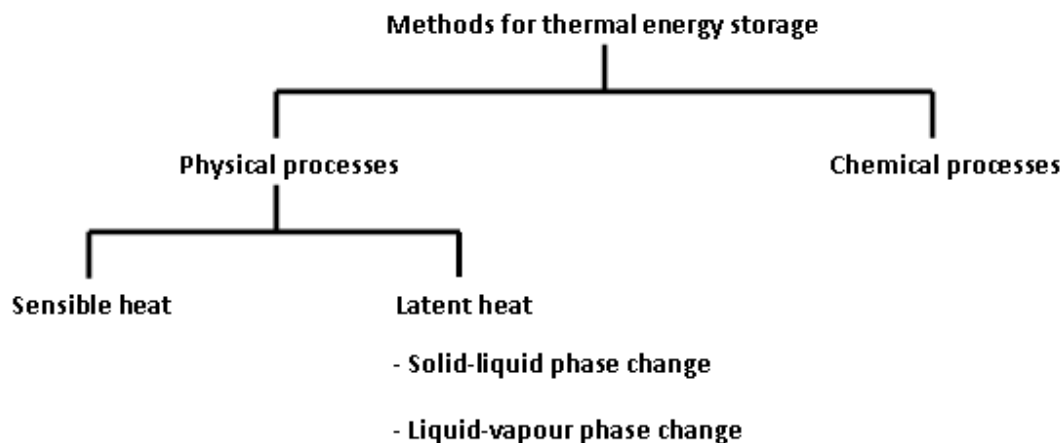
Figure 3. Classification of the available thermal energy storage methods 10]

3.2 Sensible heat storage (SHS)

3.2.1 Definition

The general definition of sensible heat is given as "Sensible heat energy is the amount of stored energy measured by sensor when the temperature of the storage material is

subjected to increase" [10]. In SHS, energy is stored or extracted by heating or cooling a storage media (liquid or solid), which does not change its phase during this process [12]. Figure 4 shows mechanism of the heat storage in the sensible heat storage media. From Figure 4, it could be understood that when heat is absorbed by a substance, it causes a rise in temperature. In terms of energy it is a potential energy in the form of thermal energy (heat). The amount of the stored heat during the temperature increment is the heat capacity "c_p" of the storage medium and it can be calculated using the following equation [10]:

$$\Delta Q = m \cdot c_p \cdot \Delta T \qquad\qquad (1)$$

Where,

ΔQ = amount of stored heat

c_p = specific heat capacity

ΔT = temperature increament

m = mass of the storage medium
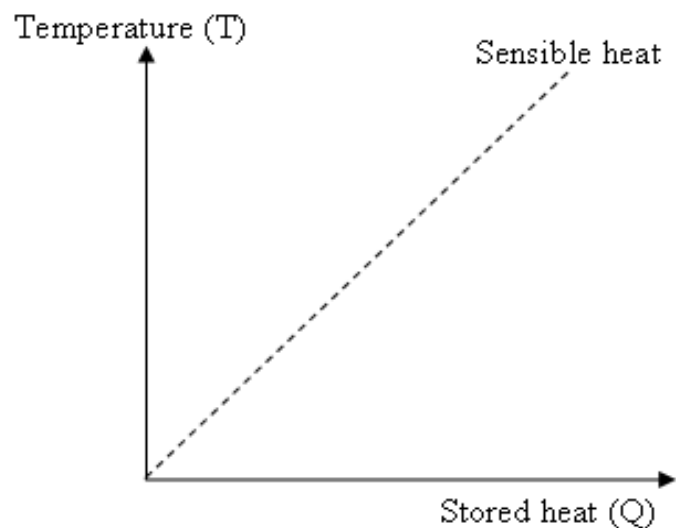
Figure 4. Heat storage as sensible heat leads to a tempeature increase when heat is stored 10]

Usually the heat capacity is given with respect to the amount of the material, the volume or the mass. In such case it is called as molar, volumetric or mass specific heat capacity. Equation (1) indicates mass specific heat capacity [10].

It is desirable for the sensible heat storage materials to have high specific heat capacity, long term stability under thermal cycling, and compatibility with the container materials

and to be available at low cost [7]. The storage of sensible heat uses movements of atoms and molecules and it requires high amount of storage materials [10]. Liquid storage media and solid storage media are described in details in the next sections.

3.2.2 Liquid storage media

Many heat storage liquid media are available for heat storage. For the purpose some liquid media such as (a) water, (b) salt water solutions, (c) oil and oil based fluids, and (d) molten salts are used [13].

Water could be selected for the low temperature applications (below the boiling point) over a wide range of temperature that is 5-90 ° C. Because it has higher specific heat capacity (being 4.2 kJ/kg) than other materials and it is cheap and widely available. It can be used as storage and transport medium for solar based warm water (i.e., solar domestic hot water tanks (SDHW)) and space heating applications. And large scale storage applications, underground natural aquifers have been considered.
The main drawback of water as heat storage media is its high vapour pressure hence it requires pressure tolerable container for high temperature applications [13].

Salt water solutions are also easily available at low cost. For example, solar ponds propose a simple and low cost method for collection and storage of large amount of solar energy for low temperature applications (5-95 ºC). They can be utilized in space heating and cooling applications, in industrial process heat and in electrical power generation. Salts such as sodium chloride (NaCl) and magnesium chloride ($MgCl_2$) are most commonly used for the purpose [13].

Other storage fluids consist of petroleum based oils and molten salts. Compared to the water, heat capacities of such fluids are merely 25-40% (on a weight basis) nevertheless, these fluids have lower vapour pressure than water and could be used as heat transfer media for high temperature applications with the temperatures higher than 300 ºC. For instance, therminol and caloria-HT oils. Some molten salts of inorganic salts have been considered for the high temperature applications (300 ºC and more) such as sodium hydroxide (NaOH). The main drawbacks of the oils are that their usage are limited to less than 350 ºC considering the stability and safety reasons and also it could

be fairly expensive. Focusing on the molten salts, they might be highly corrosive (ex. NaOH) and there may be inconvenience in storing energy at high temperatures [13].

Liquid metals are also probable sensible heat storage media. Most of their properties are similar to water but they have low specific heat capacities. However they have higher thermal conductivity. Some other liquid storage mediums are presented in Table 2 and Table 3 [13 - 15].

3.2.3 Solid storage media

For the low as well as high temperature applications many storage medias such as, rocks, metals, concrete, sand, bricks, pebble beds, rock piles and many more could be used. They do not have limitations for using in the low or high temperature applications such as liquid media [14, 15].

Rocks are used in pebble beds and rock piles. Such systems are frequently used for temperatures up to 100 ºC in combination with solar air heaters. Such systems can also be used for higher temperature applications up to 1000 ºC [14, 15].

Ceramic bricks are widely used as storage material in building fabrics including combination systems with air and water. Floor warming is the most common technique for the thermal storage along with building inertia and hollow core construction under the building mass storage sources [14, 15].

Metals (and inorganic salts) are useful for high temperature energy storage applications. They possess high thermal conductivity. For instance, aluminium, magnesium, zinc and industrial wastes like copper slag, iron slag, cast iron slag, aluminium slag and copper chips could be used as the energy storage media [13]. Cast iron is one of the sensible heat storage materials that have higher energy density than water. However, it is more expensive than stone or brick [14, 15].

Details of solid media for the thermal energy storage application are presented in Table 2 and [14, 15].

Table 2. Thermal capacities of some sensible heat storage materials at 20 ºC [14]

Material	Density (kg/m^3)	Specific heat (J/kg·K)	Volumetric thermal capacity (10^6 J/m^3·K)$^{-1}$
Clay	1458	879	1.28
Brick	1800	837	1.51
Sandstone	2200	712	1.57
Wood	700	2390	1.67
Concrete	2000	880	1.76
Glass	2710	837	2.27
Aluminium	2710	896	2.43
Iron	7900	452	3.57
Steel	7840	465	3.68
Gravelly earth	2050	1840	3.77
Magnetite	5177	752	3.89
Water (liquid media)	988	4182	4.17

Table 3. Characteristics of candidate solid and liquid sensible heat storage materials [15]

Storage medium	Temperature (ºC)		Average density (kg/m^3)	Average heat conductivity (W/mK)	Average heat capacity (kJ/kgK)	Volume specific heat capacity (kWh$_t$/m^3)	Media costs per kg ($/kg)	Media costs per kWh$_t$
	Hot	Cold						
Solid media								
Sand-rock-mineral oil[a]	200	300	1,700	1.0	1.30	60	0.15	4.2
Reinforced concrete	200	400	2,200	1.5	0.85	100	0.05	1.0
NaCl (solid)	200	500	2,160	7.0	0.85	150	0.15	1.5
Cast iron	200	400	7,200	37.0	0.56	160	1.00	32.0
Cast steel	200	700	7,800	40.0	0.60	450	5.00	60.0
Silica fire bricks	200	700	1,820	1.5	1.00	150	1.00	7.0
Magnesia fire bricks	200	1200	3,000	5.0	1.15	600	2.00	6.0
Liquid media								
Mineral oil	200	300	770	0.12	2.6	55	0.30	4.2
Synthetic oil	250	350	900	0.11	2.3	57	3.00	43.0
Silicone oil	300	400	900	0.10	2.1	52	5.00	80.0
Nitrite salts	250	450	1,825	0.57	1.5	152	1.00	12.0
Nitrate salts	265	565	1,870	0.52	1.6	250	0.70	5.2
Carbonate salts	450	850	2,100	2.0	1.8	430	2.40	11.0
Liquid sodium	270	530	850	71.0	1.3	80	2.00	21.0

3.2.4 Advantages and disadvantages of SHS

Both liquid and solid SHS materials are generally cheap and widely available. In addition, they could be useful for both low and high temperature applications. For low temperature (5-95 ºC) applications water and salt water solutions could be used since,

water has higher specific heat capacity than other materials. And for high temperature applications (more than 300 ºC) petroleum based oils, molten salts and liquid metals could be used. Solid storage materials such as rocks, metals, concrete, sand, bricks, pebble beds, rock piles, etc., could be used for low as well as high temperature applications [14, 15].

On the other hand, some restrictions are also related with these mateials. For example, water has high vapour pressure which limits its use. Oil could be used for high temperature applications but safety, stability and cost could be disadvantages for its use. And molten salts might be highly corrosive. In addition, SHS needs high amount of storage material which makes it inconvenient where the space, storage mass and cost are the dominant factors [7]. Some of the examples for the sensible heat storage such as, solar power plant and old age buildings made up of heavy stones are presented in Figure 5.

(a)   (b)   (c)
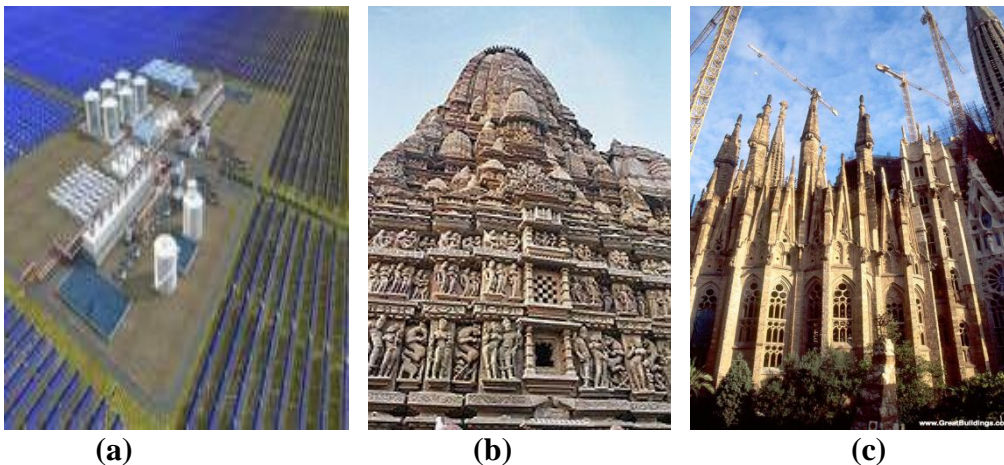
Figure 5. Applications of sensible heat storage: (a) Solar power plant - Gila Bend, Arizona, USA, (b) the temple complex at Khajuraho at Madhya Pradesh, India, (C) Sagrada familia at Barcelona, Spain

3.3 *Heat of chemical reactions*

Chemical energy is the potential of a chemical substance to undergo a transformation through a chemical reaction or to transform other chemical substances. Breaking or making of chemical bonds involve energy. When a chemical reaction takes place there is energy difference between the initial chemical substances and the final product at the end of the reaction. The chemical reactions may be endothermic process (energy consuming) or may be exothermic process (energy producing). Generally chemical processes produce large amount of energy exchange. For such systems it is necessary

that the chemical reactions involved are completely reversible. Some of the advantages of TES using reversible thermochemical reactions include high energy storage densities, indefinitely long storage duration at near ambient temperature, and heat-pumping capability. There are also some disadvantages such as their cycling stability [10], storage due to the volume expansion, and corrosivity in high or less amount with different metal containers, complexity, uncertainties in the thermodynamic properties of the reaction components and of the reaction's kinetics under the wide range of operating conditions, high cost, toxicity, and flammability. Due to such disadvantages the technique is at a very early stage of development [15].

3.4 Latent heat storage using phase change materials

3.4.1 Definition

Thermal heat storage by latent heat was recognized early as an attractive alternative to sensible heat storage in various applications, for example latent heat storage (LHS) in building materials [16]. LHS system is proved as a viable option for solar heat energy storage compared to SHS [17]. Thermal energy can be stored isothermally in some substances as *solid-solid crystalline phase transformation,* heat of vaporization (*liquid to vapour transition*), and latent heat of phase change, that is as heat of fusion (*solid to liquid transition*) [15]. And the materials which can change their phase are called phase change materials (PCM). Classification of the three basic types of PCM can be seen in the Figure 3 [10]. In the present work solid to liquid phase change (latent heat storage) materials are focused and will be followed. Nevertheless, solid to solid and liquid to vapour transition materials are described in short.

3.4.2 Latent heat of liquid-vapour phase change

The liquid-vapour phase change involves evaporation and condensation of the materials. They also possess high phase change enthalpy. But there are some disadvantages in using liquid-vapour phase change materials. For instance, in closed system where the volume is constant, evaporation leads to a large increase of the vapour pressure leading to high phase change Temperature. In the other case where the pressure is kept constant in a closed system leads to a large volume change. In contrast to the closed systems (that is open system) at ambient pressure, the material is evaporated on heating due to

the open system. To extract the stored heat from the storage (in the case of open system), the storage material has to be retrieved from the nature and that could be possible in the case of water, because it is a natural part of the environment. In some liquid-vapour storage media the heat storage and heat release may occur at different temperatures. Thus the evaporation strongly depends upon the boundary conditions that make limited use of such materials as PCM [10].

3.4.3 Solid to liquid phase change materials

Solid to liquid phase change materials store high amount of heat at nearly constant temperature while changing the phase from solid to liquid [10] and release the stored heat when solidified. Melting is characterized by a small volume change (less than 10%). But for this kind of phase transition the container should be large enough and made up of suitable material so that pressure does not change significantly and consequently the melting and solidification of the material occurs at a constant temperature.

During melting, heat is transferred to the storage material and the material will keep its temperature constant at the melting temperature and will store high amount of energy. The constant temperature is called as phase change temperature and such materials are called phase change materials. Phase change materials (PCM) (solid to liquid) are also called latent heat storage materials. Solid-liquid PCM are suitable for heat or cold storage. Due to the small volume change, the stored heat is equal to the enthalpy difference. This can be calculated using the following formula [10]:

$$\Delta Q = \Delta H = m \cdot \Delta h \qquad (2)$$

Where,

ΔQ = stored heat

ΔH = enthalpy difference between the solid and the liquid phase

m = mass of the sample

Δh = heat of fusion

Figure 6 shows two ways of using the stored heat taking advantage of the phase change. It shows that PCM can provide temperature control and high energy storage. Such advantages favour the PCM compared to sensible heat storage materials. Figure 6 (a)

and (b) show the PCM mechanism. Figure 6 (a) shows that as the temperature increases and reaches the melting temperature it remains at the constant temperature and after the material has changed its phase the temperature of the material will increase or decrease (this is sensible heat storage part of the PCM). Whereas, Figure 6 (b) indicates that during the phase change temperature the material stores high amounts of energy and while the solidification the material releases the stored energy during the phase change temperature [10].

(a)   **(b)**
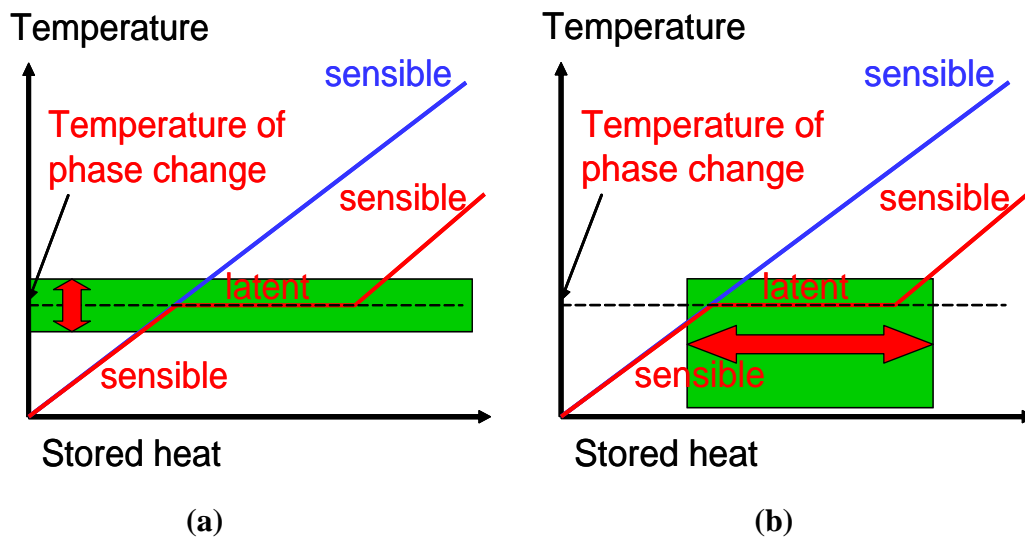
Figure 6. (a) Stabilization of temperture and (b) Storage of heat or cold in solid-liquid phase change materials 18]

3.4.4 Solid to solid phase change materials

Some solid-solid PCM have the same characteristics as solid-liquid PCM, and usually they have a large phase change enthalpy as the solid-liquid PCM [10].

4 Phase change materials (PCM)

Latent heat storage materials (PCM) store large amounts of energy during melting and release the stored energy during their solidification. There is a number of organic, inorganic and eutectic mixtures which are identified by different researchers as potential PCM. In this section, some requirements on the PCM and different types of the PCM are discussed in details.

4.1 Requirements of phase change materials

For the selection of a PCM for any application, the material should fulfil some basic requirements such as having

- A suitable phase change temperature for the application (to assure storage and release of heat at the desired temperature),
- A congruent melting temperature,
- A large melting enthalpy density per unit volume (to achieve high storage density), and
- Reproducible phase change (for long term usage of the PCM for the given application) [10].

Other than these, there are other expected requirements such as,

- It should not have phase separation (in the case a PCM consists of several components). Phase separation is a state where components with the different densities of a material settle down in a stratified pattern according to ascending density values. The different layers of the material can be seen in the Figure 7 [10].

Figure 7. Segregation of a salt hydrate 19]

- It should not present subcooling (or little subcooling). Subcooling is the effect under which many PCM do not solidify immediately upon cooling below the melting temperature, but start crystallization only after a tempeature well below the melting temperature is reached. Subcooling of eutectic salt-water solutions can be seen in Figure 8 [10].
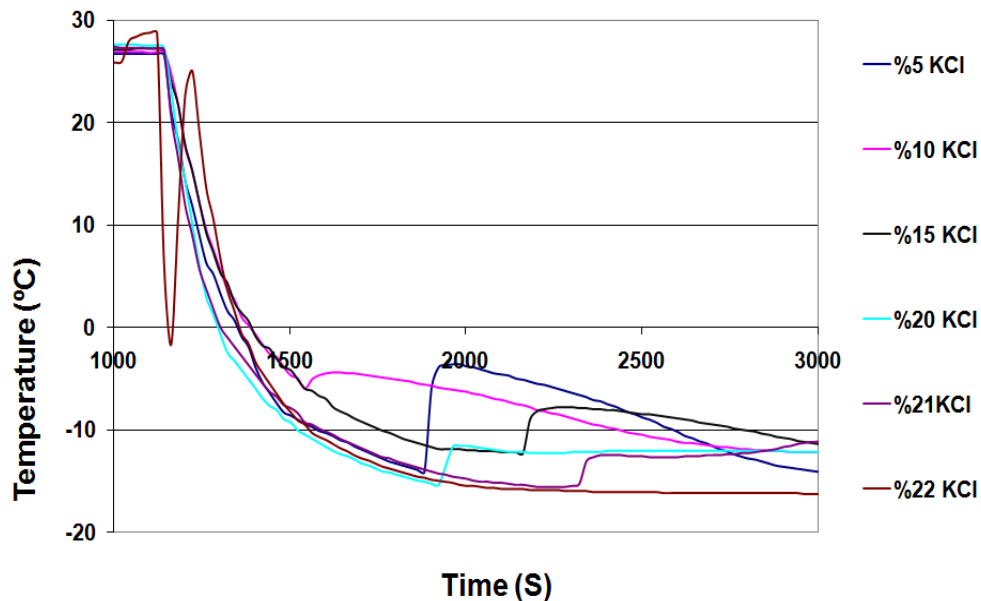
Figure 8. Subcooling effect of eutectic salt-water solutions 20]

- It should have good thermal conductivity [9, 10] but infact, generally PCM have low thermal conductivity.
- It should have low vapour pressure [10].
- It should have small volume change during the phase change [10].
  It should have chemical stability. The PCM should have long term stability over number of cycles.
- Chemical compatibility of the PCM with other materials (containers). If PCM and its container do not have good compatibility corrosion [20, 23] with the metal containers may arise and the effect can be seen in Figure 9. PCM in contact with plastic containers may cause softening of the plastic materials [21].

Figure 9. Galvanized steel treated with an eutectic salt water mixture. From left: After treatment and before treatment[20]

- It should be non-toxic [10].

- It should be non-flammable [10].

- It should be available at low price (but generally PCM are costly).

- It should have good recyclability [10]

Such requirements should also be considered to correctly design the TES system using PCM.

However, except the melting point in the operating range, the majority of PCM do not satisfy required criteria mentioned above. But, using different techniques (or combination) an improvement could be achieved to develop the properties. For instance, the thermal conductivity could be improved by adding graphite in the PCM [10], metallic fins can be used to increase the thermal conductivity of PCM, subcooling might be overcome by introducing nucleating agents or a "cold finger" in the storage material and incongruent melting can be inhibited by using suitable thickening agents [9].

4.2 Classification of phase change materials

4.2.1 Classification

There are plenty of materials that could be used as PCM and many of them have been analysed as PCM. PCM are classified into three major classes [9] as, (1) organic PCM, (2) inorganic PCM and (3) eutectic mixtures. The available classification of different materials that can be used as PCM is presented in the Figure 10 and their melting temperature and enthalpy range are presented in Figure 11.
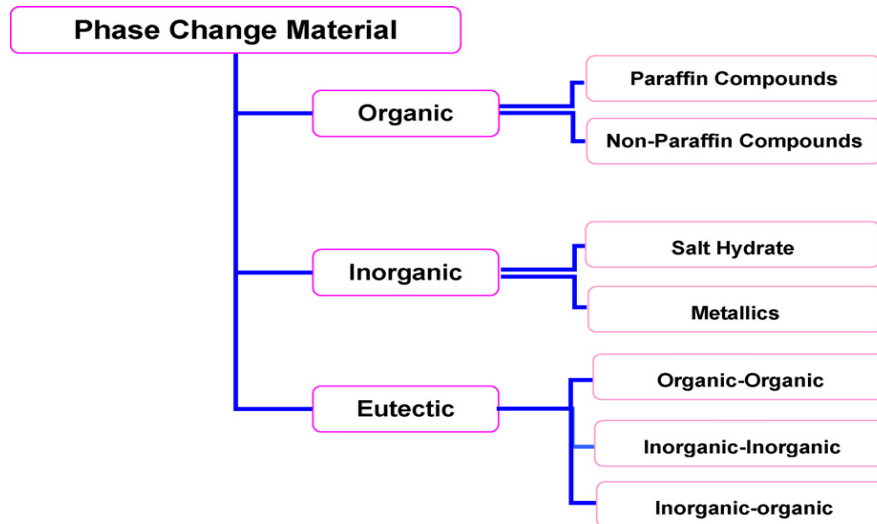
Figure 10. Classification of energy storage materials [9]
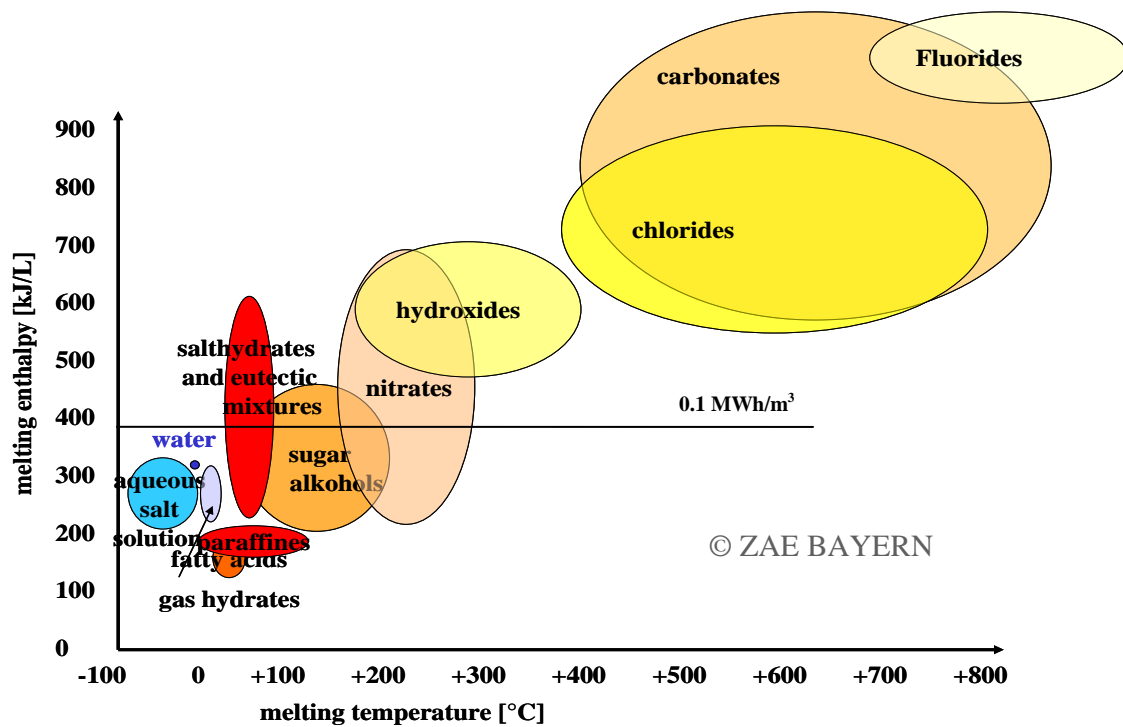
Figure 11. Classes of materials that can be used as PCM with their typical melting temperature and enthalpy range [10]

4.2.2 Organic phase change materials

4.2.2.1 Definition

Organic materials possess congruent melting and freezing temperatures without phase segragation and subcooling. Hence, they do not show consequent degradation of the latent heat of fusion. They are self-nucleating (means they solidify with little or no subcooling without any nucleating agent), generally safe, non-reactive and non-

corrosive, chemically stable and possess high heat of fusion. They are compatible with conventional construction material and recyclable. On the other hand they possess low thermal conductivity, low volumetric latent heat storage capacity, they are flammable (depending on the compostion), and they show problems with plastics [9, 25]. They are further classified as, (i) paraffins and (ii) non-paraffins.

4.2.2.2 Paraffins

The word paraffin comes from Latin and it means little reactive. The most commonly used organic PCM are paraffins and it is a technical name of an alcane (it is also called saturated hydrocarbon). Most paraffin, PCM is straight chain n-alcanes with the general formula C_nH_{2n+2} [CH_3-$(CH_2)_n$-CH_3] [10] and they have similar properties to each other. As the chain length increases the melting point and the latent heat also increases [9]. They have almost all advantages as mentioned in section 4.1.

On the other hand, paraffins also have some disadvantages, such as:

- They have low thermal conductivity, but metallic fins can be used to increase the thermal conductivity of PCM [9].
- They might be combustible (there is a controversy regarding this point).
- Unsufficient compatibility with plastic containers (they can cause softening of the plastic materials) [24].
- Paraffins are costly if they are pure alkanes (generally less expensive commercial paraffins are used) [10].

Some of the paraffins that have been analyzed as PCM are presented in and some commercial paraffins are presented in Table 5.

Table 4. Some paraffins that have been analysed as PCM [10]

Material	Melting temperature (°C)	Heat of fusion (kJ/kg)	Thermal conductivity (W/m·K)	Density (kg/m^3)
n-Tetradecane ($C_{14}H_{30}$)	6	230	- 0.21 (solid)	760 (liquid, 20 ℃) -
n-Pentadecane ($C_{15}H_{32}$)	10	212	- -	770 (liquid, 20 ℃) -
n-Hexadecane ($C_{16}H_{34}$)	18	210, 238	- 0.21 (solid)	760 (liquid, 20 ℃) -
n-Heptadecane ($C_{17}H_{36}$)	19	240	- -	776 (liquid, 20 ℃) -
n-Octadecane ($C_{18}H_{38}$)	28	200, 245	0.148 (liquid 40 ℃) 0.358 (solid 25 ℃)	774 (liquid, 70 ℃) 814 (solid, 20 ℃)
n-Eicosane ($C_{20}H_{42}$)	38	283	- -	779 -
n-Triacontane ($C_{30}H_{62}$)	66	-	- -	775 -
n-Tetracontane ($C_{40}H_{82}$)	82	-	- -	- -
n-Pentacontane ($C_{50}H_{102}$)	95	-	- -	779 -
Polyethylene (C_nH_{2n+2}, n upto 100000)	110-135	200	- -	- 870-940 (solid, 20 ℃)

Table 5. Commercial PCM available in the market [19]

PCM name	Type of product	Melting temperature (°C)	Heat of fusion (kJ/kg)	Density (kg/L)	Source
RT20	Paraffin	22	172	0.88	Rubitherm GmbH
ClimSel C 24	n.a.	24	108	1.48	Climator
RT26	Paraffin	25	131	0.88	Rubitherm GmbH
STL27	Salt hydrate	27	213	1.09	Mitsubishi Chemical
AC27	Salt hydrate	27	207	1.47	Cristopia
RT27	Paraffin	28	179	0.87	Rubitherm GmbH
TH29	Salt hydrate	29	188	n.a.	TEAP
STL47	Salt hydrate	47	221	1.34	Mitsubishi Chemical
ClimSel C 48	n.a.	48	227	1.36	Climator
STL52	Salt hydrate	52	201	1,3	Mitsubishi Chemical
RT54	Paraffin	55	179	0,90	Rubitherm GMBH
STL55	Salt hydrate	55	242	1,29	Mitsubishi Chemical
TH58	n.a.	58	226	n.a.	TEAP
ClimSel C 58	n.a.	58	259	1,46	Climator
RT65	Paraffin	64	173	0,91	Rubitherm GmbH
ClimSel C 70	n.a.	70	194	1,7	Climator

n.a.: not available or not known at the time of writing

4.2.2.3 Non-paraffins

The non-paraffin class is further grouped into fatty acids, alcohols and glycols [9, 10]. Non-paraffin based organic PCM also have almost similar properties as paraffins. Among the non-paraffin organic materials, fatty acids are given more importance as PCM. Hence, in this section fatty acids are discussed in detail.

Fatty acids as PCM:

Fatty acids are carboxylic acids having long unbranched aliphatic chains and are formulated as $CH_3(CH_2)_{2n} \cdot COOH$ [7, 10]. From the thermophysical properties point of view, fatty acids also have congruent melting and freezing points, good reproducibility, low thermal conductivity, no phase segregation, mild corrosivity and no or little subcooling. In contrast to paraffin, generally fatty acids have high heat of fusion and they are expensive (2-2.5 times expensive than commercial paraffins) [9, 10, 26]. Some of the fatty acids with potential use as PCM are presented in Table 6.

Table 6. Fatty acids with potential use as PCM [19]

Compound	Melting temperature (°C)	Heat of fusion (kJ/kg)	Thermal conductivity (W/m·K)	Density (kg/m³)
Propyl palmiate	10 16-19	186	n.a.	n.a.
Caprylic acid	16 16.3	148.5 149	0.149 (liquid, 38.6°C) 0.145 (liquid, 67.7°C) 0.148 (liquid, 20°C)	901 (liquid, 30°C) 862 (liquid, 80°C) 981 (solid, 13°C) 1033 (solid, 10°C)
Capric-lauric acid (65 mol%-35 mol%)	18.0 17-21	148 143	n.a.	n.a.
Butil stearate	19 18-23	140 123-200 200	n.a.	n.a.
Capric-lauric acid (45%-55%)	21	143	n.a.	n.a.
Dimethyl sabacate	21	120-135 135	n.a.	n.a.
Octadecyl 3-mencaptopropylate	21	143	n.a.	n.a.
34% Mistiric acid + 66% Capric acid	24	147.7	0.164 (liquid, 39.1°C) 0.154 (liquid, 61.2°C)	888 (liquid, 25°C) 1018 (solid, 1°C)
Octadecyl thioglycate	26]	90	n.a.	n.a.
Vinyl stearate	27-29 27	122	n.a.	n.a.
Myristic acid	49-51 54 58	204.5 187 186.6	n.a.	861 (liquid, 55°C) 844 (liquid, 80°C) 990 (solid, 24°C)
Palmitic acid	64 61 63	185.4 203.4 187	0.162 (liquid, 68.4°C) 0.159 (liquid, 80.1°C) 0.165 (liquid, 80°C)	850 (liquid, 65°C) 847 (liquid, 80°C) 989 (solid, 24°C)
Stearic acid	69 60-61 70	202.5 186.5 203	0.172 (liquid, 70°C) [49]	848 (liquid, 70°C) 965 (solid, 24°C)

% in weight

n.a.: not available or not known at the time of writing

4.2.3 Inorganic phase change materials

Generally inorganic materials have higher volumetric latent heat storage capacity than the organic materials due to their high density. They show sharp phase change, high thermal conductivity and they are non-flammable. Moreover, they are easily available at low cost. The main drawback of these materials is incompatibility with metals because severe corrosion effect is proven for some PCM-metal combinations [20 - 23]. They may show volume expansion on cooling [20], they show subcooling and segregation

[25]. These materials are further classified as (1) salt hydrates (2) salts, and (3) metals [9, 10].

Salt hydrates as PCM:

Salt hydrates are the most important group among the PCM which have been extensively studied for their use in latent heat thermal energy storage systems. Salt hydrates may be regarded as alloys of discrete ratio of inorganic salts and water forming a typical crystalline solid bounded through ion-dipole or hydrogen bonds with the general formula $AB \cdot nH_2O$. Salt hydrates are available in wide temperature range from 5 to 130 ºC. Generally, they have high volumetric energy density due to their high density. But they can potentially separate into two different phases since the presence of salt and water molecules which have different densities. Actually, the solid-liquid transformation of salt hydrates is a process of dehydration of hydration of the salt, although this process resembles melting or freezing thermodynamically. When a salt hydrate undergoes melting, it gives either salt hydrate with fewer amounts of water molecules (lower hydrate) or the anhydrous form of the salt. When the salt hydrate solidifies it releases water and the released amount of water is not enough to dissolve all the solid phase present and consequently causing the incongruent melting. Since there is density difference between water and salt, the lower hydrate (or anhydrous salt) settles down at the bottom of the container. Most of salt hydrates melt incongruently which is the main disadvantage of using salt hydrates as PCM [9, 10]. Different suggestions to overcome phase segregation and subcooling are mentioned by Farid et al. [26]. Table 7 shows some examples of salt hydrates with their physico-chemical properties.

Table 7. Inorganic substances with potential use as PCM [19]

Compound	Melting temperature (°C)	Heat of fusion (kJ/kg)	Thermal conductivity (W/m·K)	Density (kg/m³)
Na2CrO4·10 H2O	18	n.a.	n.a.	n.a.
KF·4 H2O	18.5	231	n.a.	1447 (liquid, 20°C) 1455 (solid, 18°C) 1480
Mn(NO3)2·6 H2O	25.8	125.9	n.a.	1738 (liquid, 20°C) 1728 (liquid, 40°C) 1795 (solid, 5°C)
CaCl2·6 H2O	29 29.2 29.6 29.7 30 29-39	190.8 171 174,4 192	0.540 (liquid, 38.7°C) 0.561 (liquid, 61.2°C) 1.088 (solid, 23°C)	1562 (liquid, 32°C) 1496 (liquid) 1802 (solid, 24°C) 1710 (solid, 25°C) 1634 1620
LiNO3·3 H2O	30	296	n.a.	n.a.
K3PO4·7 H2O	45	n.a.	n.a.	n.a.
Zn(NO3)2·4 H2O	45.5	n.a.	n.a.	n.a.
Ca(NO3)2·4 H2O	42.7 47	n.a.	n.a.	n.a.
Na2HPO4·7 H2O	48	n.a.	n.a.	n.a.
Na2S2O3·5 H2O	48 [48-49	201 209,3 187	n.a.	1600 (solid) 1666
Zn(NO3)2·2 H2O	54	n.a.	n.a.	n.a.
NaOH· H2O	58.0	n.a.	n.a.	n.a.
Na(CH3COO)· 3 H2O	58 58.4	264 226	n.a.	1450
Cd(NO3)2·4 H2O	59.5	n.a.	n.a.	n.a.
Fe(NO3)2·6 H2O	60	n.a.	n.a.	n.a.
NaOH	64.3	227.6	n.a.	1690
Na2B4O7·10 H2O	68.1	n.a.	n.a.	n.a.
Na3PO4·12 H2O	69	n.a.	n.a.	n.a.
Na2P$_2$O7·10 H2O	70	184		n.a.

n.a.: not available or not known at the time of writing

They have properties such as:

- Generally having high volumetric energy density due to their high density.
- They have high thermal conductivity, similar to water (that is 0.58 W/m·K) [24] and eutectic water-salt solutions, and almost double than the conductivity of paraffins.
- They show small volume change on melting.
- They are chemically stable.
- They are compatible with plastics.
- They might be slightly toxic.
- They are available at low cost [9, 10].

On the other hand they also show some disadvantages such as:

- Incongruent melting [9, 10].

- Phase separation is the main problem due to the salt and water components with different densities [20]. That can result as a decrease in the heat absorbed on melting and released on crystallization, and in the spreading of the enthalpy peak over a wide range of temperature [27].

- Due to the phase separation they show problem with the cycling stability [9, 10].

- Almost all the salt hydrates show subcooling.

- They have low vapour pressure.

- Many salt hydrates are potentially corrosive [9, 10].

But some solutions could be helpful to overcome phase separation, subcooling and incongruent melting, such as,

- Subcooling can be counteracted by rough surfaces [26].

- Subcooling can also be prevented by introduction of crystal seeds [26].

- Subcooling can also be overcome by violent motion of the PCM [26].

- Direct contact heat transfer between hydrated salts and an immiscible fluid for the solution to subcooling [26].

- Use of nucleating agents is the most fruitful for the PCM application [27, 28] to overcome the phase separation.

- Subcooling can be suppressed by cold finger and

- Preservation of some crystals (in a small cold region) could also be useful for the prevention of subcooling [9, 10].

- Addition of another salt could be useful to provide congruent melting to the PCM [27] and

- Addition of thickening agents to make the mixture congruent [9, 10, 26].

Salts as PCM:

Different salts which have melting point above 150 ºC can also be used as PCM. The heat of fusion roughly rises as the metling temperature increases. A salt always consists of more than one component, so theoretically phase separation is a potential problem. The thermal conductivity of the salts could be good, data of subcooling are not available and they have very low vapour pressure. The volume change could be upto 10% upon

melting, many salts are chemically stable, they could be corrosive with metals, their safety and price differs for different salt samples [10].

Metals as PCM:

This class of PCM covers low melting metals and metal eutectics. Because of the weight this class is not considered seriously but when the volume is the key point they are candidate PCM because of the high heat of fusion per unit volume, high thermal conductivity and relatively low vapour pressure. But they have low specific heat [9].

Eutectics as PCM:

Eutectic PCM solutions are mixtures of two or more chemical compounds which, when mixed in a particular ratio, have a congruent freezing and melting point below or above freezing temperature of water. They offer a thermal energy storage facility in negative temperature range [20, 26, 29, 30].

They provide some advantages such as:
- Thermal energy storage in negative temperature range due to presence of the salt.
- They show similar thermal conductivity as water.
- They show good energy storage density.

Simultaneously, they also have disadvantages such as:
- They show subcooling [10].
- They present phase separation also because of the stratification of the salt and the water.

Eutectics had attracted interest until the late 18th century for some applications, however due to phase separation and because the life expectancy of these mixtures were unpredictable, their wide spread usage was limited [26]. Some examples of inorganic and organic eutectics with potential use as PCM are shown in Table 8.

Table 8. Inorganic and organic eutectics with potential use as PCM [19]

Compound	Melting temperature (°C)	Heat of fusion (kJ/kg)	Thermal conductivity (W/m·K)	Density (kg/m³)
Inorganic eutectics with potential use as PCM				
45-52% LiNO3·3H2O + 48-55% Zn(NO3)2·6H2O	17.2	220	n.a.	n.a.
66.6% CaCl2·6 H2O + 33.3% MgCl2·6 H2O	25	127	n.a.	1590
48% CaCl2 + 4.3% NaCl + 0.4% KCl + 47.3% H2O	26,8	188,0	n.a.	1640
Organic eutectics with potential use as PCM				
37.5% urea + 63.5% Acetamide	53	n.a.	n.a.	n.a.
67.1% naphthalene + 32.9% benzoic acid	67	123.4	0.136 (liquid, 78.5°C) 0.130 (liquid, 100°C) 0.282 (solid, 38°C)	0.257 (SOLID, 52 °c)

% in weight

n.a.: not available or not known at the time of writing

5 Applications of phase change materials

To fulfil the demand for lowering the electricity consumption, many researches have considered use of PCM in different applications. Some of the available applications of PCM in the literature are,

- Thermal storage of solar energy [11].
- Cooling: use of off-peak rates and reduction of installed power, icebank [11, 25, 31, 32].
- Heating and sanitary hot water: using off-peak rate and adapting unloading curves [11, 25, 31, 32].
- Safety: temperature maintenance in rooms with computers or electrical appliances [11].
- Thermal protection of food: transport, hotel trade, ice-cream, food agroindustry, wine, milk products, for pizza-heaters, self-chilling beverage keg, etc [11, 19].
- Thermal protection of electronic devices (integrated in the appliance)
- Medical applications: transportation of blood and its byproducts, other medical applications (such as, mattress for operating tables, hot or cold pads to treat local pain in the body) [11, 19].
- Cooling of engines (electric and combustion) [11].
- Thermal comfort in vehicles [11].
- Softening of exothermic temperature peaks in chemical reactions [11].
- For heat exchanging ventilation system using PCM [33].
- Applications to reduce the power demand [11, 25, 31, 32] in buildings such as:
  - Passive solar collecting walls
  - Indoor walls
  - Floors and ceilings
  - Green houses.
- For the containers such as rigid and soft containers, PCM pads, and isothermal water bottle [19].

Some of commercial PCM products are shown in the Figure 12.

(a) Rigid container by Sofrigam

(b) PCM pad by TCP RELIABLE, Inc.

(c) Isothermal water bottle by Sofrigram
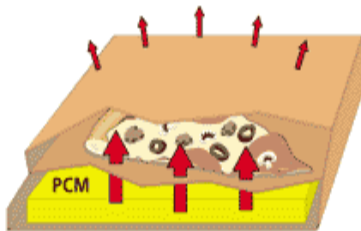
(d) pizza-heater (Merck KGaA)

(e) Hot cushion for medical purposes, by Rubitherm®

(g) All Purpose delivery transporters, by PCM Thermal Solutions

(h) Containers for blood products transport, by BIO TRANS

(i) Rubitherm® cold product for cooling therapy

Figure 12. Different applications of PCM [34]

6 Techniques for the thermal analysis of PCM

6.1 Available techniques for the thermal analysis of phase change materials

Some techniques are available for the thermal analysis of chemical materials. Thermal analysis is a branch of materials science where the properties of materials are studied as they change with temperature. Thermal analysis techniques help to select and to determine thermodynamic properties of the materials which are essential for understanding the behavior of material under different conditions. Calorimetric methods are the methods to determine the change of heat in any kind of process ("calor" comes from Latin) [10, 35, 36]. Numerous research groups have been using different traditional methods such as, differential scanning calorimetry (DSC) [10, 37–40], conventional calorimetry, and differential thermal analysis (DTA), for analyzing PCM to reveal the thermal properties of these materials. Recently, T-history method was proposed by Zang et al. [41] for the thermal analysis of PCM and later improvements to this method was proposed by Marín et al. [42], which in addition facilitate to determine enthalpy as function of temperature [9–11, 39, 41–43]. Hong et al. [43] also proposed a new method which is a combined method of modified T-history method [44, 45] and heat flux meter method proposed by Saito et al. [46] for measuring the latent heat of PCM with a melting point lower than room temperature. Another method called "air-flow chamber" is also proposed by Günther et al. [39].

The DTA and DSC methods are used for studying phase transition under different atmospheric influences, temperatures and heating/cooling rates in the field of metallurgy, material science, pharmacy, and food industry [36].

Since, the method used for the present experimental studies are based on the differential scanning calorimetry (DSC), different DSC types and methods are described in detail in the next section.

6.2 Types of differential scanning calorimeter

Differential Scanning Calorimetry (DSC) is a thermoanalytical technique and it was developed by E.S. Watson and M.J. O'Neill in 1960 [47]. DSC measures the change of heat flow rate difference which is normally released due to an alteration of the sample temperature. In the DSC heat only flows if the temperature difference is present [48]

and therefore the samples are subjected to temperature program to produce temperature difference for measurement of the heat flow. It measures energy directly and allows precise measurements of heat capacity [47] and thermal conductivity [36]. DSC quickly allows the measurements of reaction heats and heats of transition (heat flow rates) and their changes at characteristic temperatures for small sample masses (in milligrams and in grams for classic calorimetry), in wide temperature ranges with high accuracy [48].

DSC are mainly classified into two different classes [10, 36, 48] such as,

-   Power compensation DSC, and

-   Heat flux DSC

The primary measurement signal for all three types is a temperature difference; it determines the intensity of the exchange of the heat between the furnace and the sample-reference part. The resulting heat flow rate (Φ) is proportional to the temperature difference [10].

Since, the experiments were performed using heat flux DSC, this class of DSC is discussed in detail in the next section.

6.2.1 Power compensation DSC (PC DSC)

The power compensation DSC can be seen in Figure 13. The power compensation DSC belongs to the heat-compensating calorimeter. In which, the heat to be measured is compensated with electric energy, by increasing or decreasing an adjustable Joule's heat. PC DSC consists of two identical micro-furnaces, one for the sample and the other for the reference with individual heater. The sample furnace is heated with a temperature – time program, while the reference furnace tries to follow this program. It results in increment and decrement of the temperature in the reference furnace following a reaction. In this case the compensating heating power is measured which is actually the heat flow difference. The very light weight individual furnace is advantage of the PC DSC (1 g) over the HF-DSC (up to 200 g). That favors extremely short responding time. The heating and cooling rates can be up to 500 °C/min. When an exothermic (heat releasing, i.e. solidification) or endothermic (heat absorbing, i.e. solidification) reaction appears the energy is accumulated or released to compensate the energy change in both

furnaces. The power required to maintain the system in equilibrium is proportional to the energy changes occurring in the sample [10, 36, 48].
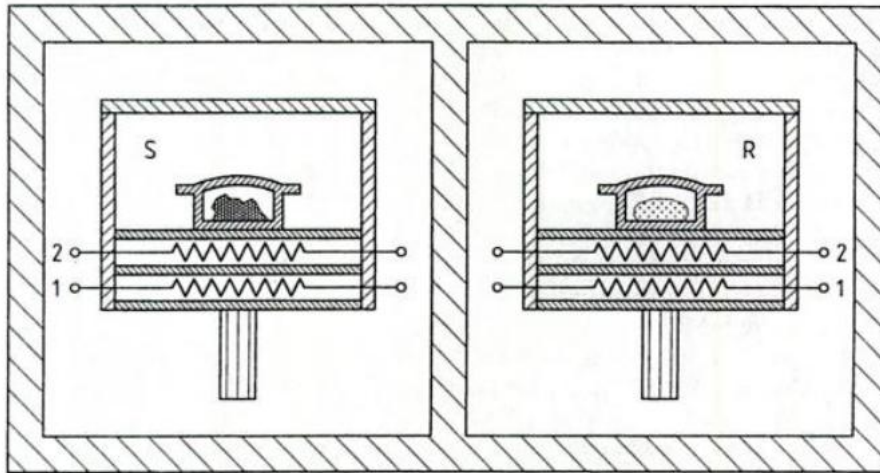
Figure 13. Sketch of a power compensation dsc 48]

6.2.2 Heat flux DSC (hf-DSC)

The hf-DSC is also known as a type of Boersma DTA [36]. The heat flux DSC belongs to the class of heat-exchanging calorimeters. In which measurement of the heat flow rate between sample and surroundings due to the heat is measured. And the exchange of the heat with the environment takes place via a well-defined heat conduction path with given thermal resistance [48].

The heat flux DSCs are further classified into three most important fundamental types such as [36, 48],

- Disk type measuring system
- Turret type measuring system
- Cylindrical type measuring system

6.2.2.1 Heat flux DSC with Disk type measuring system

Figure 14 shows the disk type DSC. In this measuring system, sample and reference containers are placed symmetrically to the centre and the temperature sensors are

integrated in the disk of medium thermal conductivity, which serves as solid samle support. When the furnace is heated, the heat flows through disk to the samples. . It has a simple and easily realizable design with a high sensitivity for the small sample volume. But the heat exchange between furnace and sample is limited which allows only meadium heating and cooling rates [36, 48]. If the samples of same kind are analyzed in an ideally symmetrical arrangement, the same heat flows into sample and reference sample. Then the differential temperature signal ΔT is zero. But in real, neither ideal thermal symmetry of the measuring system at all operating temperatures nor thermal identity of the samples can be attained in practical application, not even outside the transition interval. Hence, there will always be a signal ΔT which depends on the temperature and the sample properties. When a sample transition takes place, steady state equilibrium is interrupted and a differential signal, proportional to the difference between the heat flow rates to the sample and to the reference samples is generated. It can be presented as [48],

$$\Phi_{FS} - \Phi_{FR} \sim T_S - T_R \tag{3}$$
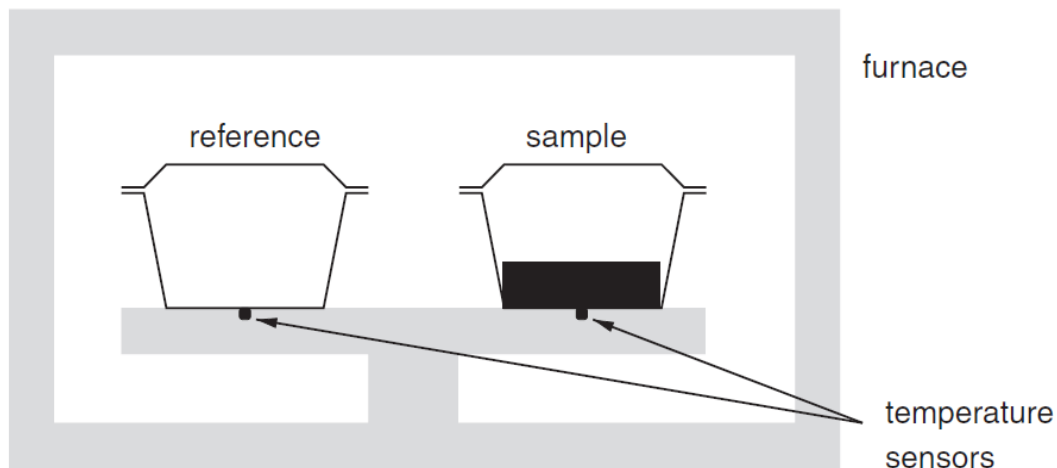
Figure 14. Sketch of a furnace of a heat flux DSC of a disk type 40]

The heat flux DSC with disk type measuring systems is available for temperature between – 190 ºC and 1600 ºC. The maximum heating rates are about 100 K/min with common heating or cooling rate is 10 K/min, typical time constants of the ΔT-sensor (empty systems, i.e. without sample) are between 3 and 10 seconds, the noise of the measurement signal lies between 0.5 μW and 20 μW (it also depends on the

temperature and the heating rate). The total uncertainty of the heat measurement amounts to about 5% [36, 48].

6.2.2.2 Heat flux DSC with turret type measuring system

The turret type DSC can be seen in Figure 15. In the turret type DSC, the heat exchange takes place via small hollow cylinders which also serve as elevated sample support. This system is ideal for determining the purity of metals. The design is more sophisticated with high sensitivity and fast thermal response which allows large heating and cooling rates, the sample volume is small. It is a special type because it has a third thermocouple which measures thermal inertia (called Tzero DSC technology) [36, 48].
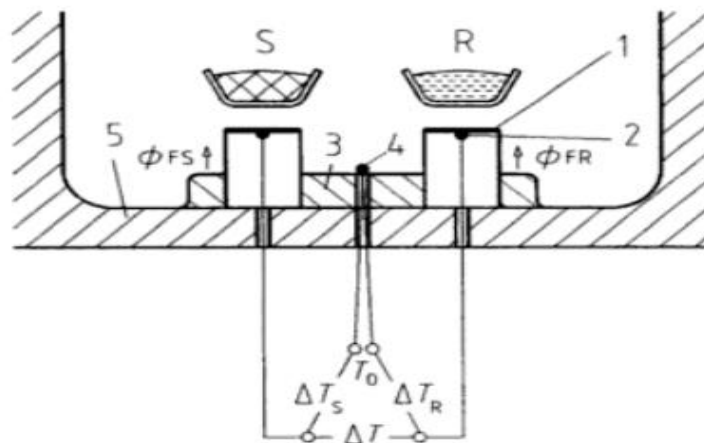
Figure 15. Sketch of a turret type heat flux DSC 48]

6.2.2.3 Heat flux DSC with cylinder type measuring system

The cylinder type heat flux DSC can be seen in Figure 16. It works on Calvet principle using a cylinder type measuring system. In which two sintered alumina cylinders set parallel and symmetrical in the heating furnace. And the heat exchange between the cylindrical sample cavities and the furnace takes place via a path with low thermal conductivity. It is very sensitive with a large sample volume but with a large time constant which allows only low heating rates, and the sensitivity per unit volume is however very high [36, 48].
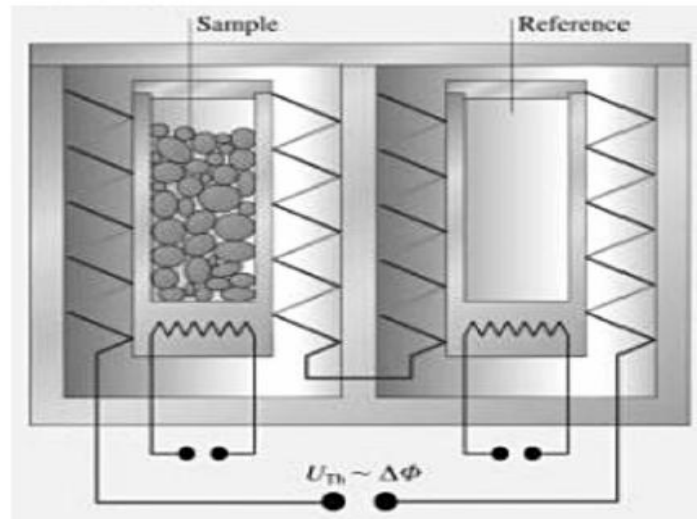
Figure 16. A cylinder-type heat flux DSC 36]

In the present experimental work, the disk type heat flux DSC (hf-DSC822[e]) from the company Mettler Toledo is used.

6.3 Principle of heat flux-differential Scanning Calorimetry (hf-DSC)

Figure 17 shows the photographic view of a DSC which is used for present experimental analysis of PCM. Differential Scanning Calorimetry (DSC) is a thermoanalytical technique. It is a standard method for thermal analysis. Heat flux DSC determines the amount of heat absorbed by a sample upon temperature change. The temperatue development of the sample in a furnace is compared with the temperature of a reference in a symmetric position. In a hf-DSC a temperature sensor is placed on the surface of the furnace (Figure 14). A hf-DSC allows measuring the heat flow with accuracy. The temperature development of the sample in the furnace is compared with the temperature of a reference in a symmetric position. Thermal effects of the sample lead to a deviation in the sample temperature from the reference temperature. This temperature difference is detected and used to determine the heat flux between the sample and the furnace. From the measured heat flux, the specific heat as a function of temperature $c_p(T)$ can be obtained. And from the specific heat values, the enthalpy (Δh) (the storage capacity) can be derived by integration over temperature (T) using following equation [39, 40]:

$$h(T) = \int_{T0}^{T} cp(\tau) d\tau \qquad (4)$$
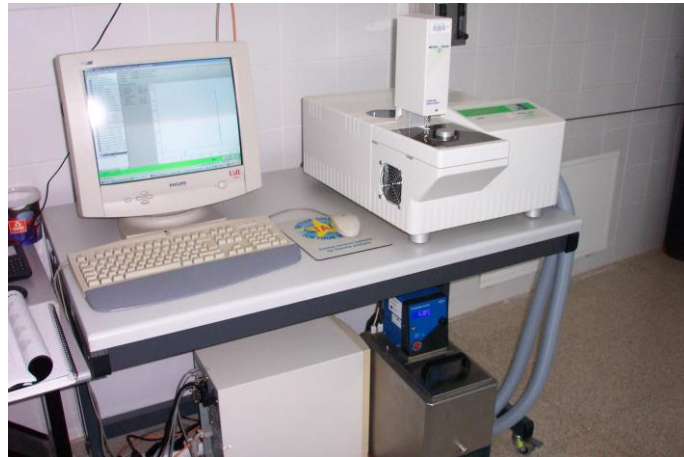
Figure 17. Photographic view of a hf-DSC of the GREA used for present thermal analysis of PCM samples

The start of the integration range T_0 can be chosen freely to normalize h(T) curves.

Since the DSC allows measuring the heat of fusion and their changes at characteristic temperatures with high accuracy, it could be useful to obtain thermophysical properties of PCM. These properties would be, c_p solid, c_p liquid, melting temperature (T_m) and phase change enthalpy (Δh) [10, 37, 40].

6.4 Different modes of DSC operation

DSC could be mainly operated using two different modes such as, (1) dynamic mode and (2) isostep mode [10, 39, 40]. These modes are discussed in detail in the following sections.

6.4.1 DSC dynamic mode

The most widely used scanning mode is the dynamic mode. It consists of heating and cooling segments at constant rates [39, 40]. Since the method involves constant (and continuous) heating and cooling rates, the time duration for the method analysis is short. A typical dynamic mode temperature program and a signal are shown in Figure 18.
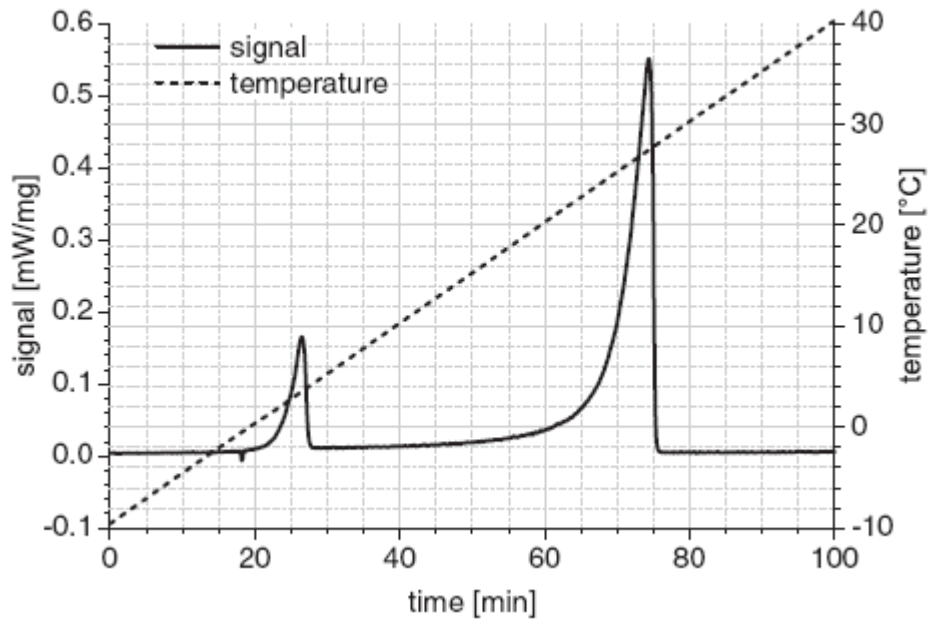
Figure 18. Typical heat flow and temperature evolution during a dynamic DSC measurement with constant heating rate. The peaks indicate strong thermal effects of the sample at the corresponding temperatures [40]

Enthalpy (h) can be determined by executing a dynamic program for three times. Such as,

- First, a reference is compared with the blank crucible (empty crucible): to generate the baseline (it is a thermal response of the crucible material).
- Second, the reference is compared with the standard material (usually sapphire): for calibration (for assuring good sensitivity for small signals).
- And at last, the reference is compared with the sample material: to generate the sample line.

Then the resulting specific heat of the sample as function of temperature c_p (T) is given by [39]:

$$c_{p,\ sample}\ (T) = c_{p,\ standard}\ (T) \cdot [\frac{U_{sample} - U_{empty}}{U_{standard} - U_{empty}}]\ (T) \cdot \frac{m_{sample}}{m_{standard}} \qquad (5)$$

Where,

m = masses of the sample and standard material

U = voltage signals of empty, sample and standard run

Since the method involves continuous heating/cooling there are some related uncertainties to the dynamic mode which are discussed next.

6.4.2 Uncertainties related to dynamic mode operation

The temperature sensors are at the surface of the furnace (Figure 14). Hence, the measured temperature at the surface of the furnace is higher than the average sample temperature for heating and lower than the average sample temperature for cooling runs. Thus, the *effect of continuous heating and cooling of the dynamic mode* leads to temperature gradient in the sample temperature [39, 40].

Moreover, if the applied *heating and cooling rates are very high*, then it leads to a temperature gradient in the sample and the resulting heat flux signal originates from a temperature range. Therefore the resulting enthalpy values from heating and (or) cooling are systematically shifted to higher and (or) lower temperatures. This effect can be seen in Figure 19. In the calculation of the thermal effect, the temperature of the material is assumed to be the same throughout the whole sample (solid lines). In reality, due to heat transfer limitations, the temperature is not uniform (dashed lines) [40].

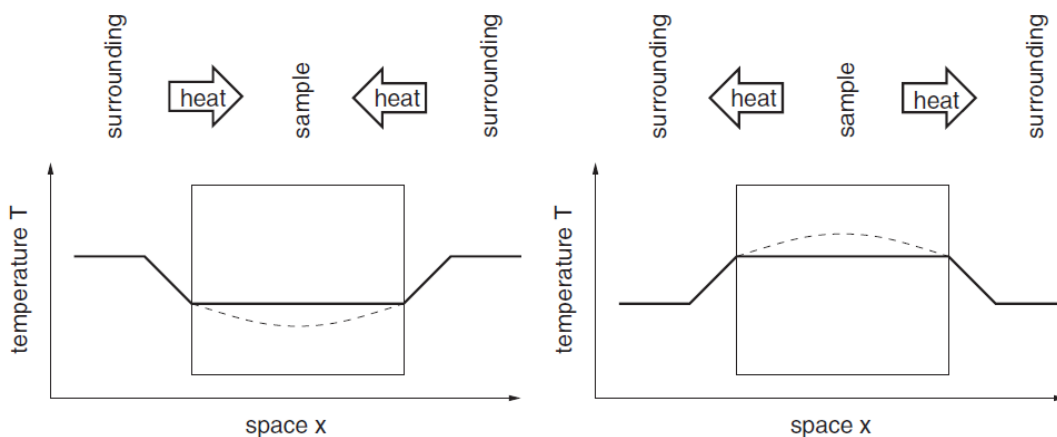**Figure 19. Temperatures inside the sample during heating (left) and cooling (right) [40]**

When doing both heating and cooling measurements, the real temperature of a thermal effect can be confined to a value between both extremes. If the thermal effect does not occur in thermal equilibrium, a further shift due to kinetic or dynamic reasons can increase the thermal shift [40]. Therefore, the heating or cooling rate has to be slow

enough to assure thermodynamic equilibrium within the sample. If not, the heat supplied at each data recording (dH = dQ) cannot be assigned to the measured temperature resulting into significant errors in the data of the heat stored as a function of temperature [10]. Due to this reason and because the exact form of the gradient is not known, it cannot be assumed that the real value is indeed at the centre. Therefore, the distance between heating and cooling curves indicates the uncertainty of the measurement [40].

The *sample size* also affects the signal of the sample. If a small sample size is selected with low heating and cooling rates, the temperature shift inside the sample will be reduced. But this is not the solution. Because, both the small sample size and low heting and cooling rate lead to a weak signal and hence, decreasing the accuracy in enthalpy. Moreover, the small sample could not be a representative of the bulk material to be analyzed [40].

The effect of different heating/cooling rates and the sample size can be clearly seen in Figure 20 and Figure 21 [39]. Figure 20 and Figure 21 show the deviation in the resulting signal. Figure 20 shows that as the heating rate or sample mass increases the peak has shifted to higher temperature values. It can also be seen that as the heating rates increse the peaks shift towards higher temperatures and as the cooling rates increase the peaks shift towards lower temperatures leading to the thermal gradients in the sample. In DSC analysis, initially the sample has to be isothermal at the initial and final temperatures. If the sample is not in the isothermal state during this period, these states are not well defined and the heat supplied is not determinded correctly hence, resulting to wrong values [10]. When the sample undergoes the dynamic method, continuous heating (or cooling) is applied to the sample and thus the temperature gradient originates. These gradients vary consequently as the heating rate or the sample mass varies. As a result, the measured values are not the real values but the overestimated values due to the continuous heating or underestimated due to the continuous cooling which is responsible for the temperature shift to the high or the low temperature values. As a consequence, the signal of the sample being attributed to too high temperatures, the shift of the melting peak increases with increasing gradient, i.e., heating rate or sample mass.
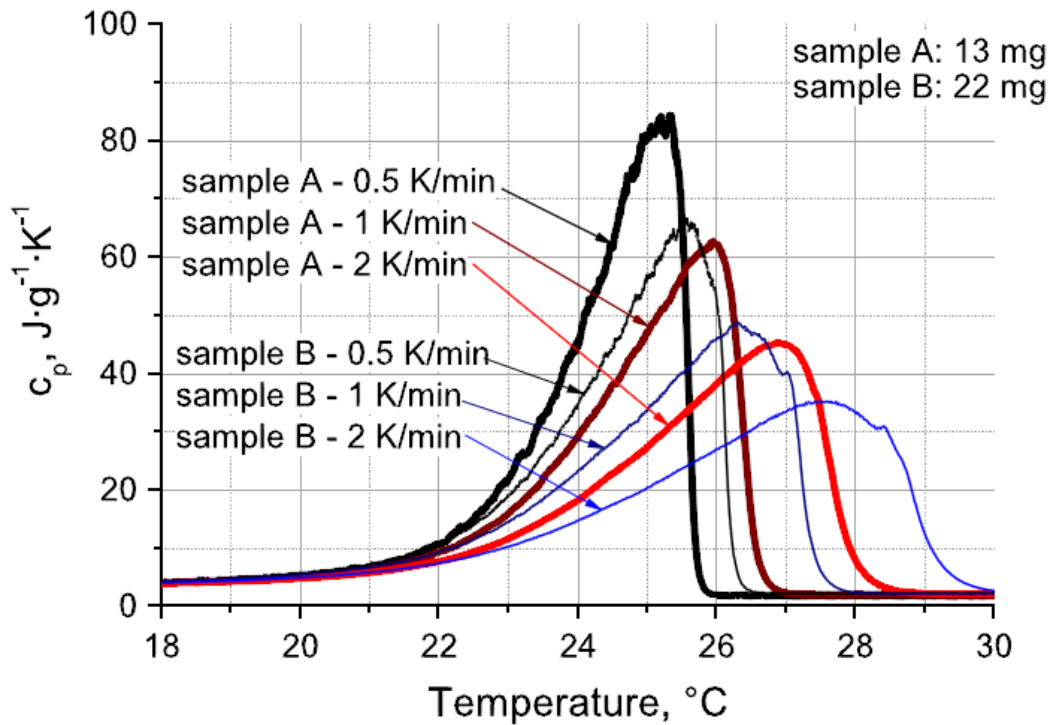
Figure 20. Effect of different sample mass and different heating rates [39]
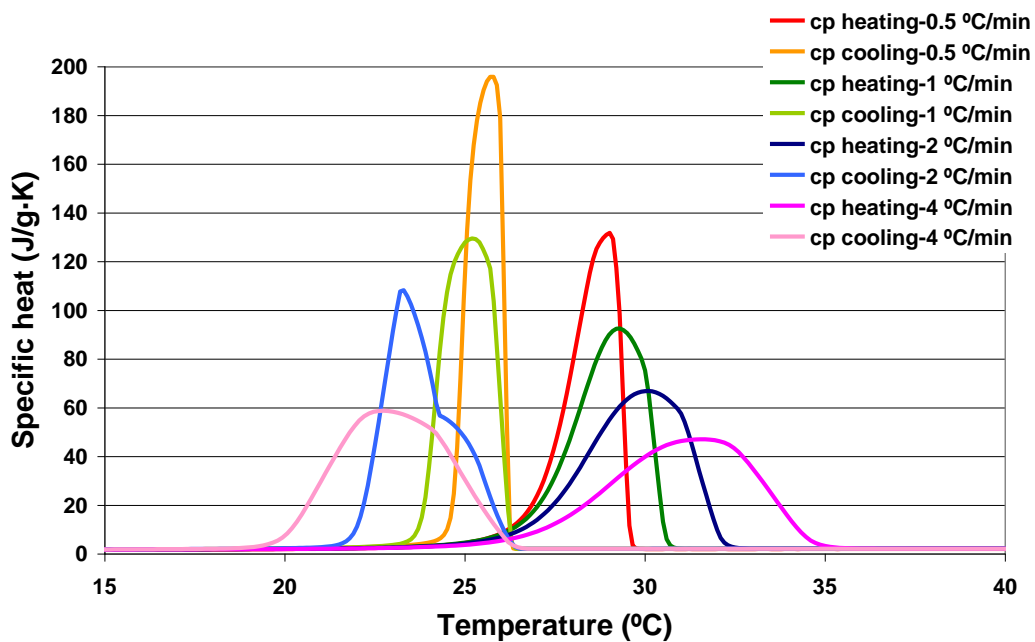
Figure 21. Effect of different heating rates [49]

Due to the reasons of uncertainties, for pure materials, the onset of the peak is commonly used to mark the melting temperature and the integral of the peak denotes the melting enthalpy. But this effect is more dominant for the PCM, because when the PCM is analyzed using DSC, the heat transfer problem increases because they have a high heat capacity and a low thermal conductivity than the other samples. Due to these two major factors the effect of internal temperature gradient is higher than the other samples

and especially near to the phase change temperature ranges which is of interest for the selection of the PCM [39, 40].

Because of the PCM properties the $c_p(T)$ curve is highly nonlinear during this temperature range. The consequences of the thermal gradient inside the sample can be experimentally quantified by reversing the ramp by means of cooling down the sample and comparing the heating and cooling measurements. During the cooling process the temperature gradient is reversed and the sample temperature is underestimated. Hence, the true sample temperature is thus enclosed by the heating and cooling measurement data. If the difference between the results of heating and cooling is within the desired uncertainty range, then the gradient is small enough. If it is larger, a variation of the heating and respectively cooling rate can show whether the results are dependent on the measurement variables. If they are not, the difference can be considered as the material property. That can be achieved by thermal hysteresis. By plotting the thermal hysteresis with different heating and cooling rate for dynamic method for DSC, a suitable heating rate could be found [39].

The adverse effect of the too high heating/cooling rate is well described above. If the too high heating/cooling rate is an adverse effect, then low heating/cooling rate could be an option. Nevertheless, lower heating/cooling rate is also not a solution for the dynamic method for the DSC. Because the signal-to-noise ratio and the errors in the Δh values increase with the very low heating rates [39, 40].

6.4.3 DSC step mode

In this method, continuous heating or cooling is not applied to the sample. But small ramps of heating and cooling are applied followed by constant temperature period to ensure the thermal equilibrium at the beginning and at the end of each heating/cooling ramp. These small ramps are called steps, and the final resulting signal is the sum of these heating/cooling ramps. Using this method it is possible to increase the temperature resolution of the stored heat. Hence, the method is more reliable compared to the dynamic method because the uncertainty in the temperature is now precisely known, as it is confined to the step size. In this method the resolution of the temperature is

proportional to the height of the temperature steps. A typical step method temperature program and its resulting signal are shown in Figure 22.
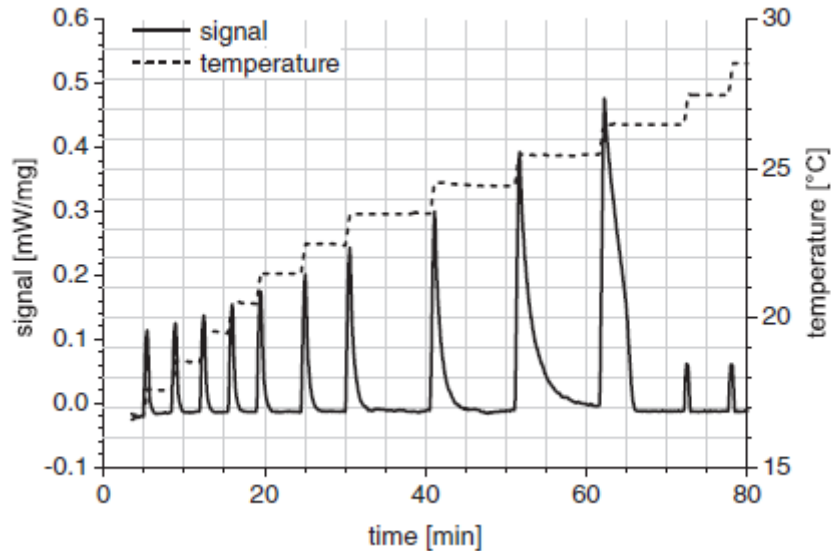
Figure 22. Typical heat flow and temperature evolution during a DSC step method for heating process [40]

In this mode, the furnace is heated in stepwise intervals in the predetermined temperature range. These steps are followed by the predetermined time delay without heating (or cooling) such that the signals for the sample and the reference become isothermal at the end of each step and return to zero. Thus confirmning that the sample (and reference) is isothermal and the area below that period gives the amount of stored heat during the corresponding temperature. Hence, there is no temperature gradient. It should be taken into account that a reduction of the step size leads to better temperature resolution but it should also be considered that the step size should not be too small because if the step size is too small then the corresponding temperature signal will not be isothermal (not reach zero), the signal will vanish and the precision of the measurement will be lost.

The evaluation of the signal considers only peak areas and the exact shape of the baseline has no influence on the resulting h(T) relationship. From the sample heat-flux signal, the enthalpy h(T) is determined by integration of every peak within the phase change range. For checking the accuracty of this method, the heat calibration is performed by the comparison of the measured peak areas of phase change of standard

materials to literature values of the phase change enthalpies. A sensitivity profile for the instrument is created and used to convert the directly measured thermovoltage signal into the heat-flux signal. The calibration needs to be repeated time to time, to ensure the correct performance of the instrument [10, 39, 40].

6.5 Temperature-history (T-history) method

The T-history method was proposed by Zhang et al. [41]. T-history installations are not readily available in the market, but can be assembled using standard laboratory components. The T-history installation is shown in Figure 23. The method was improved by Marín et al. [42] to obtain temperature dependent properties such as enthalpy vs. temperature curve and specific heat vs. temperature curves for the larger sample size.

The set up of the method consists of [42]:

- Test tubes haveing Bi (biot number) < 0.1,
- Insulated cool down chamber,
- Hot water bath for heating the sample and reference to initial temperature,
- Temperature sensors, to measure the temperature of the PCM, water and ambient, and
- Data acquision equipment connected to a computer.

In this method, two identical test tubes, one with PCM and the other with a reference substance (with known specific heat, i.e. distilled water) are heated in the water bath to the required temperature and then these tubes are placed in the cool down chamber to cool down the tubes. During this period the temperature-history is recorded [10, 42]. Following this method they analyzed paraffin, $C_{16}H_{34}$ and their obtained temperature-time curve is presented in Figure 24 [42].
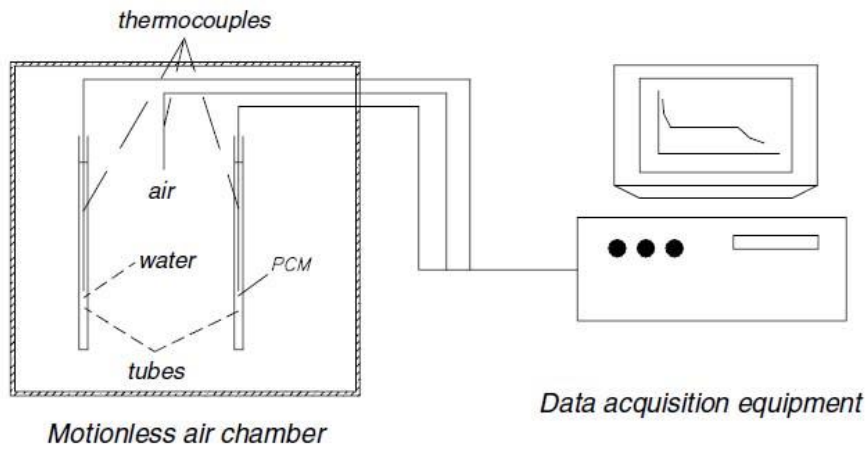
Figure 23. T-history experimental set-up 42]

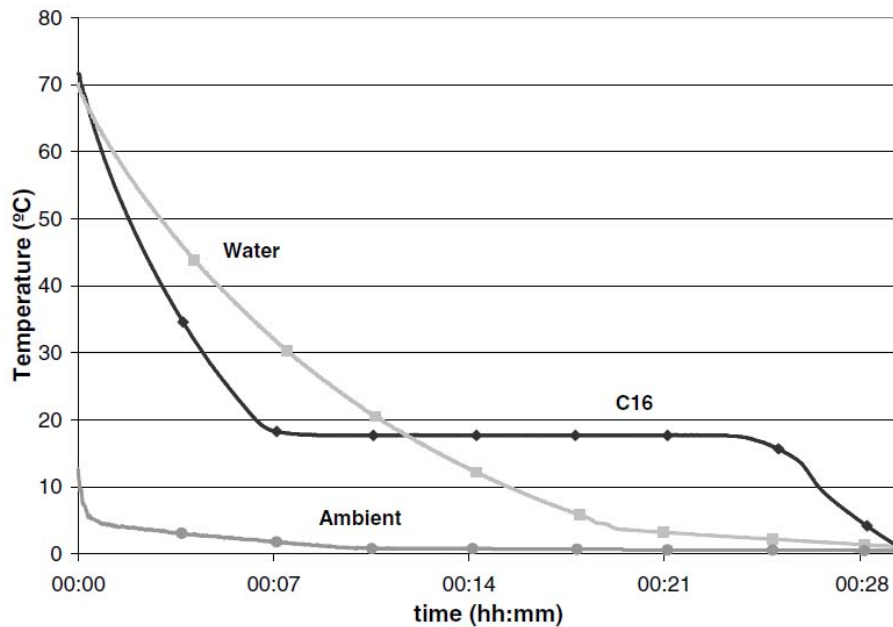**Figure 24. Experimental temperature–time curve obtained for paraffin C$_{16}$ 42]**

Günther et al. [39] used a T-history installation with 20 ml of sample size which is approximately 1000 times more than the DSC sample size. They studied mixed linear alkanes using DSC dynamic mode, DSC isothermal step mode and T-history method. Their results obtained by using the three methods are presented in Figure 25.
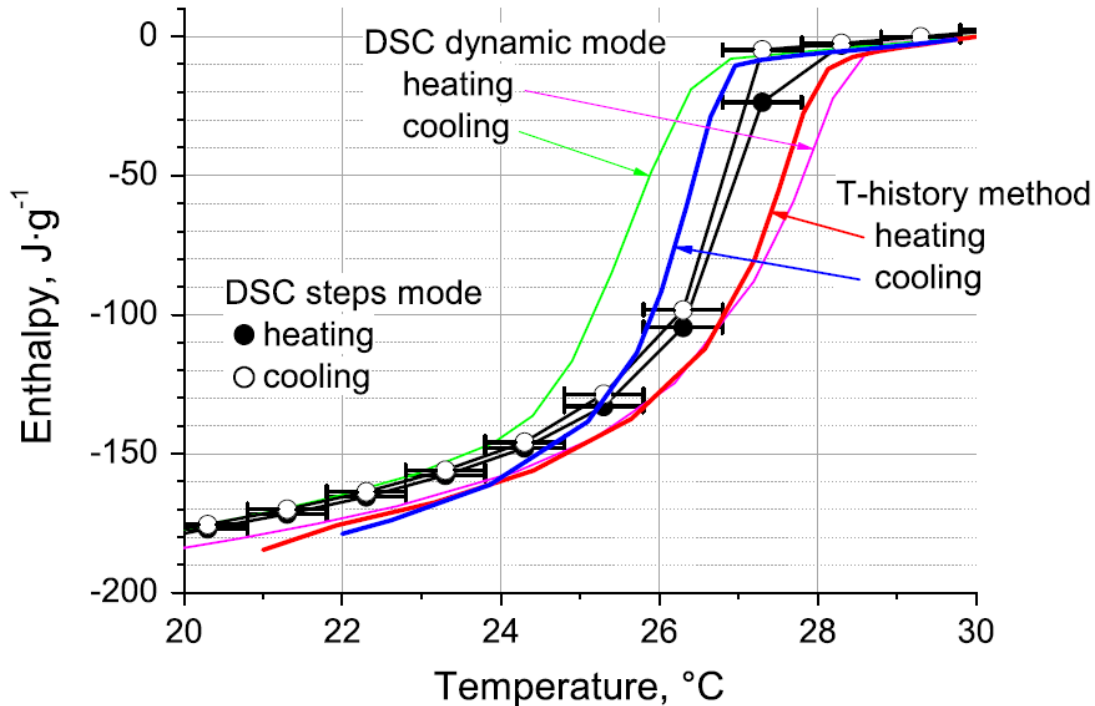
Figure 25. Comparison of heating and cooling enthalpy curves of one sample material with different methods 39]

They found that with the step method the uncertainty in temperature was reduced from 2 K, with the slowest dynamic method (0.5 K/min) the uncertainty was found to about 1 K and they also found that the T-history method presented similar precision with large sample size [39].

6.6 Problems related with PCM analysis using DSC

There are some problems in analyzing PCM due to their high enthalpy density per unit volume. Such as,

- *Sample size*: Sample should be representative of the material for being sure about the homogeneity of the sample material. Many PCM contain nucleating agents, heat transfer enhancing additives, gelling materials, etc. Hence, analysis on very small sample size of PCM (typically 20 μL for the DSC analysis) is not completely representative of the thermal properties of the PCM bulk material and it could not be assumed that the sample composition is same as the bulk material. Moreover, if the PCM sample size is very small for the analysis, pseudo-subcooling may occur [10, 39].

- *Subcooling***:** Subcooling is often stronger for small sample sizes than in large sample sizes. Therefore the sample size should be large enough to obtain the real behaviour of the sample. If the sample present strong subcooling in DSC analysis, it deforms the cooling DSC curve. Due to the subcooling, it becomes difficult to quantify internal gradients by comparing heating and cooling curves. Consequently, the maximum subcooling determined by a DSC is not a representative of the PCM nature [10, 39]. Hence, as a solution to the subcooling, the large sample size should be analyzed before applying the PCM for any real TES system.

- *Correct determination of the exchanged heat and temperature of the sample***:** For obtaining the correct results it is necessary to calibrate the DSC time to time using standard material. For the PCM used for the heat storage applications, the sum of the latent heat and sensible heat is important. For this purpose, good sensitivity for small signals is necessary. And it can be achieved using the heat flow rate calibration. A calibration of the heat flux is done using the melting enthalpies of standard materials ('heat calibration') or the sensible heat of a standard without phase change ('heat flow rate calibration') [10, 39, 40].

- *Thermal equilibrium***:** For achieveing thermal equilibrium the sample should be isothermal, otherwise the heat flux cannot be attributed to a single temperature as indicated by the sensor. To maintain the isothermal condition of the sample, the heating or cooling should be slow enough or the sample size should not be too large. This is contradictory to the requirement of enough large samples for being a representative of the sample as mentioned above [10, 39, 40].

- *Reaction equilibrium***:** The sample should be in reaction equilibrium, otherwise the enathalpy at the measured temperature has no defined value and consequently enthalpy differences are also not well defined. It refers to two aspects: first, the dynamic process has to proceed to a stable state and second, there should be only one stable state at the same temperature. Some occasions such as, very slow reactions, metastable states like amorpohous instead of crystalline structures, subcooling and different crystalline structures cause problems with regard to reaction equilibrium (This requirement=reaction

59

equlibrium is violated during subcooling of a sample or if cooling crystals form slowly. That indicates that the heating/cooling rates should be small.) [10, 39].

- *Hysteresis***:** Most calorimeters are constructed to provide accurate results for sensible heats of ordinary materials. But while analysing the PCM a significant offset can be seen in the melting range of the PCM due to their high energy storage density. This effect could become worse while cooling down of the PCM. Hence, as mentioned previously, for the correct analysis of the PCM, the heating and cooling of the PCM should be performed. Due to the high energy storage density of the PCM hysteresis could be obtained while presenting the values of enthalpy as a function of temperature. But this hysteresis could be apparent or real hysteresis. Some factors might be the reason for the apparent hysteresis, such as continuous heating and cooling, and it could be because of the analysing equipment. There are several real causes for the hysterisis which include: subcooling, or if the latent heat is released too slowly on cooling because the crystal lattice forms very slowly, or because diffusion processes are necessary to homogenize the sample, or different solid phase after the solidification compared the initial solid phase [10, 39].

7 Experimental part

The objective of the present work is mentioned in chapter 2. In the present work commercially available PCM which have melting temperature in the thermal comfort range according to Spanish climate were selected for the analysis.

7.1 Sample selection

In total four commercially available PCM samples were selected for the analysis of the thermal properties. Two of them were paraffins and two were salt hydrates. The selected paraffins were RT 20 and RT 27, and the selected salt hydrates were SP 22 A17 and SP 25 A8. The thermal properties of these samples given by the manufacturer are presented in Table 9. All the samples were from the company Rubitherm GmbH.

Thermal properties of selected paraffins (RT 20 and RT 27)

The paraffin samples are based on the mixtures of n-alkanes. They have high thermal energy storage density, relatively constant temperatures for storage and extraction of heat, no subcooling effect, allow long life utilization with stable performance through the phase change cycles, they are ecologically harmless and non-toxic and chemically inert [50, 51].

Thermal properties of latent heat blend SP 22 A17 and SP 25 A8

The materials are latent heat blend type and composed of salt hydrates and paraffins. The materials are preferably processed into sustaining and/or absorptive structure (e. g. foams). They have high material densities (as seen in the Table 9). They can be used in the construction industry and possibly they could be useful for passive and active cooling (e.g. in wall elements and air conditioners). The materials show stable performance throughout the phase change cycles, they possess high thermal storage capacity, limited subcooling, low flammability and they are non toxic. But, these materials have hygroscopic nature. Hence, they should be stored in a completely self contained container because these materials may absorb moisture, the original thermal properties of the materials could change [50, 51].

Table 9. Thermal properties of selected PCM given by the manufacturer [50]

Properites	RT 20	RT 27	SP 22 A17	SP 25 A8
Melting point/area	22 ℃	25-28 ℃ (typically being 27 ℃)	22-24 ℃ (typically being 23 ℃)	26 ℃
Congealing point/area	22 ℃	28-25 ℃ (typically being 27 ℃)	21-19 ℃ (typically being 20 ℃)	25 ℃
Heat storage capacity	172 kJ/kg	184 kJ/kg	150 kJ/kg (13-28 ℃)	180 kJ/kg
Specific heat capacity	-----	-----	-----	2.5
Density solid	-----	0.88 kg/l (at 15 ℃)	1.49 kg/l (at 15 ℃)	1.38 kg/l
Density liquid	-----	0.76 kg/l (at 40 ℃)	1.43 kg/l (at 35 ℃)	-----
Volume expansion	-----	16%	4.03%	0.001 l/K
Heat conductivity	-----	0.2 W/m·K	0.6 W/m·K	0.6 W/m·K
Corrosion	-----	Chemically inert with respect to most materials	Corrosive compared to metal	-----

7.2 Methodology

The instrument used for thermal analysis was a hf-DSC. The model was DSC822^e and it was manufactured by Mettler Toledo. A water-bath (OVAN) was used for cooling purposes and nitrogen gas was used as a purge atmosphere. The standard aluminum crucibles of 100 μl volume were used as the sample container. Sapphire was used as a standard material was used for heat flow calibration. The calibration of the instrument was previously done by the technician from the manufacturing company. To determine the sample mass, an analytic balance AG – 135 also from Mettler Toledo was used. The calibration of the balance was also previously done by the technician from the manufacturing company. It has linearity of ±0.2 mg/±0.03 mg (in the temperature range 10 … 30°C).

The samples were preheated before sampling in order to facilitate sampling and to assure the homogeneity of the samples. Both dynamic and step methods were used to find out the suitable method for the thermal analysis of both PCM. The dynamic method program applied to all samples is presented in Figure 26. During the dynamic method all samples were heated and cooled down during 5 to 50 ℃ with the heating rate of 0.5 ℃. The nitrogen gas flow was constant (80 ml/min) during all the experiments. General temperature range of 5 to 50 ℃ was applied in order to make sure complete melting and

freezing of the samples. The low heating /cooling rate of 0.5 ºC was used considering the previously mentioned causes.

The samples were also analyzed to check repeatability of the results. For that purpose three sub-samples of all four samples (RT 20, RT 27, SP 22 A17, and SP 25 A8) were analyzed using the same dynamic method and each sub-sample was cycled three times.
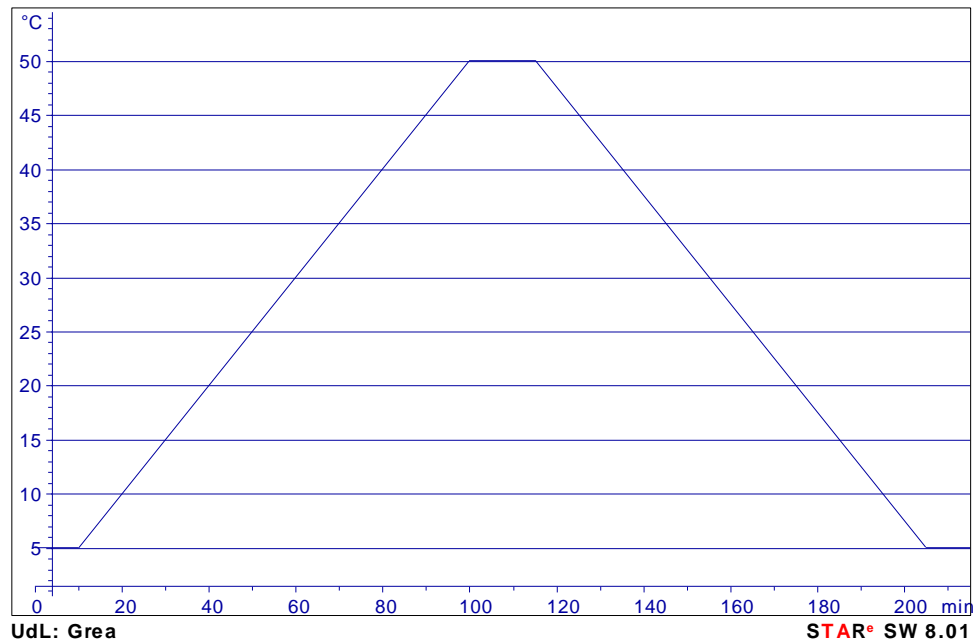

Figure 26. Dynamic method program applied to all samples from 5 to 50 ºC with heating/cooling rate of 0.5º/min

From the dynamic method results, the phase change range of each sample was decided and consequently step method for each sample was created, and applied since the step method is more accurate method. More delay time during isothermal step was allowed during the phase change temperature range in order to assure the thermal equilibrium at each corresponding temperature. For the step method, new samples of all the samples were prepared in the same manner as for the dynamic method. During the step method the applied heating and cooling rate was the same as the dynamic method (that is 0.5 ºC/min).

The step method for RT 20 is presented in Figure 27. For this sample, the applied temperature range was shortend during 5 to 30 ºC. In this method, delay time of 20 min was applied during 16 to 24 ºC (for heating) and 22 to 14 ºC (for cooling).
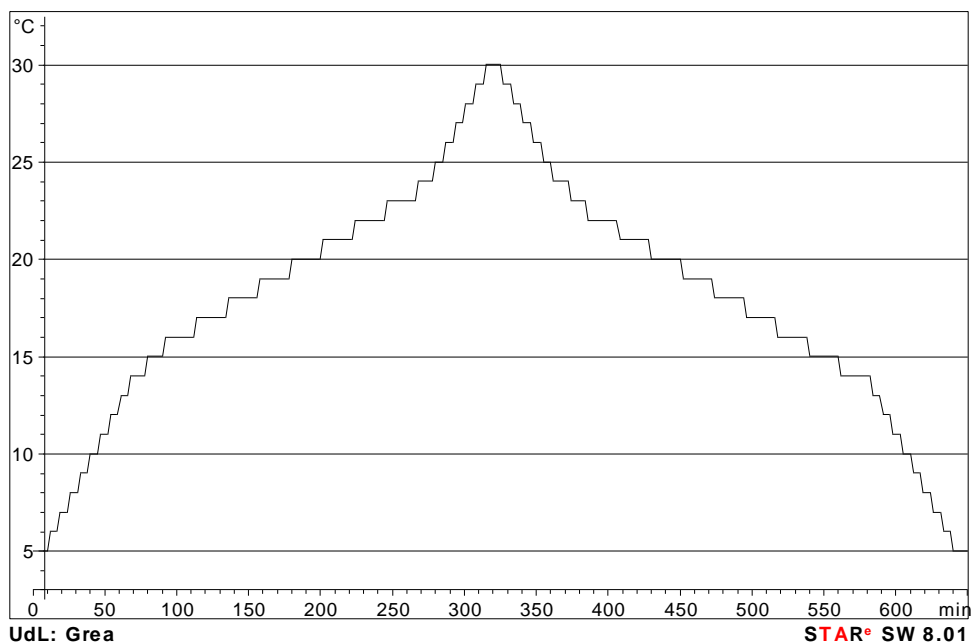
Figure 27. Step method program from 5 to 30 ºC with heting/cooling rate of 0.5 ºC/min for RT 20

Figure 28 shows step method for RT 27. For this sample, the applied temperature range was shortend during 5 to 35 ºC. In this method, delay time of 20 min was applied during 21 to 29 ºC (for heating) and 27 to 18 ºC (for cooling).
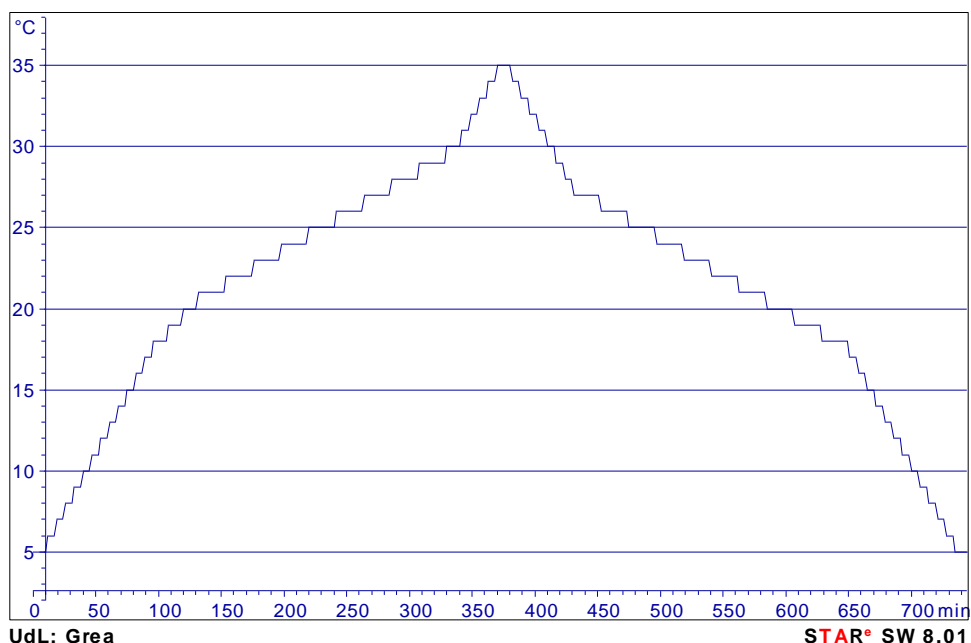

Figure 28. Step method program from 5 to 35 ºC with heating/cooling rate of 0.5 ºC/min for RT 27

The step method for SP 22 A17 is shown in Figure 29. For this sample, the applied temperature range was shortend during 5 to 30 ºC. In this method, delay time of 20 min was applied during 12 to 22 ºC (for heating) and 22 to 12 ºC (for cooling).

Figure 29. Step method program from 5 to 30 ºC with heating/cooling rate of 0.5 ºC/min for SP 22 A17

Figure 30 shows step method for SP 25 A8. For this sample, the applied temperature range was shortend during 5 to 37 ºC. In this method, delay time of 20 min was applied during 23 to 32 ºC (for heating) and 32 to 22 ºC (for cooling).
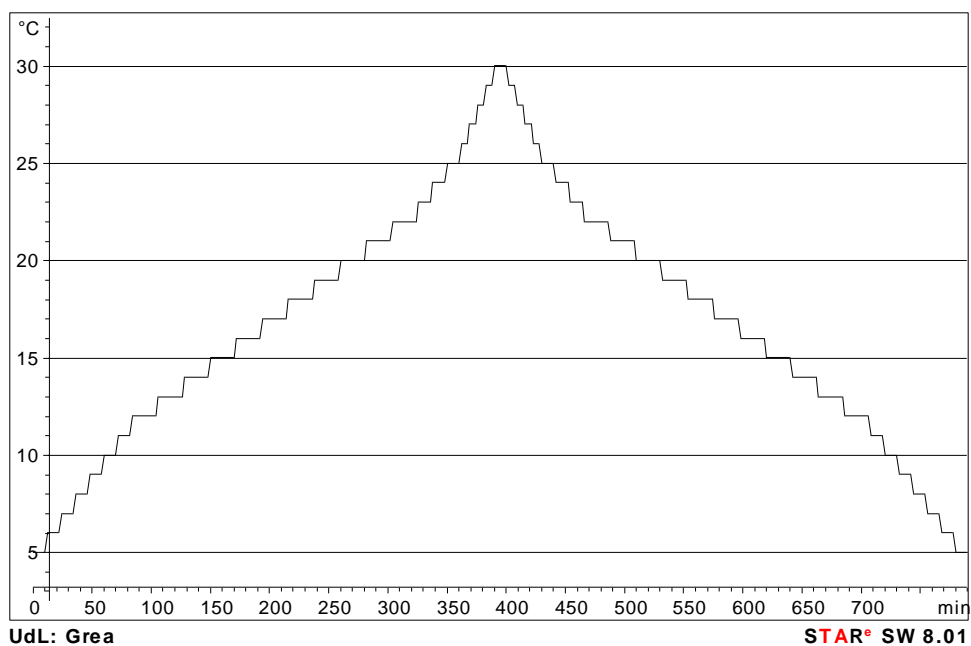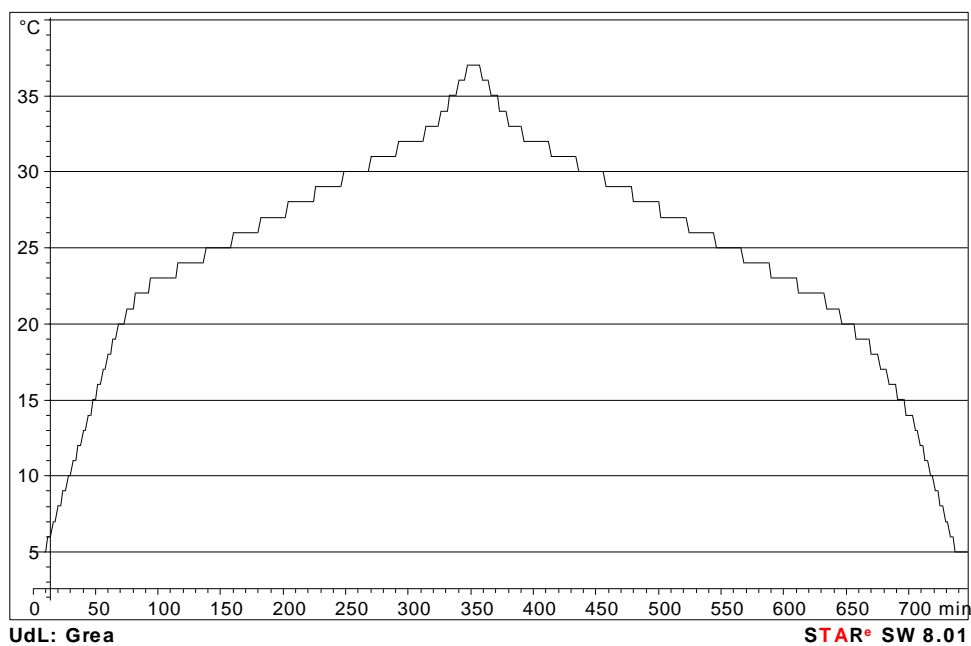

Figure 30. Step method program from 5 to 37 ºC with heating/cooling rate of 0.5 ºC/min for SP 25 A8

7.3 Results and discussion

The three sub-samples of the RT 20, RT 27, SP 22 A17 and SP 25 were named as sample A, B and C for the dynamic method experiments and D, E and G for the step method experiments. And the number of the each cycle was given as the suffix for the name of the sample cycle.

7.3.1 Results of paraffin samples

7.3.1.1 Results of RT 20

7.3.1.1.1 Dynamic method results

Output results of the dynamic method of RT 20 for all three sub-samples obtained using DSC star[e] software are presented in Figure 31. And the phase change area of each sample cycle was integrated and the temperature and enthalpy values were obtained by integrating the melting and the solidification peaks. For an example integrated sub-sample A − 1D (where, D = dynamic method cycle) is presented with melting and solidification enthalpy values in Figure 32. Extracted specific heat values as a function of temperature are presented in Figure 33. The enthalpy values were derived from the specific heat values and are presented in Figure 34. Figure 34 shows the hysteresis due to the difference in the peak melting and solidification temperatures, and it can also be seen in Figure 33.

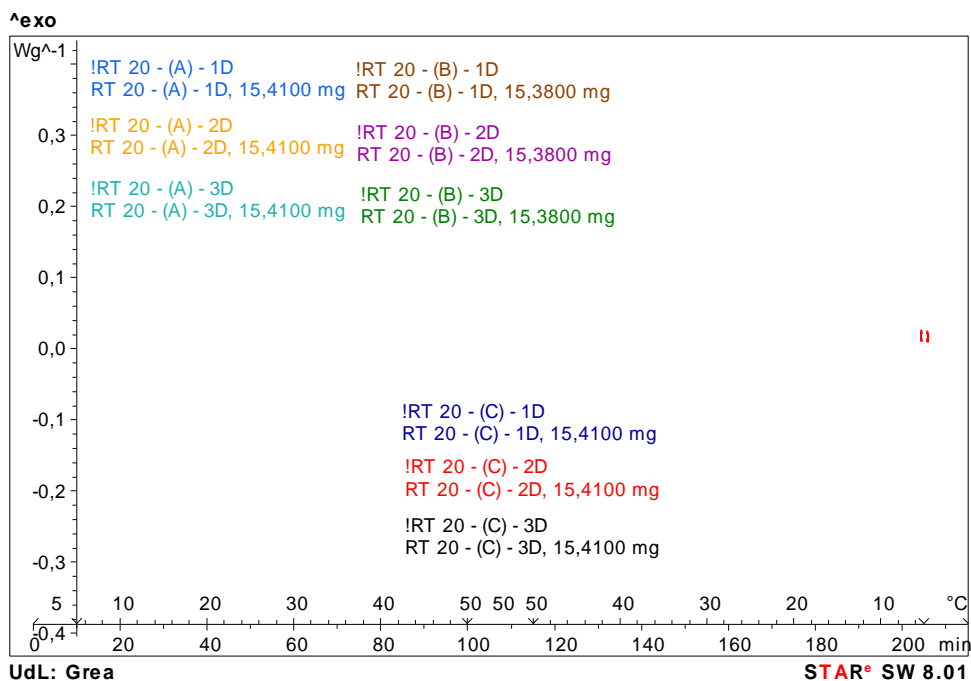**Figure 31. Heat flow vs. time and temperature of RT 20 for three sub-samples (A, B and C with their three cycles) using dynamic method**
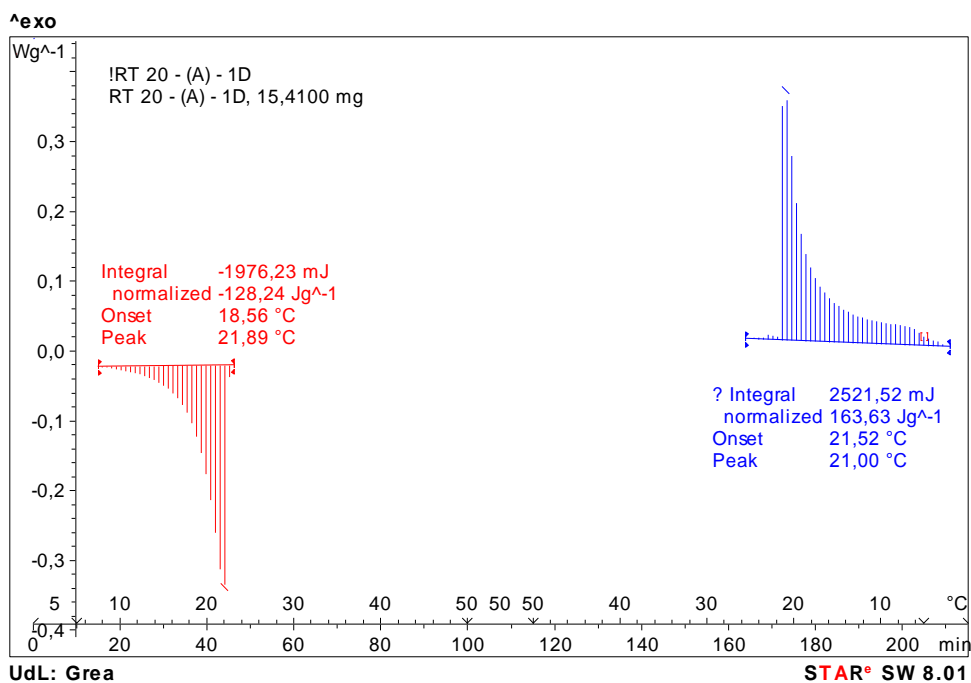

Figure 32. Heat flow vs. time and temperature and enthalpy values (left to right: melting and solidification peaks) during phase change temperature range (7.5 to 24.5 ºC for melting and 25.5 to 5 ºC for solidification) of the sub-sample (A) of RT 20 using dynamic method
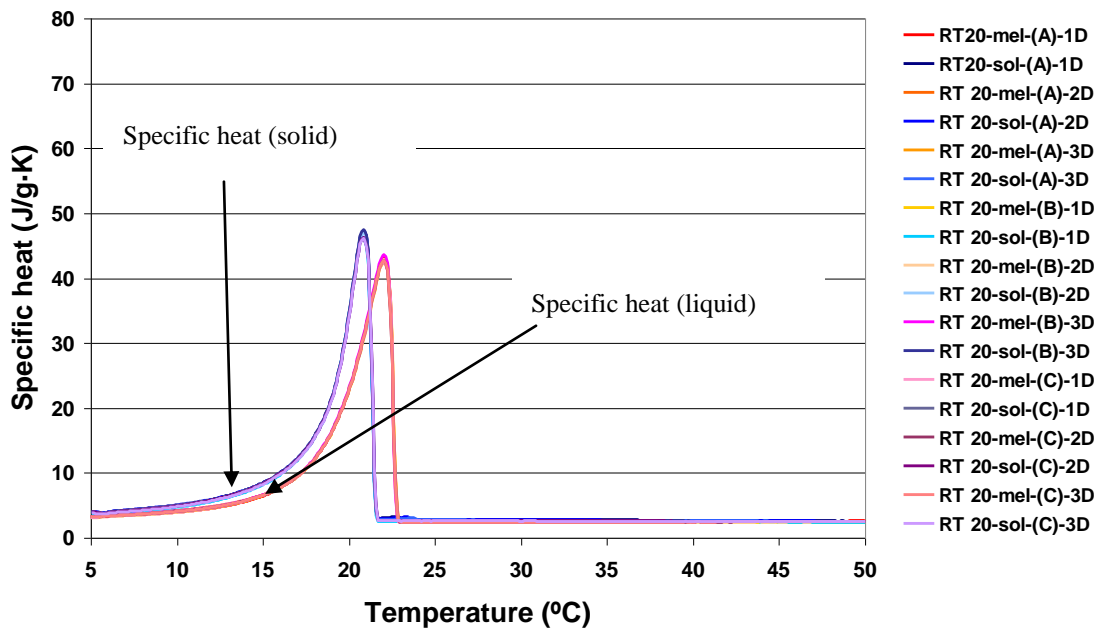
Figure 33. Specific heat vs. temperature of RT 20 for the three sub-samples (A, B and C) with three different cycles (dynamic method)
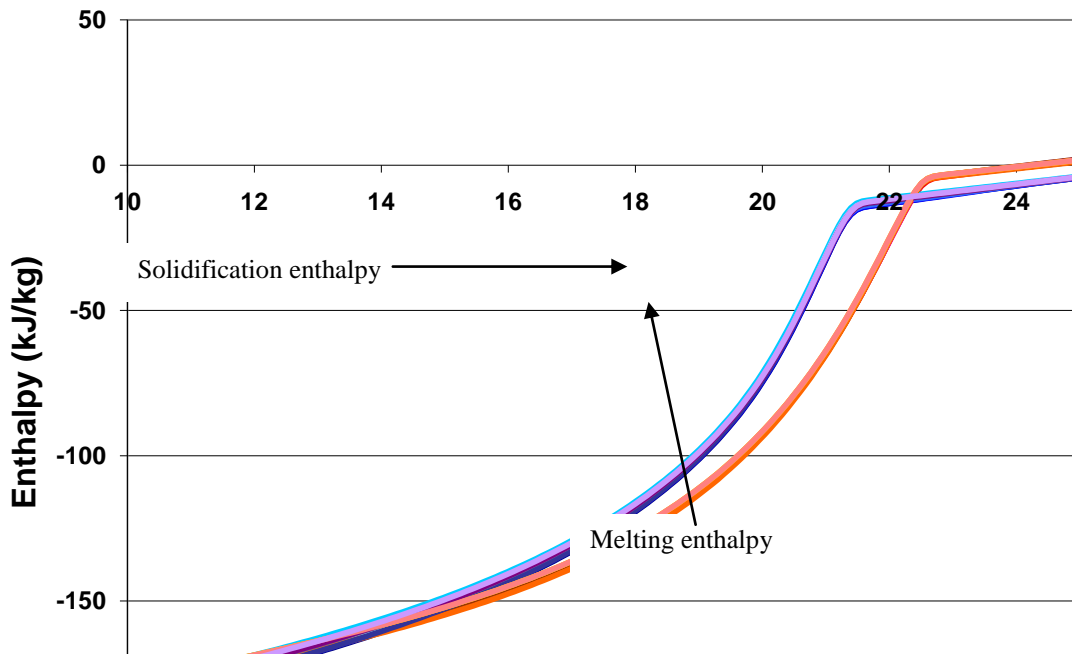
Figure 34. Enthalpy vs. temperature of RT 20 for the three sub-samples (A, B and C) with three different cycles (dyanamic method)

The dynamic method experimental values for the enthalpy, and melting and freezing temperatures obtained by the DSC software are presented in Table 10. The melting was started from 7.5 ℃ and was ended at 24.5 ℃, hence the melting peaks of all cycles of all sub-samples were integrated within this phase change temperature range. While the solidification started from 25.5 ℃ and ended at 5 ℃, therefore the solidification peaks

for all cycles of all sub-samples were integrated within this phase change temperature range. The average measured melting enthalpy within above mentioned phase change temperature range is approximately 128 kJ/kg which is less (44 kJ/kg) than the commercial value (172 kJ/kg). The difference in the experimental enthalpy value and the commercial value could be due to the instrument sensitivity or change in the phase change range of the commercial values and the experimental values. The average measured melting tempeature (obtained by Mettler Toledo DSC822^e) is 21.90 ℃ which shows good agreement with the commercial data. And the standard deviation for the peak temperatures is less than 0.02 ℃ and for the melting enthalpy it is less than 0.70 kJ/kg. Hence, it can be said that temperature equilibrium was attained during the thermal analysis. Finally, from the results obtained during the present analysis it can be said that there is a good repeatability of the sample behaviour for all the three sub-samples.

Table 10. Comparison bettween the experimental values (dynamic method) and the commercial values of RT 20

Sample name	Mass of the sample (mg)	Latent heat capacity given by manufacturer (kJ/kg) (Table 9)	Enthalpy values measured in present work using DSC (kJ/kg)		Melting temperature given by manufacturer (ºC) (Table 9)	Peak temperature values measured in present work using DSC (ºC)	
			Melting enthalpy*	Solidification enthalpy**		Melting point	Solidification point
RT 20-(A)-1D	15.41	172	128.24	163.63	22	21.89	21.00
RT 20-(A)-2D	15.41	172	127.54	162.14	22	21.90	21.01
RT 20-(A)-3D	15.41	172	127.08	161.26	22	21.87	21.03
RT 20-(B)-1D	15.38	172	127.89	160.63	22	21.92	20.96
RT 20-(B)-2D	15.38	172	128.43	161.93	22	21.89	20.98
RT 20-(B)-3D	15.38	172	129.06	162.18	22	21.91	21.01
RT 20-(C)-1D	15.41	172	127.27	160.41	22	21.88	21.00
RT 20-(C)-2D	15.41	172	127.23	160.99	22	21.90	20.98
RT 20-(C)-3D	15.41	172	127.22	160.79	22	21.89	21.00
Average values	-----	172	127.77	161.55	22	21.89	21
Standard deviation	-----	-----	0.64	0.96	-----	0.014	0.019

*Phase change range = 7.5 to 24.5 ºC
**Phase change range = 25.5 to 5 ºC

7.3.1.1.2 Step method results

Output results of the step method of RT 20 (D) for all three cycles obtained using DSC star[e] software are presented in Figure 35. The phase change area of each cycle was integrated and the temperature and enthalpy values were obtained by integrating the melting and the solidification peaks. For an example integrated first sample cycle D − 1S (where, S = step method cycle) is presented with melting and solidification enthalpy values in Figure 36. Extracted specific heat values as a function of temperature obtained with the step method are presented in Figure 37. The enthalpy values were obtained by the derivation of the specific heat values and are presented in Figure 38 . It can be seen that there is a very small temperature difference between melting and solidification temperatures and the melting and solidification temperatures are congruent for the three cycles.

The hysteresis area between the melting and the solidification enthalpy value has been decreased during the step method analysis and that can be seen in the comparison between the dynamic and step method analysis (Figure 39). Hence, it is proved that the step method is more accurate method than the dynamic method.
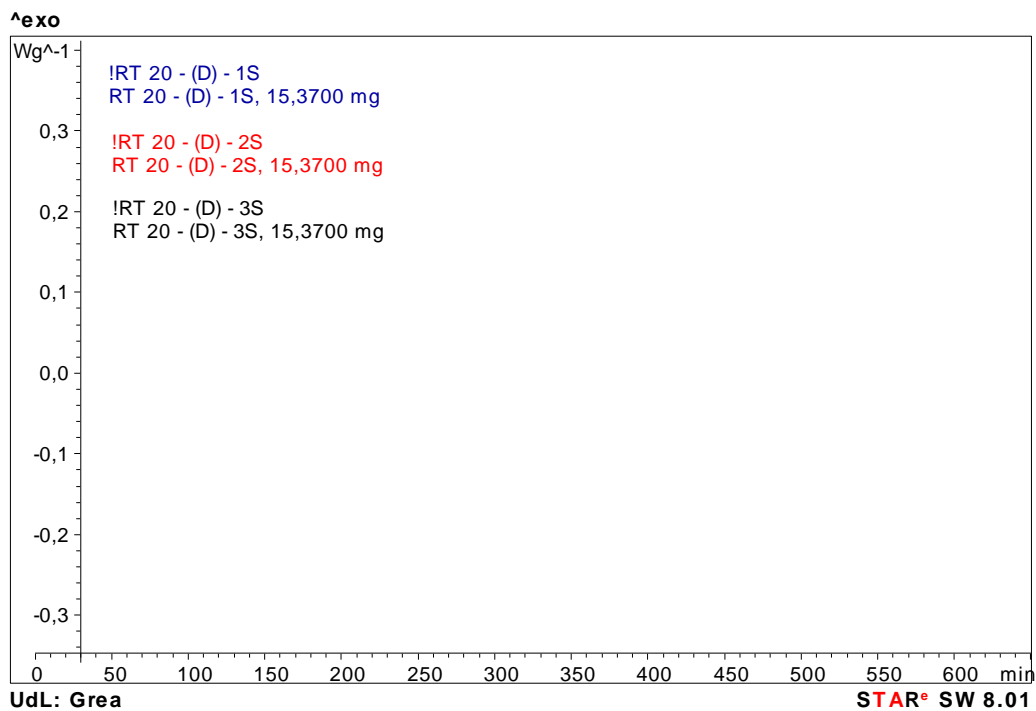

Figure 35. Heat flow vs. time of RT 20 for the three cycles using step method
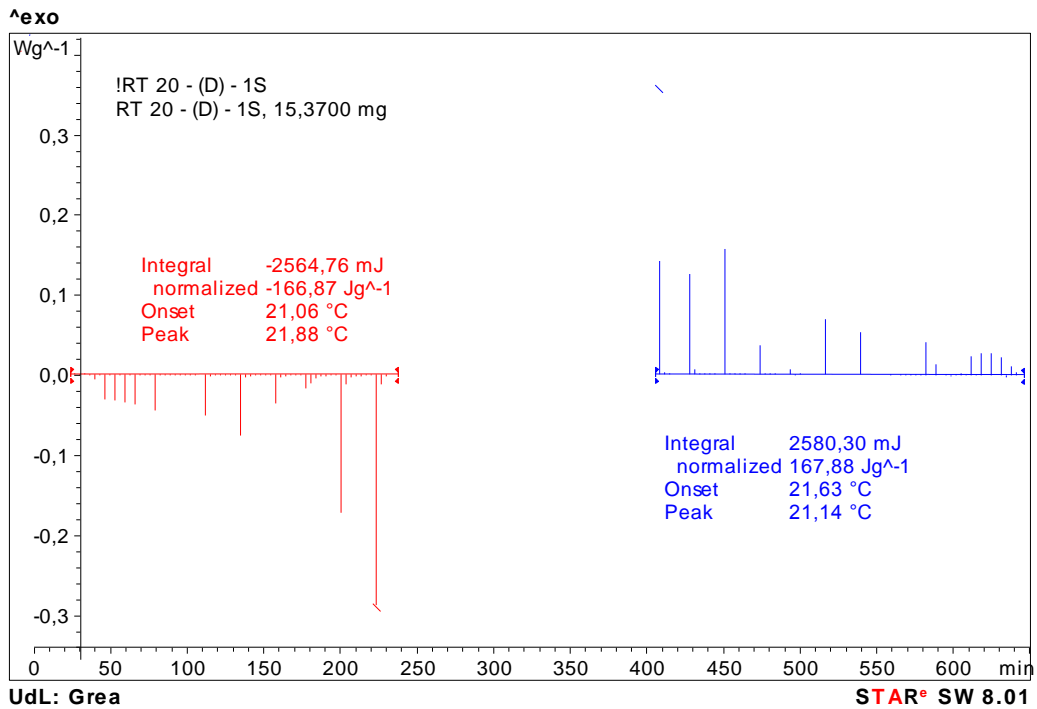
Figure 36. Heat flow vs. time and enthalpy values (left to right: melting and solidification) during phase change temperature range (7 to 22 ºC for melting and 22 to 5 ºC for solidification process) for the first sample cycle (D-1S) of RT 20 using step method
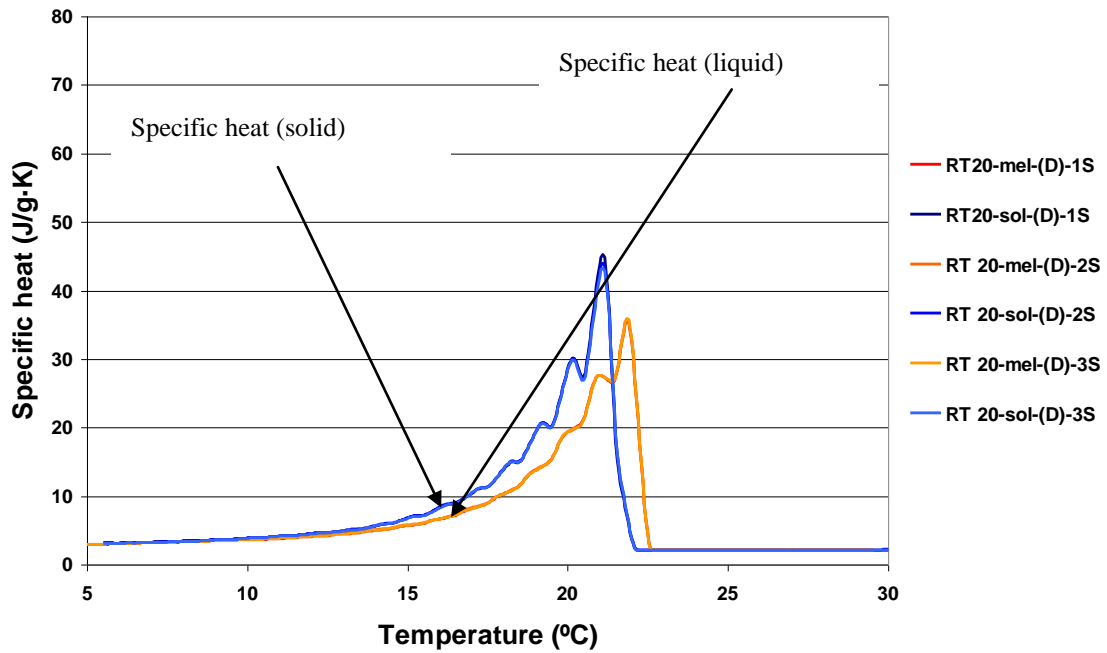

Figure 37. Specific heat as a function of tempeature of RT 20 for three cycles (Step method)
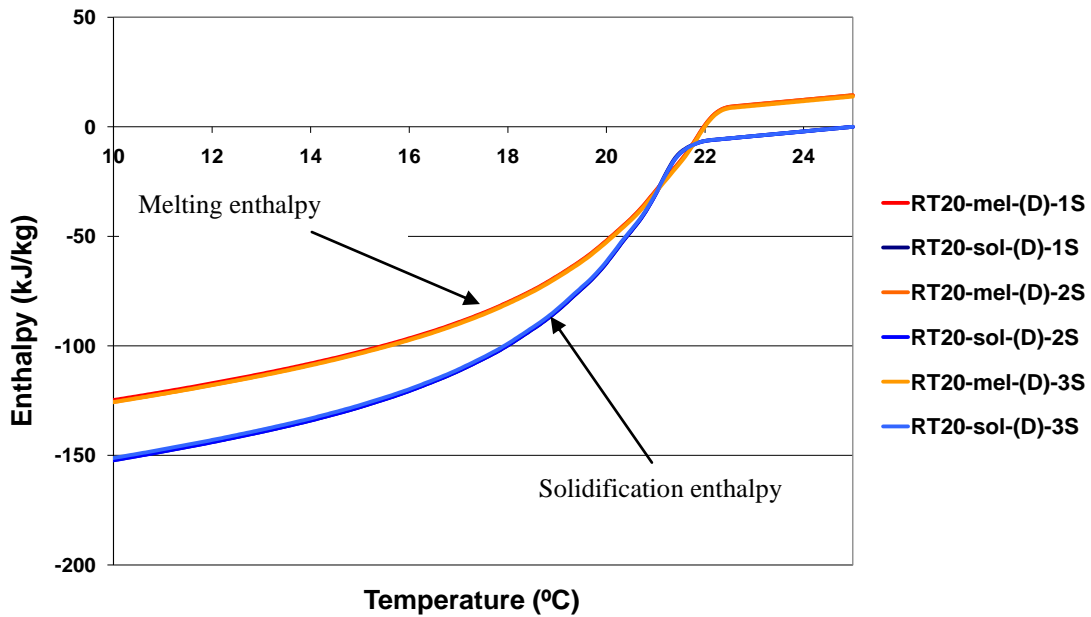
Figure 38. Enathalpy vs. temperature of RT 20 for the three cycles (Step method)
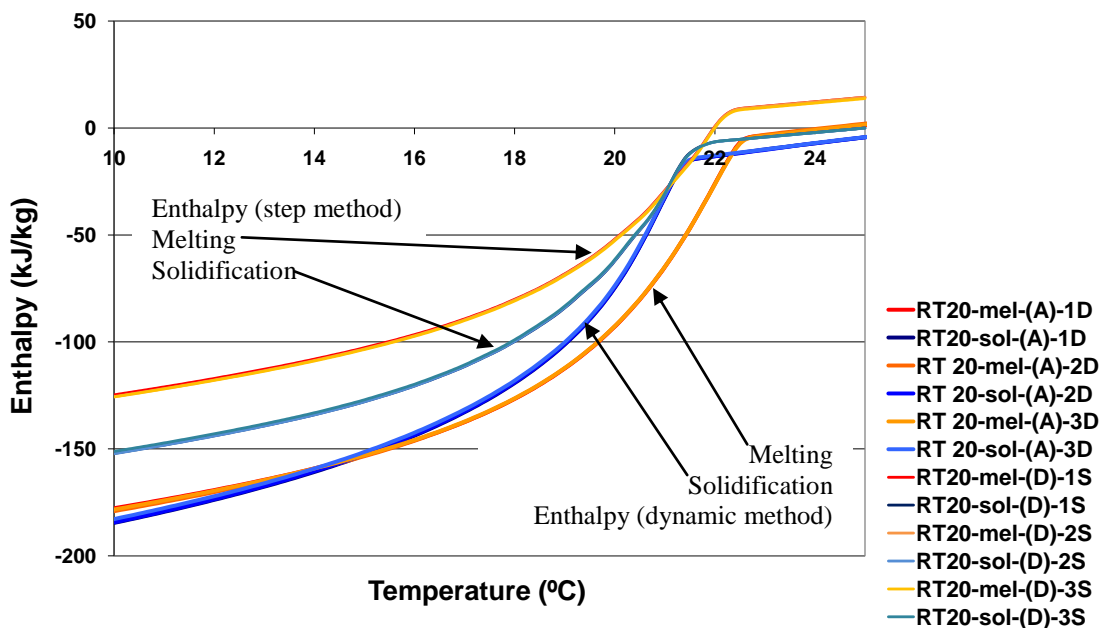
Figure 39. Comparison between dynamic and step method for enthalpy vs. temperature curves of RT 20

The experimental values for the enthalpy and melting and freezing temperatures obtained by the DSC software are presented in Table 11. The melting was started from 7 ºC and was ended at 22 ºC, hence the melting peaks of all the cycles were integrated within this phase change temperature range. While the solidification started from 22 ºC and ended at 5 ºC, therefore the solidification peaks for all the cycles were integrated

within this phase change temperature range. Table 11shows that the measured peak temperature values are identical to each other and these values are similar to the commercial data. Moreover, there is not a huge difference (around 5 kJ/kg) for the enthalpy values between experimental data (obtained by Mettler Toledo DSC822e) and commercial data. The average measured melting enthalpy is around 167 kJ/kg and the average measured melting tempeature is 21.88 ºC. The standard deviation obtained was nil. Hence, with this method it was possible to get good conformity for the enthalpy values and the temperature values with the commercial data.

Table 11. Comparison between the experimental values (step method) and the commercial values of RT 20

Sample name	Mass of the sample (mg)	Latent heat capacity given by manufacturer (kJ/kg) (Table 9)	Enthalpy values measured in present work using DSC (kJ/kg)		Melting temperature given by manufacturer (ºC) (Table 9)	Peak temperature values measured in present work using DSC (ºC)	
			Melting enthalpy*	Solidification enthalpy**		Melting point	Solidification point
RT 20-(D)-1S	15.37	172	166.87	167.88	22	21.88	21.14
RT 20-(D)-2S	15.37	172	167.79	170.21	22	21.88	21.14
RT 20-(D)-3S	15.37	172	167.80	168.18	22	21.88	21.14
Average values	15.37	172	167.49	168.75	22	21.88	21.14
Standard deviation	-----	-----	0.53	1.26	-----	0	0

*Phase change range = 7 to 22 ºC
**Phase change range = 22 to 5 ºC

7.3.1.2 Results of RT 27

7.3.1.2.1 Dynamic method results

Output results of the dynamic method of RT 27 for all sub-samples obtained using DSC star[e] software are presented in Figure 40. The enthalpy values and melting and solidification temperature values were obtained by integrating melting and solidification peaks and for an example, integrated sub-sample A − 1D (where, D = dynamic method cycle) is presented with melting and solidification enthalpy values in Figure 41. The experimental results of the specific heat values over temperature for RT 27 using dynamic method are presented in Figure 42. Figure 42 shows that there is no major difference in the specific heat for liquid phase and solid phase. The difference during

the heating and the cooling segments can be seen from the hysteresis (as seen in Figure 43) in the enthaly-temperature curves of the sample.

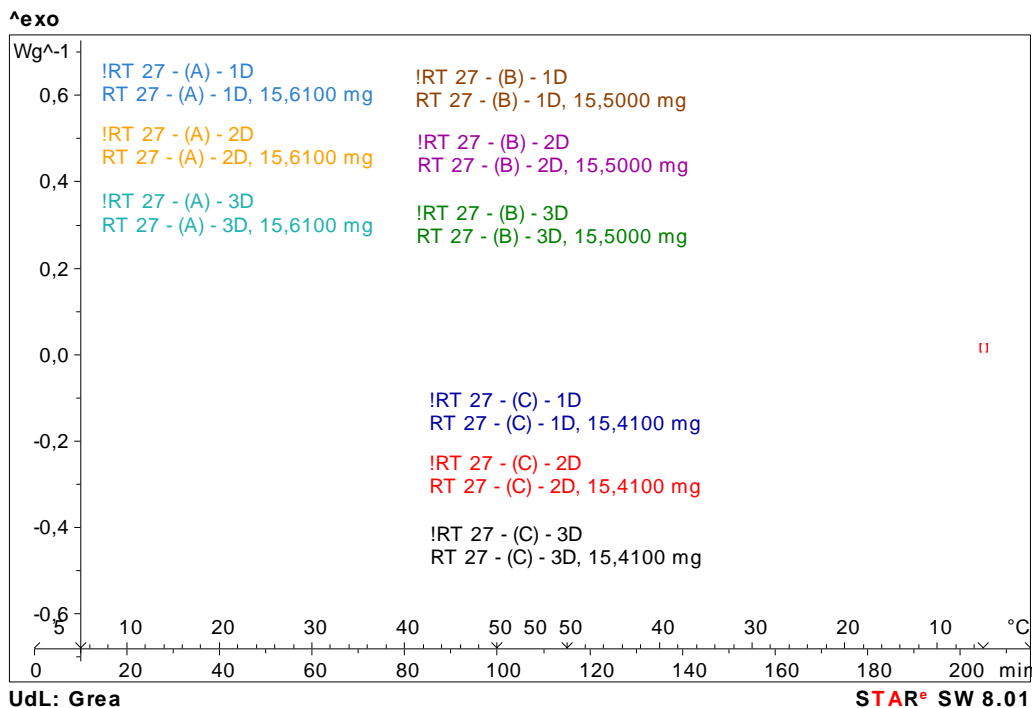**Figure 40. Heat flow vs. time and temperature of RT 27 for the three sub-samples (A, B and C with their three cycles) using dynamic method**
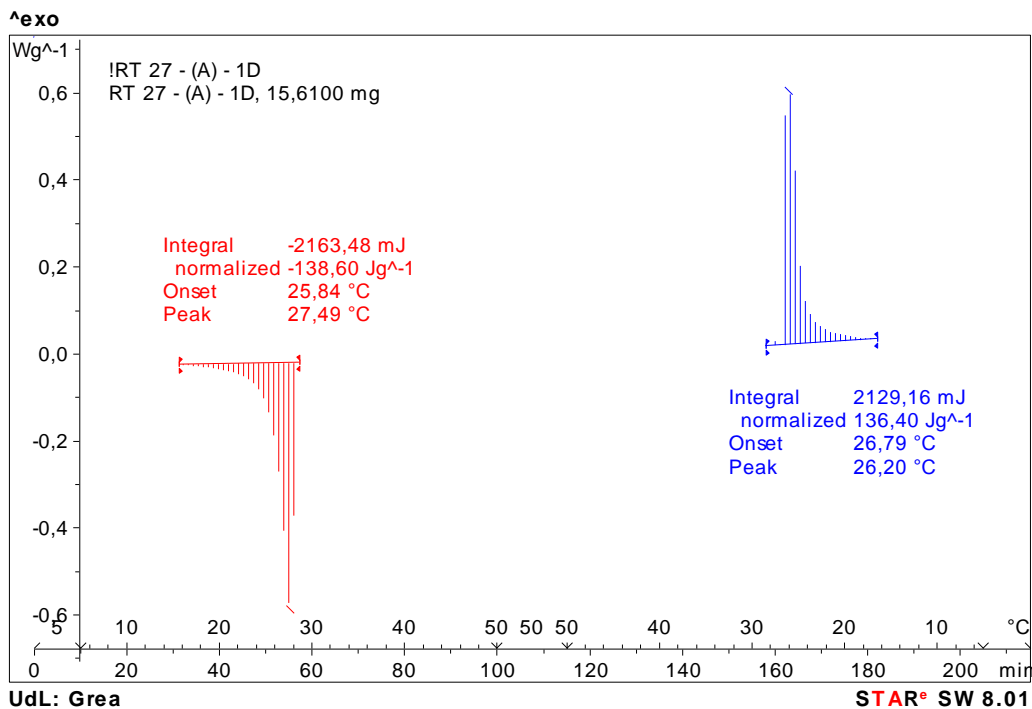

Figure 41. Heat flow vs. time and temperature and enthalpy values (left to right: melting and solidification) during phase change temperature range (15 to 28.65 ºC for melting and 28.5 to 16.5 ºC for solidification process) of sub-sample (A) of RT 27 using dynamic method
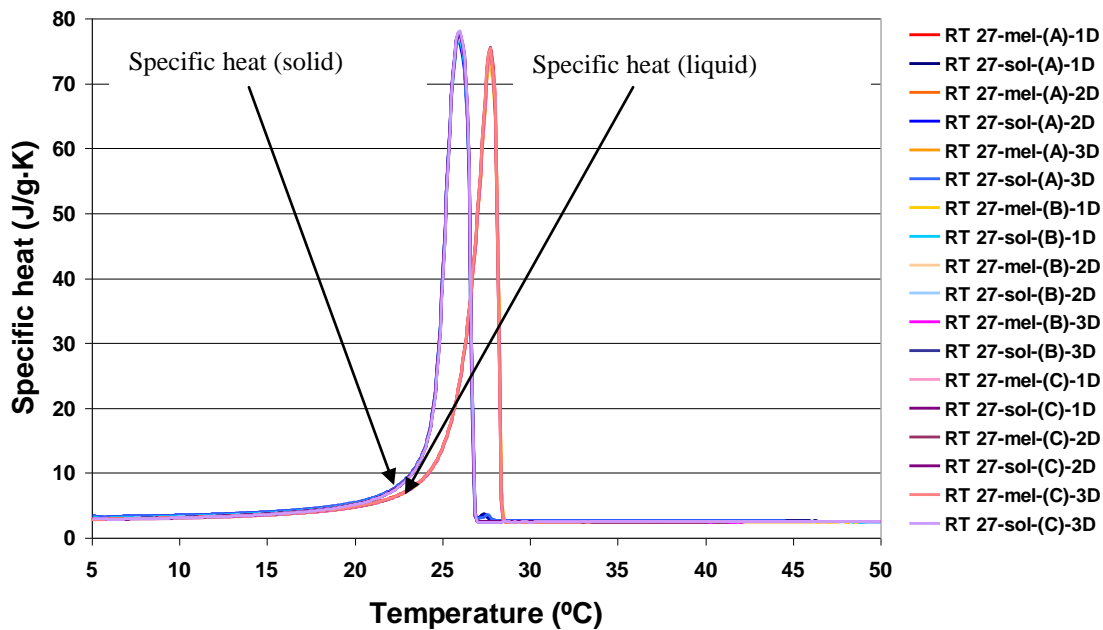
Figure 42. Specific heat vs. temperature of RT 27 for the three sub-samples (A, B and C) with three different cycles each (dynamic method)
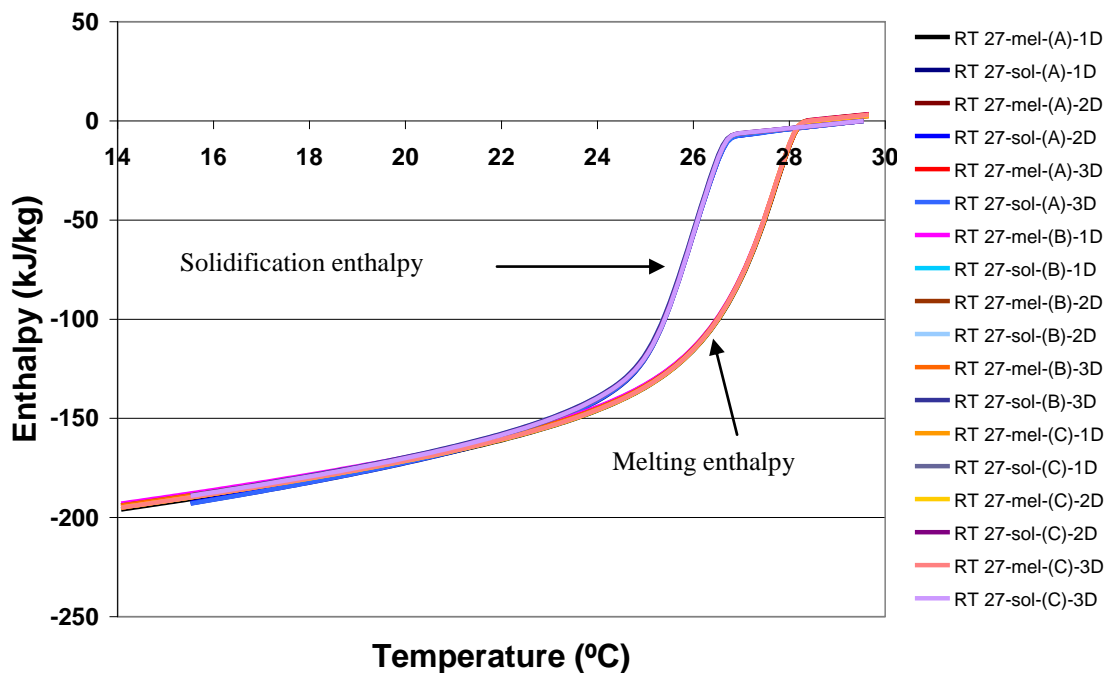
Figure 43. Enthalpy vs. temperature of RT 27 for the three sub-samples (A, B and C) with three different cycles each (dynamic method)

The experimental values for the enthalpy, and melting and freezing temperatures obtained with the DSC software compared to the commercial values are presented in Table 12. The melting was started from 15 ºC and ended at 28.65 ºC, hence the melting peaks of all the cycles of all the sub-samples were integrated within this phase change

temperature range. While the solidification started from 28.5 ℃ and ended at 16.5 ℃, therefore the solidification peaks for all the cycles of all the sub-samples were integrated within this phase change temperature range. Table 12 shows that the measured melting temperatures for all cycles are slightly higher (around 27.47 ℃) than the commercial melting temperature (27 ℃), while the solidification temperature is a little lower (26.22 ℃) than the commercial congealing temperature (27 ℃). But that is not significant because both measured melting and solidification temperatures are within the melting area (25-28 ℃) and congealing area (28-25 ℃) provided by the manufacturer and standard deviation of temperature for all cycles was less than 0.02 ℃. Thus, the DSC shows good agreement for temperature values. The average measured melting enthalpy within above mentioned phase change temperature range is around139 kJ/kg which is less than (around 45 kJ/kg) the commercial enthalpy value (184 kJ/kg). This difference of enthalpy values between the commercial value and the experimental value could be because of the used analyzing equipment and its sensitivity, and the selected phase change range for the integration of peak area. The standard deviation of all cycles for the enthalpy was less than 0.50 kJ/kg. After analyzing three sub-samples and their total nine cycles, it could be said that the repeatability of the results is assured.

Table 12. Comparison between the experimental values (dynamic method) and the commercial values of RT 27

Sample name	Mass of the sample (mg)	Latent heat capacity given by manufacturer (kJ/kg) (Table 9)	Enthalpy values measured in present work using DSC (kJ/kg)		Melting temperature given by manufacturer (ºC) (Table 9)	Peak temperature values measured in present work using DSC (ºC)	
			Melting enthalpy*	Solidification enthalpy**		Melting point	Solidification point
RT 27-(A)-1D	15.61	184	138.60	136.40	27	27.49	26.20
RT 27-(A)-2D	15.61	184	138.94	135.74	27	27.49	26.19
RT 27-(A)-3D	15.61	184	139.16	135.94	27	27.48	26.20
RT 27-(B)-1D	15.50	184	138.59	135.38	27	27.45	26.23
RT 27-(B)-2D	15.50	184	138.89	135.69	27	27.48	26.24
RT 27-(B)-3D	15.50	184	138.79	135.48	27	27.48	26.23
RT 27-(C)-1D	15.41	184	139.71	136.45	27	27.48	26.23
RT 27-(C)-2D	15.41	184	139.73	136.49	27	27.48	26.23
RT 27-(C)-3D	15.41	184	139.79	136.51	27	27.46	26.22
Average values	-----	184	139.13	136.00	27	27.47	26.22
Standard deviation	-----	-----	0.46	0.43	-----	0.012	0.016

*Phase change range = 15 to 28.65 ºC
**Phase change range = 28.5 to 16.5 ºC

7.3.1.2.2 Step method results

Output results of the step method of RT 27 (D) for all three cycles obtained using DSC star[e] software are presented in Figure 44. These outputs were integrated during phase change temperature range and for an example, integrated first cycle D – 1S (where, S = step method cycle) with melting and solidification enthalpy as well as temperature values is presented in Figure 45. The experimental results of the specific heat values over temperature for RT 27 using step method are presented in Figure 46. It can be seen in Figure 46, that the specific heat values for liquid phase and the solid phase are similar. The enthalpy values were obtained by the derivation of the specific heat values, and are presented over temperature in Figure 47 which shows the hysteresis. The area of the hysterisis loop has been decreased during the step method compared to the dynamic mehtod and that can be seen in Figure 48.
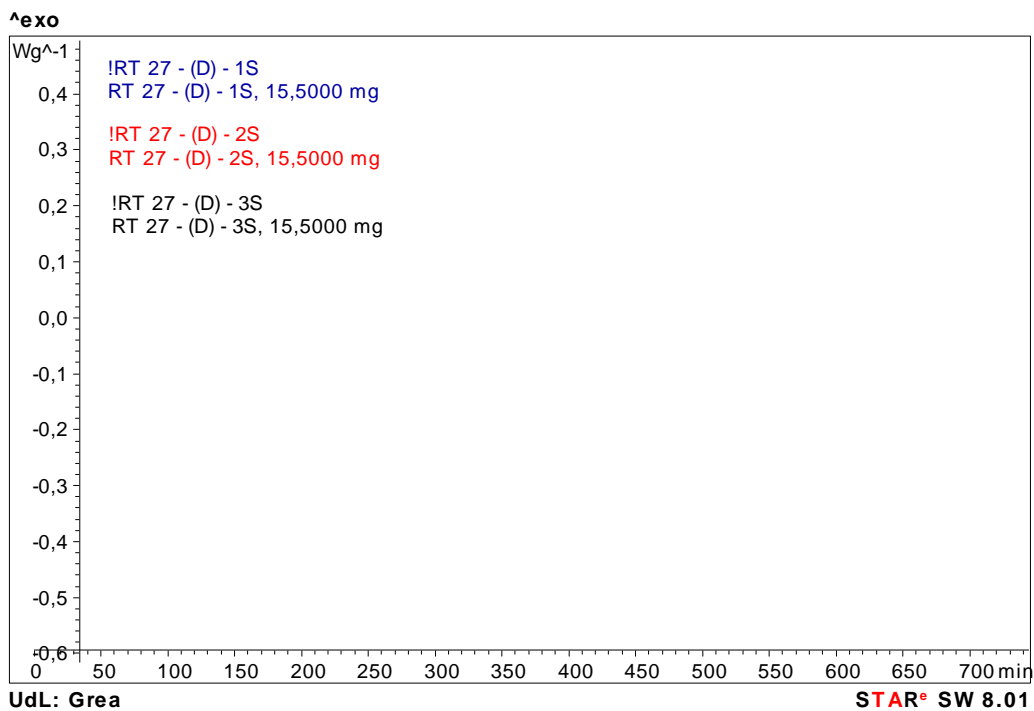
Figure 44. Heat flow vs. time of RT 27 for three cycles using step method
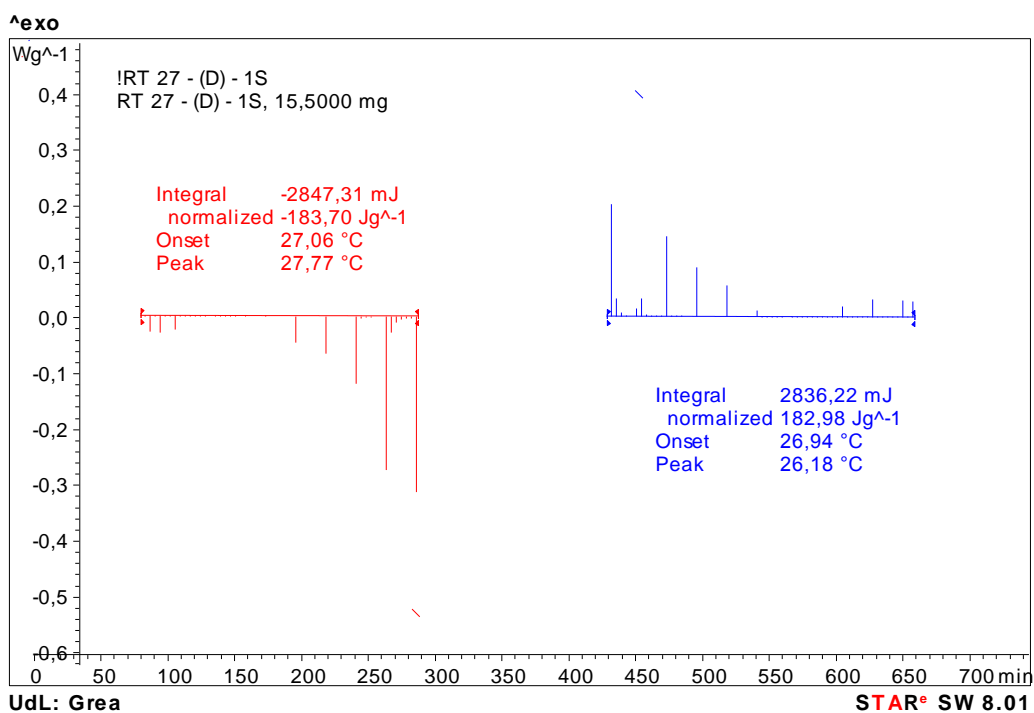
Figure 45. Heat flow vs. time and enthalpy and temperature values (left to right: melting and solidification) during phase change temperature range (15 to 28 ºC for melting and 28 to 16 ºC for solidification process) of the first cycle of sample D of RT 27 using step method

Figure 46. Specific heat vs. temperature of RT 27 for the three different cycles (step method)

Figure 47. Enthalpy vs. temperature of RT 27 for the three different cycles (step method)

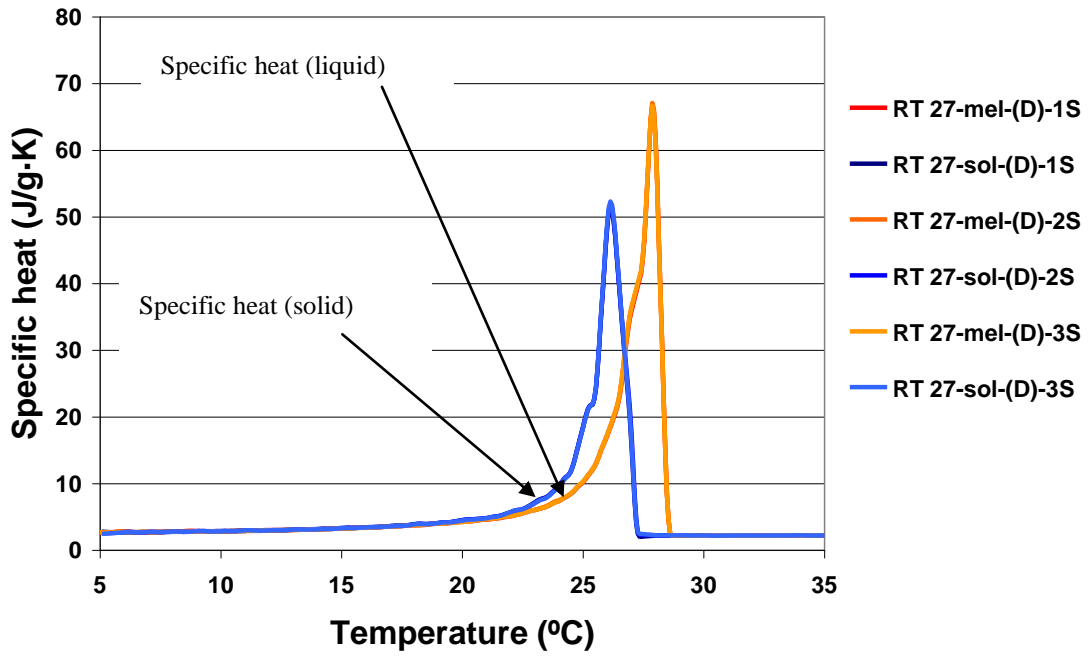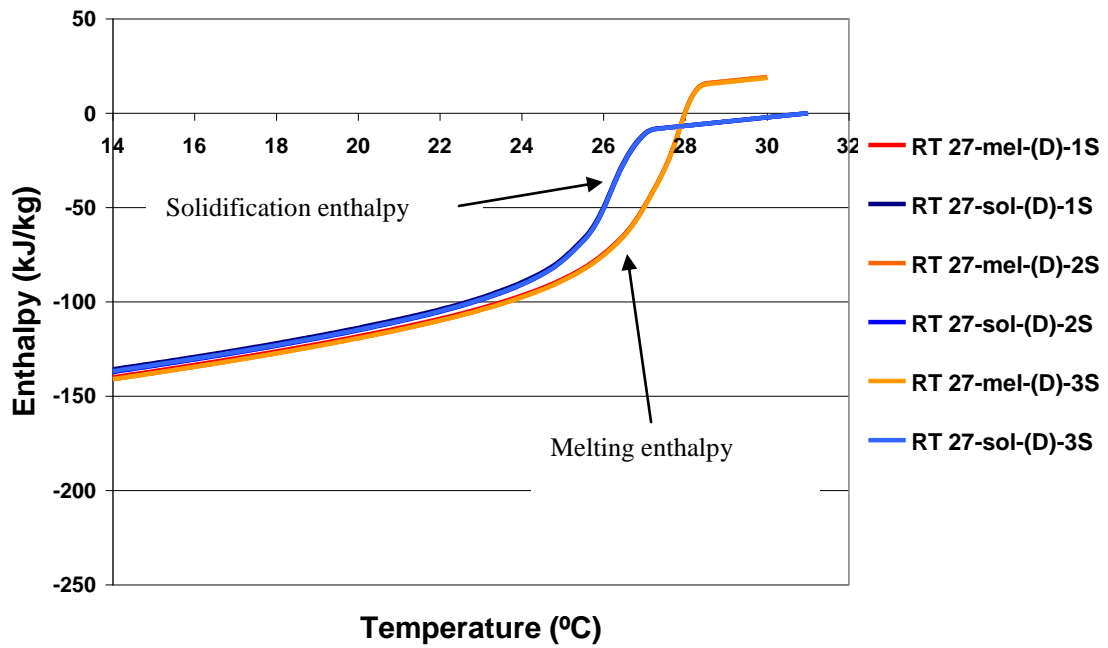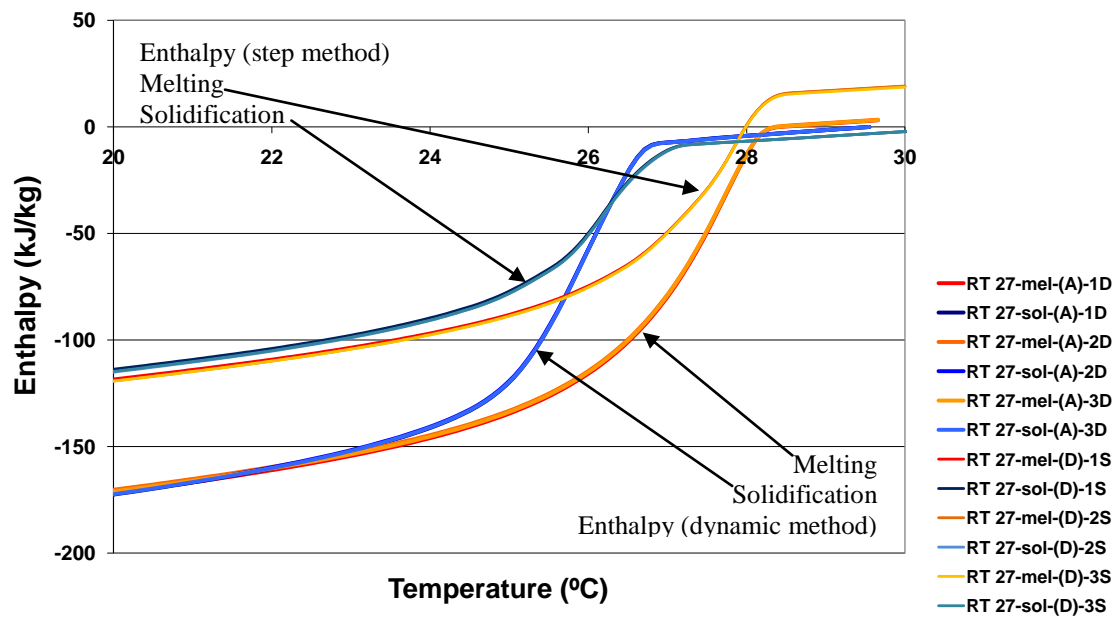**Figure 48. Comparison between dynamic and step method enthalpy vs. temperature curves of RT 27**

Table 13 shows the comparison of the experimental values and the commercial values of RT 27. In this case, the melting was started from 15 ºC and ended at 28 ºC and the solidification started from 28 ºC and ended at 16 ºC, hence the melting and solidification peaks for all cycles were integrated within this phase change temperature range. Table 13 shows that the average measured melting temperature is slightly higher (27.77 ºC) than the commercial melting temperature value (27 ºC) while the average measured solidification temperature (26.18 ºC) is lower than the commercial congealing temperature (27 ºC). But the temperature values are within the temperature ranges provided by the manufacturer (Table 9). Using this method it is possible to get enthalpy values almost similar to the commercial data. And the standard deviation for the temperature values is very low (being 0.005 ºC). It proves that the DSC shows good agreement with the commercial data for the thermophysical properties such as specific heat values, enthalpy values and the temperature values. These values are almost identical for the three cycles; therefore DSC shows good repeatability of the results.

Table 13. Comparison between the experimental values (step method) and the commercial values of RT 27

Sample name	Mass of the sample (mg)	Latent heat capacity approximate (kJ/kg) (Table 9)	Measured DSC enthalpy (kJ/kg)		Typical melting temperature (ºC) (Table 9)	Measured DSC temperature peak (ºC)	
			Melting enthalpy*	Solidification enthalpy**		Melting point	Solidification point
RT 27-(D)-1S	15.50	184	183.70	182.98	27	27.77	26.18
RT 27-(D)-2S	15.50	184	184.81	183.31	27	27.77	26.19
RT 27-(D)-3S	15.50	184	184.59	181.68	27	27.78	26.19
Average values	-----	184	184.36	182.65	27	27.77	26.18
Standard deviation	-----	-----	0.58	0.86	-----	0.005	0.005

*Phase change range = 15 to 28 ºC
**Phase change range = 28 to 16 ºC

7.3.1.3 Conclusions

Temperature values:

From the above presented paraffin results for the dynamic method (Figure 31, Figure 33, Figure 40, Figure 42) it could be concluded that the melting and freezing temperatures show small variation and the standard deviation is in the range of 0.01-0.02 ºC (Table 10 and Table 12).

The temperature values are identical during the mentioned three step method cycles for RT 20 and the standard deviation is nil (Table 11). Whereas, for RT 27 the resulting temperature values with the step method shows negligible variation giving a standard deviation of 0.005 ºC (Table 13), which is significantly small. Moreover the overall temperature values for both the methods are within the temperature range provided by the manufacturer.

Hysteresis in the enthalpy-temperature curve:

RT 20 and RT 27 samples show the hysteresis also during the step method analysis. But the area of the hysteresis during the step method is small compared to the dynamic method. That can be seen in Figure 39 and Figure 48. That also proves that the reason for the hysteresis is the applied method. Reasons for the hysteresis could be slow

formation of the crystal lattice or the diffusion process (which is necessary to homogenize the sample).

Enthalpy values:

For RT 20, the obtained heating enthalpy during the dynamic method is around 128 kJ/kg (Table 10). That is significantly less than the commercial value (172 kJ/kg). Whereas, the melting enthalpy obtained using the step method is about 168 kJ/kg (Table 11). That is quite closer to the commercial value (172 kJ/kg). And for RT 27, the obtained heating enthalpy is 140 kJ/kg (Table 12) during the dynamic method, which is significantly lower than the commercial value (184 kJ/kg). Whereas, the enthalpy value obtained using the step method is nearly 184 kJ / kg (Table 13), which is quite closer to the commercial value. Thus the enthalpy values obtained by the step method are closer to the commercial data.

The difference in the values using different methods for the same sample shows the effect of the mechanism of the applied methods. The dynamic method involves continuous heating and cooling while the step method incorporates slow heating and cooling of the sample followed by the non-reaction (heating/cooling) time period to assure the thermal equilibrium and reaction equilibrium before and at the end of each heating/cooling segment. Hence, the results obtained using the step method are more reliable compared to the dynamic method. Simultaneously the good repeatability is also obtained and that can be said from the minor standard deviation values (Table 10-Table 13). The step method was proved as comparatively more accurate method.

7.3.2 Results of salt hydrate samples

7.3.2.1 Results of SP 22 A17

Dynamic method results

Output results of dynamic method of SP 22 A17 for all sub-samples (A, B and C) obtained using DSC star[e] software are presented in Figure 49. The stored energy during the melting and the solidification was obtained by integrating melting and solidification peaks. This is shown in Figure 50, in which, first cycle of sub-sample A is integrated (A – 1D, where D = dynamic method cycle) for melting part (during 6.75-21 ºC) and

solidification part (during 50-5 ºC). The integration during mentioned phase change range gave melting enthalpy of 1.69 kJ/kg and solidification enthalpy of 52.54 kJ/kg. Which is significantly lower than the commercial value (150 kJ/kg).

The experimental results of the specific heat values over temperature and enthalpy values (derived from the specific heat values) as a function of the temperature for SP 22 A17 are presented in Figure 51 and Figure 52 using dynamic method. All nine cycles of three sub-samples of the SP 22 A17 presented almost similar behaviour.
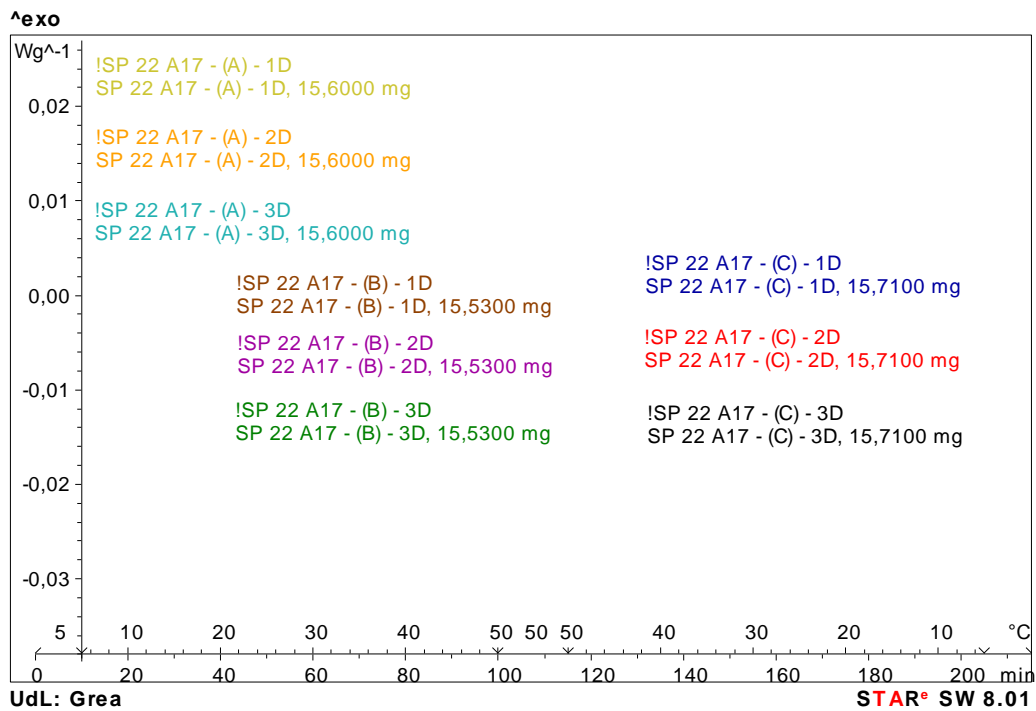
Figure 49. Heat flow vs. time and temperature of SP 22 A17 for three sub-samples (A, B and C with their cycles) using dynamic method
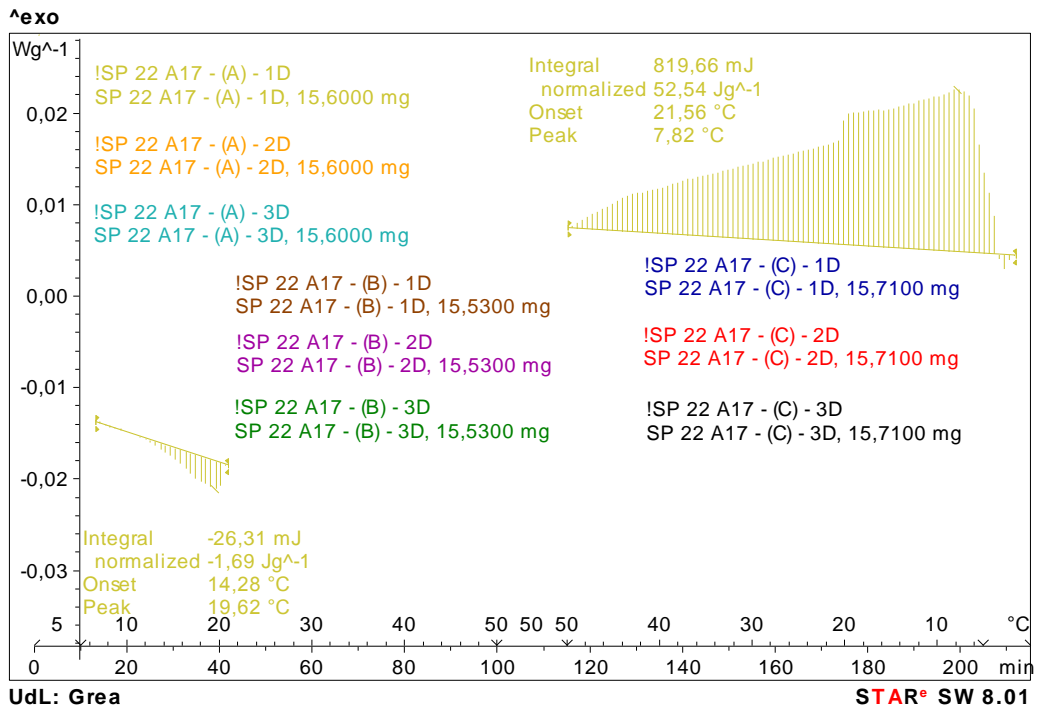
Figure 50. Heat flow vs. time and temperature and enthalpy and temperature values (left to right: melting and solidification) during phase change temperature range (6.75 to 21 ºC for melting and 50 to 5 ºC for solidification process) of the first cycle of sample A of SP 22 A17 using dynamic method
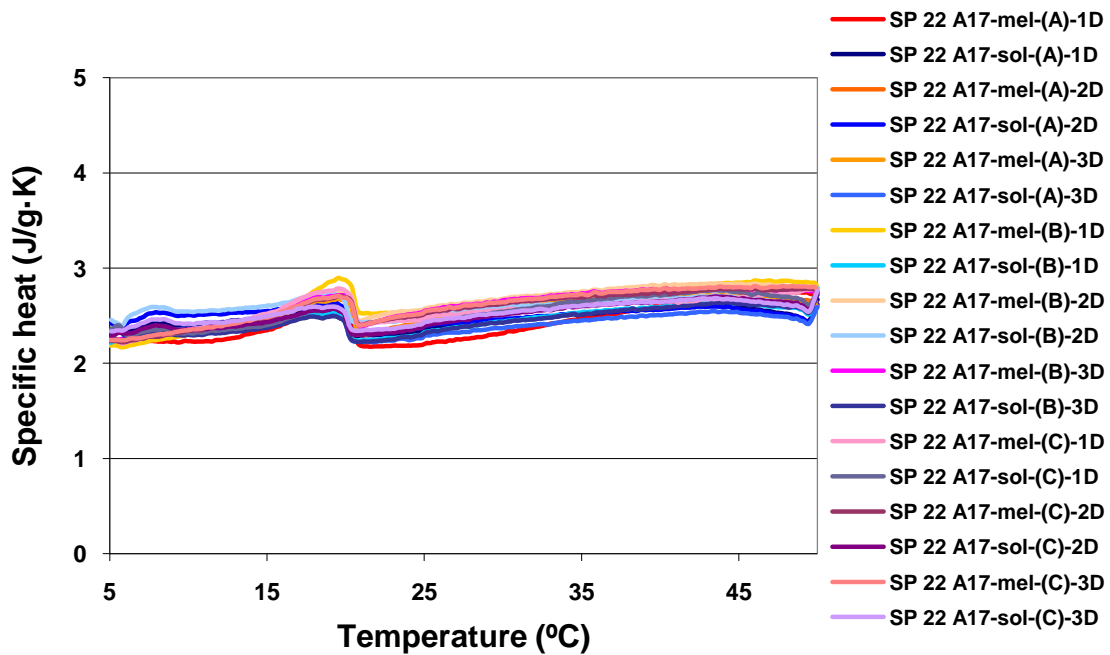

Figure 51.Specific heat vs. temperature of SP 22 A17 for three sub-samples (A, B and C) with three different cycles each (dynamic method)
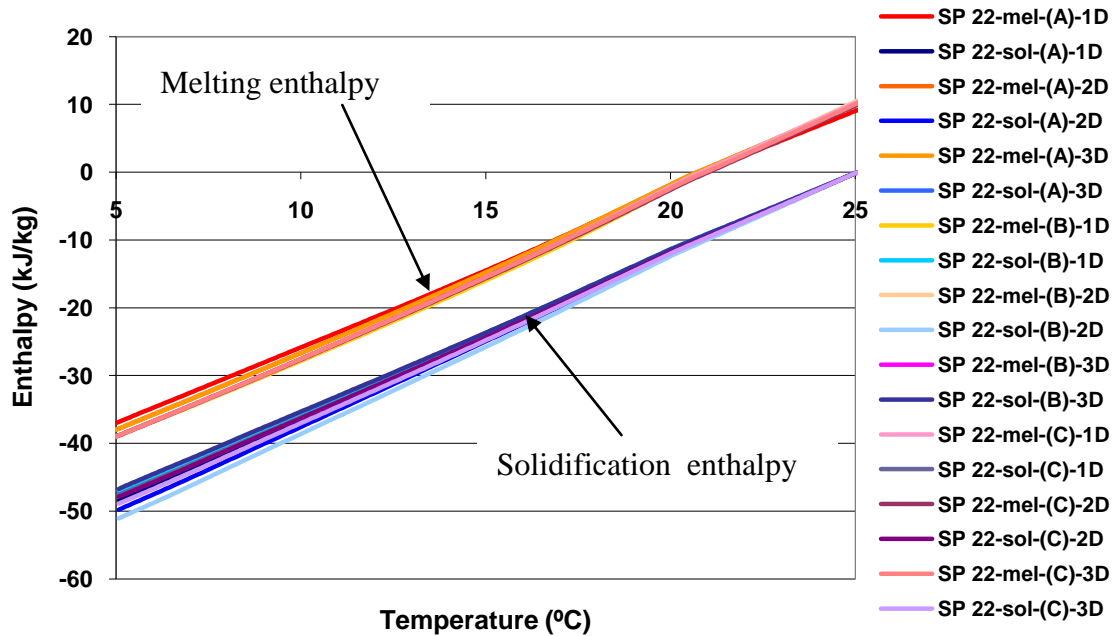
Figure 52. Enthalpy vs. temperature of SP 22 A17 for the three sub-samples (A, B and C) with three different cycles each (dynamic method)

Step method results

In the dynamic method analysis it was not possible to observe phase change. Hence, it was decided to analyze two sub-samples of SP 22 A17 using step method in order to check if its obtained behaviour using the dynamic method is correct or not. Output results of step method of SP 22 A17 for both sub-samples (D and E) obtained using DSC star[e] software are presented in Figure 53. The experimental results of the specific heat values over temperature and enthalpy values (derived from the specific heat values) as a function of the temperature for SP 22 A17 are presented in Figure 54 and Figure 55 for the step method. All six cycles of the two sub-samples of the SP 22 A17 presented almost similar behaviour. The phase change can not be observed in all three Figure 53, Figure 54 and Figure 55 during all six cycles of both sub-samples.
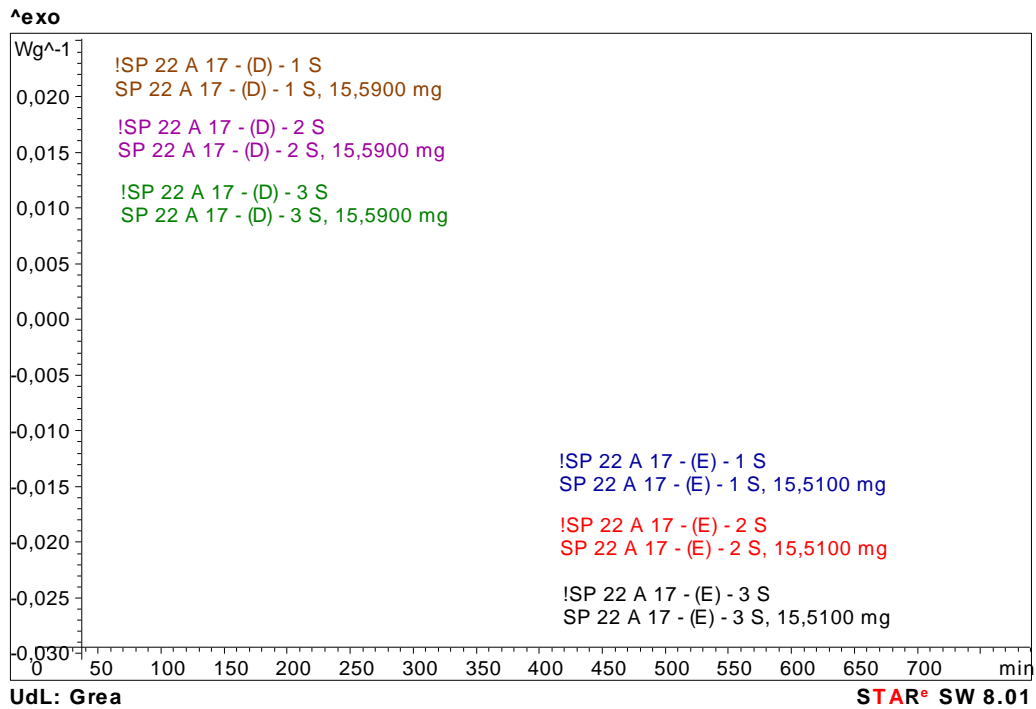
Figure 53. Heat flow vs. time of SP 22 A17 for two sub-samples (D and E with their cycles) using step method
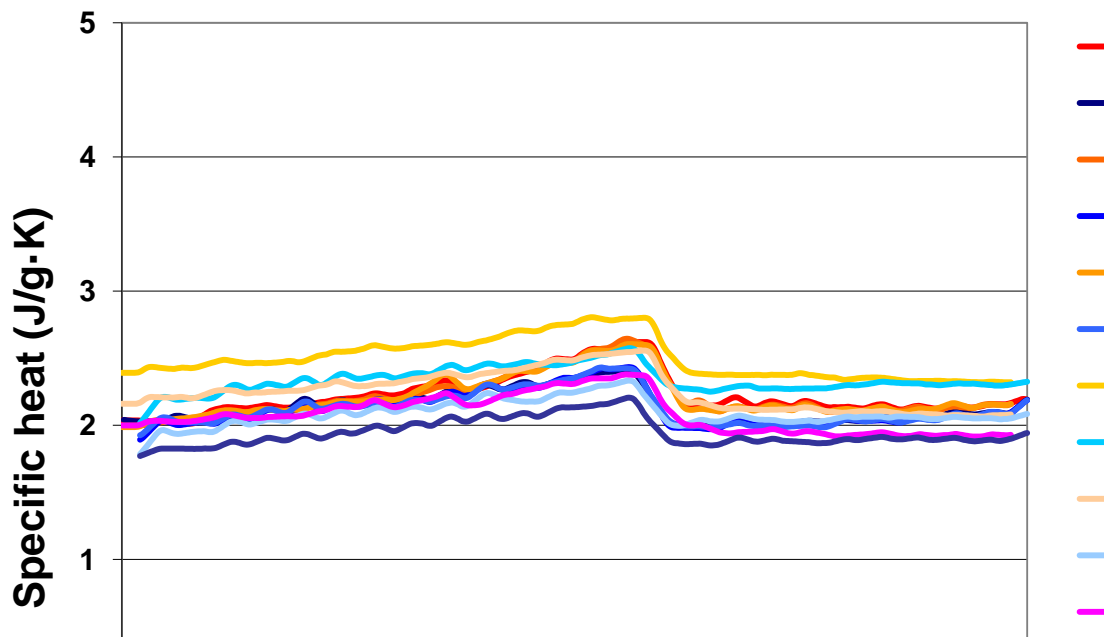

Figure 54. Specific heat vs. temperature of SP 22 A17 for the two sub-samples (D and E) with three different cycles each (step method)
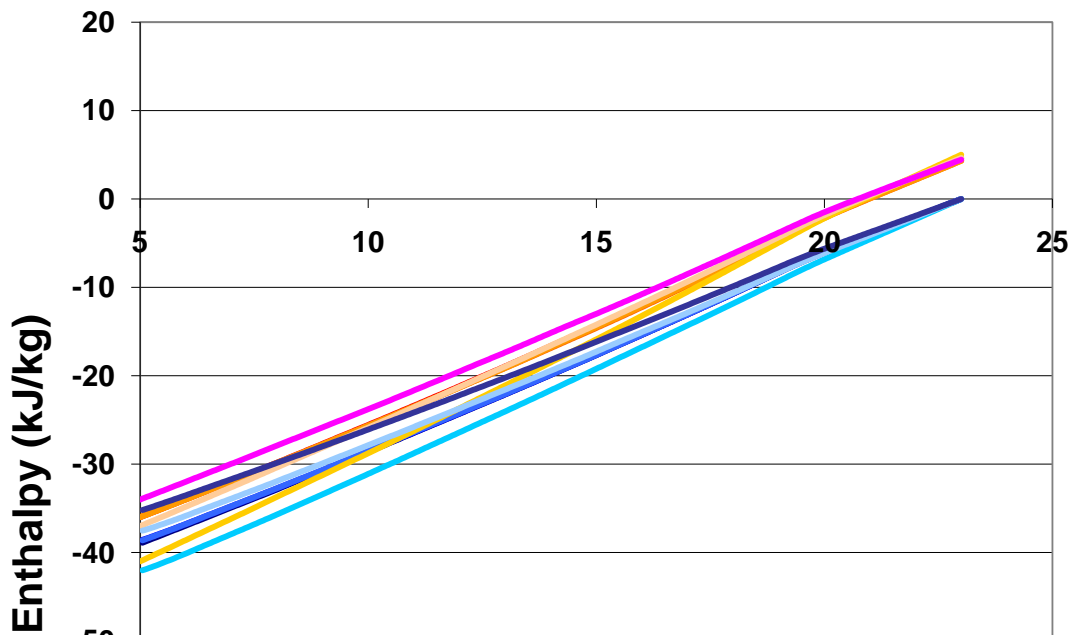
Figure 55. Enthalpy vs. temperature of SP 22 A17 for the two sub-samples (D and E) with three different cycles each (step method)

7.3.2.2 Results of sample SP 25 A8

Dynamic method results

Output results of dynamic method of SP 25 A8 for all sub-samples (A, B and C) obtained using DSC star[e] software are presented in Figure 56. In Figure 57, first cycle of sub-sample A is integrated (A – 1D, where D = dynamic method cycle) for melting part (during 7-32 ºC) and solidification part (during 32-6.6 ºC). The integration during mentioned phase change range gave melting enthalpy of 12.01 kJ/kg and solidification enthalpy of 13.66 kJ/kg. This is significantly lower than the commercial value (180 kJ/kg).

The experimental results of the specific heat values over temperature and enthalpy values (derived from the specific heat values) as a function of the temperature for SP 25 A8 are presented in Figure 58 and Figure 59 for the dynamic method. The phase change can not be observed from all four figures Figure 56, Figure 57, Figure 58 and Figure 59.

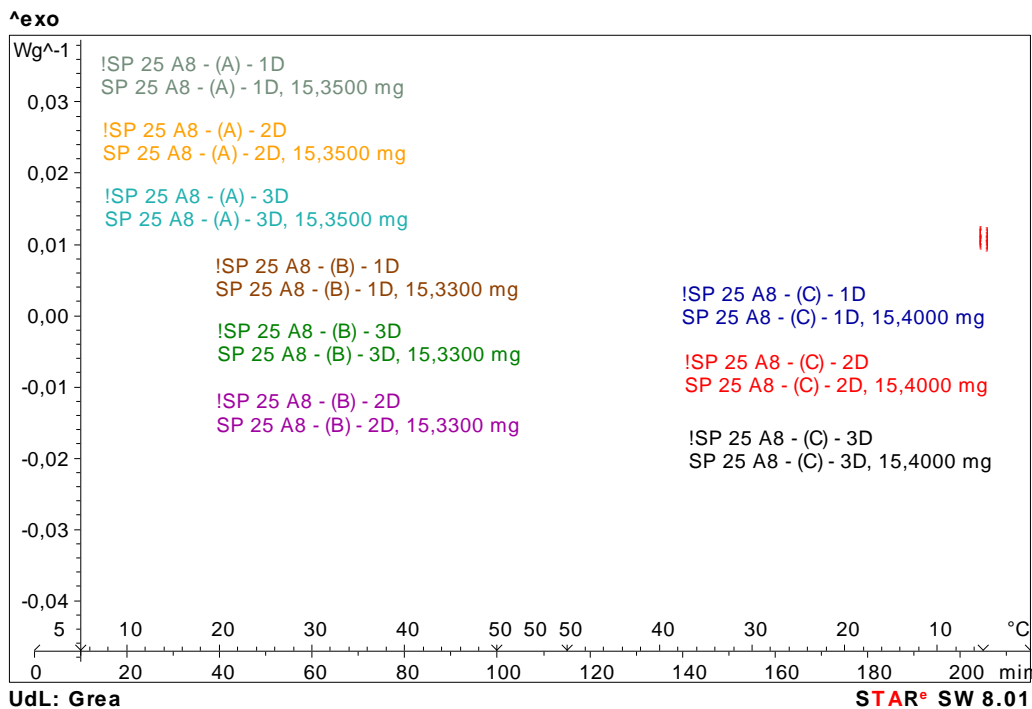**Figure 56. Heat flow vs. time and temperature of SP 25 A8 for two sub-samples (D and E with their cycles) using dynamic method**
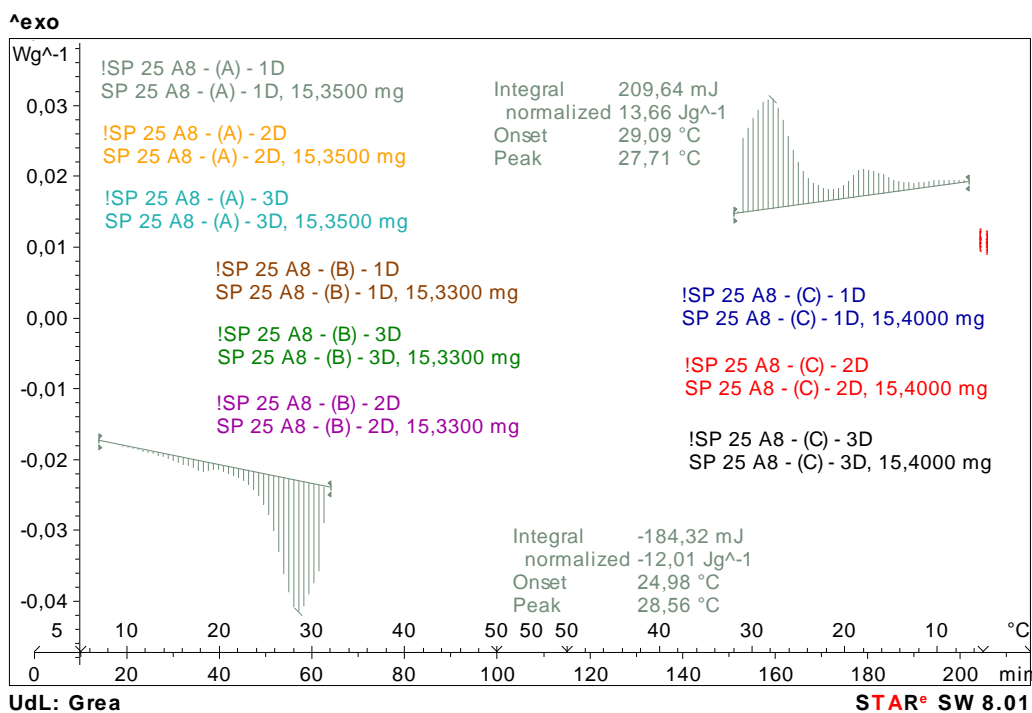

Figure 57. Heat flow vs. time and temperature and enthalpy and temperature values (left to right: melting and solidification) during phase change temperature range (7 to 32 ºC for melting and 32 to 6.6 ºC for solidification process) of the first cycle of sample A of SP 25 A8 using dynamic method
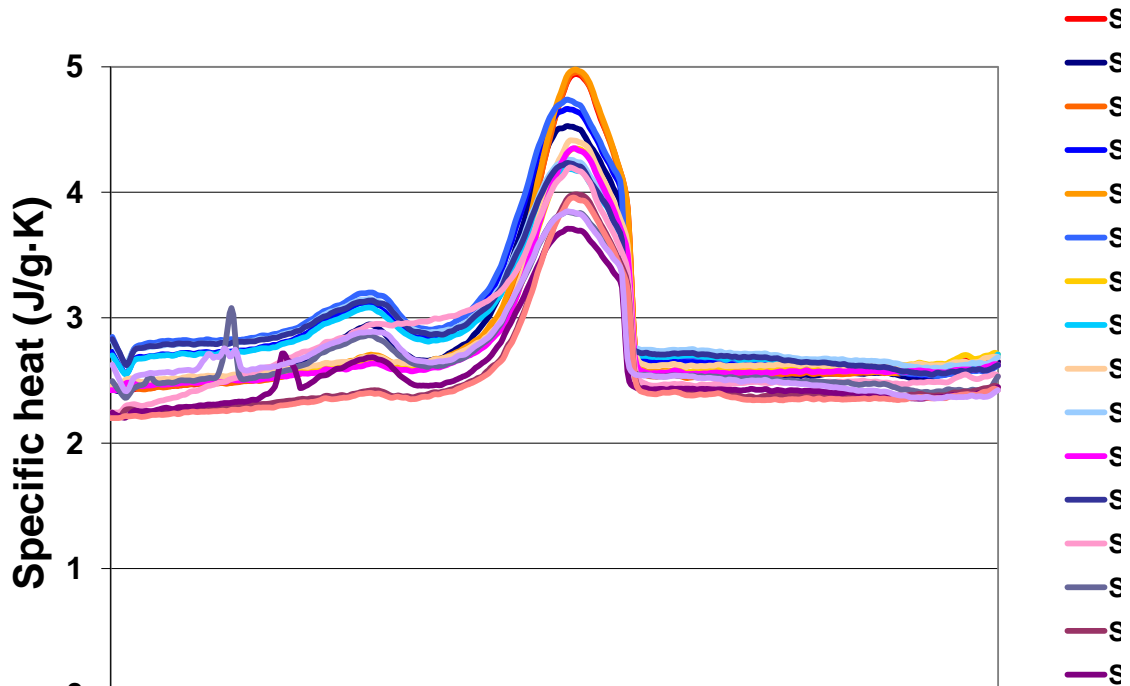
Figure 58. Specific heat vs. temperature of SP 25 A8 for the three sub-samples (A, B and C) with three different cycles each (dynamic method)
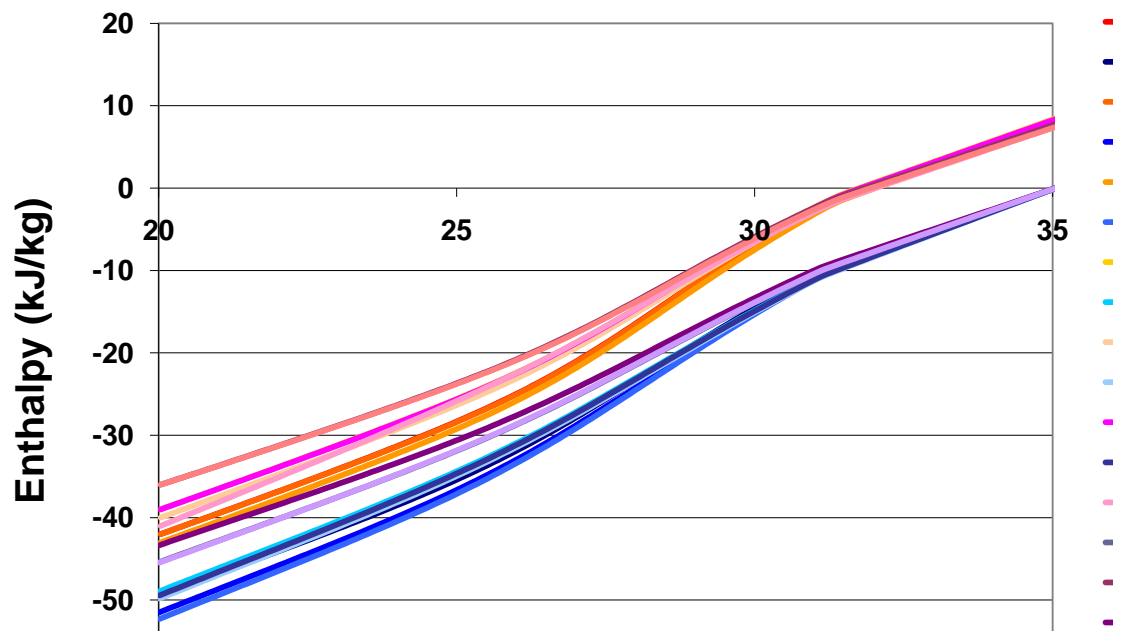
Figure 59. Enthalpy vs. temperature of SP 25 A8 for the three sub-samples (A, B and C) with three different cycles each (dynamic method)

Step method results

After analyzing SP 25 A8 with dynamic method it was again analyzed using the same dynamic method to confirm its thermal behaviour. Consequently, step method program was created with 20 min of isostep mode to achieve steps during melting and solidification. Output results of step method of SP 25 A8 for three cycles obtained using

DSC star[e] software are presented in Figure 60. The experimental results of the specific heat values over temperature and enthalpy values (derived from the specific heat values) as a function of the temperature for SP 25 A8 are presented in Figure 61 and Figure 62 for the step method. All three cycles of the SP 25 A8 presented almost similar behaviour. The phase change can not be observed in all three cycles (Figure 60).

Figure 60. Heat flow vs. time of SP 25 A8 for three cycles using step method

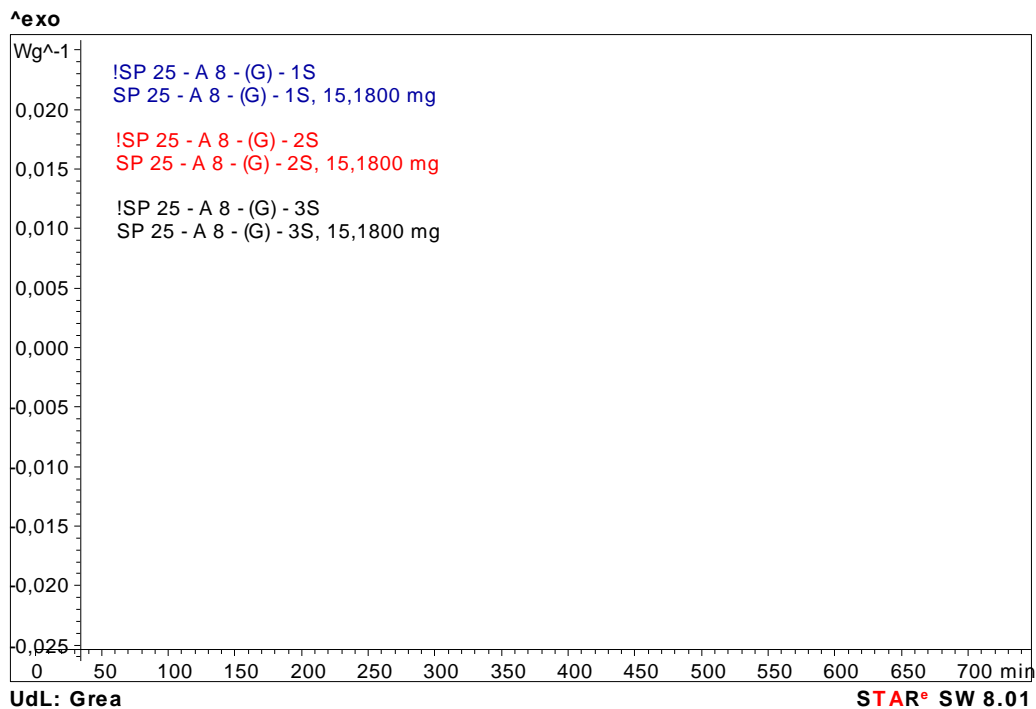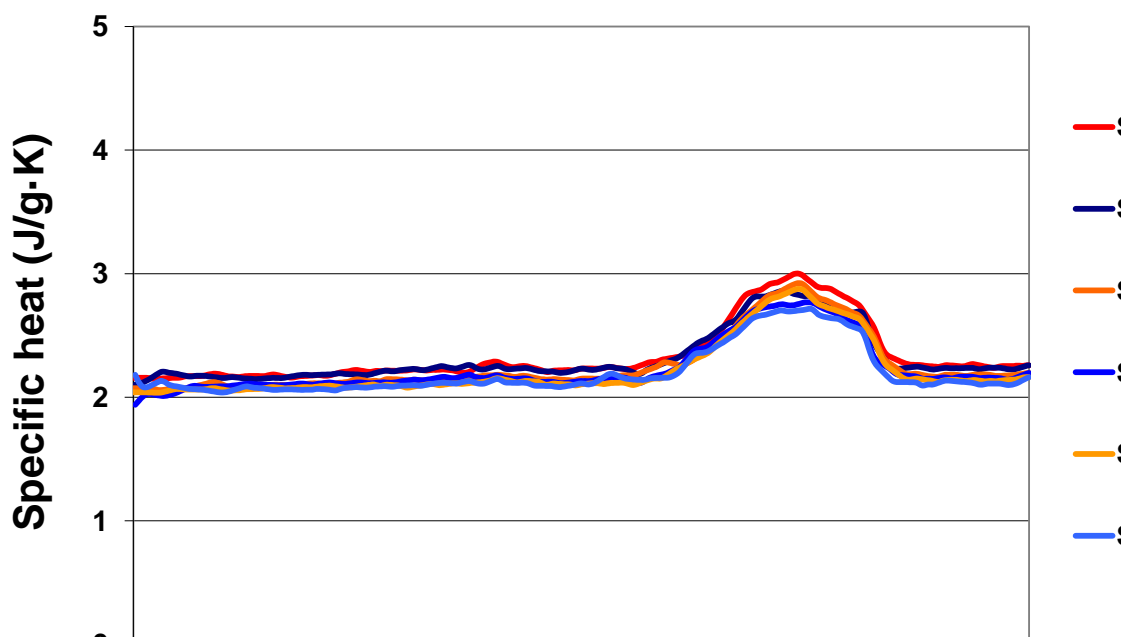**Figure 61. Specific heat vs. temperature of SP 25 A8 for the three cycles (step method)**

91
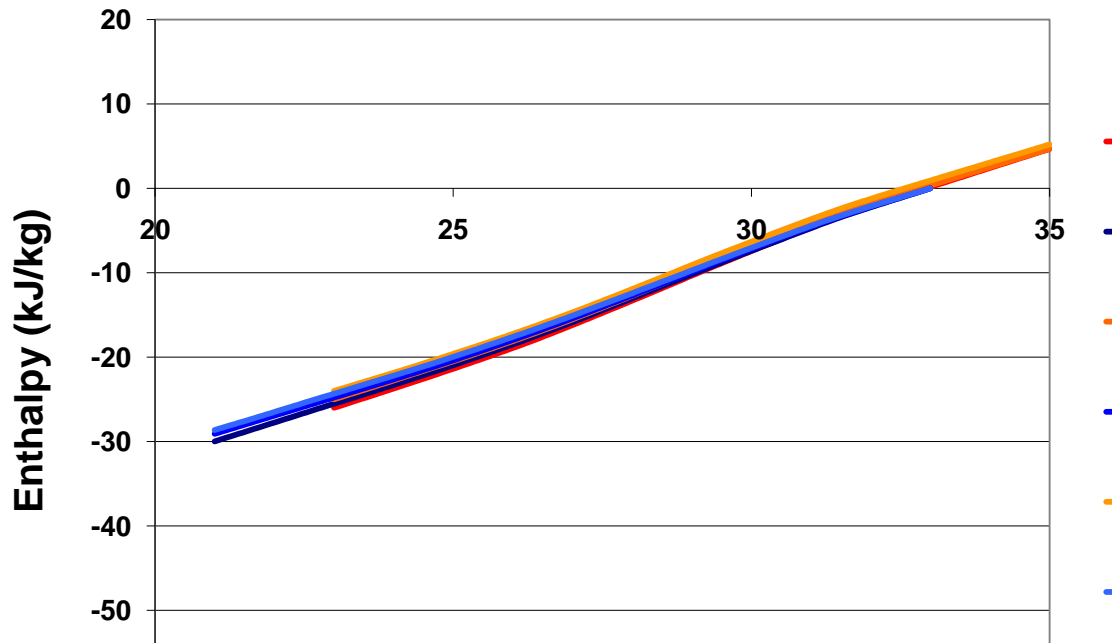
Figure 62. Enthalpy vs. temperature of SP 25 A8 for the three cycles (step method)

7.3.2.3 Discussion

The salt hydrate samples SP 22 A17 and SP 25 A8 were analyzed using both dynamic method (three sub-samples of both samples) and step method (two sub-samples of SP 22 A17 and one sample of SP 25 A8). But they did not respond during the DSC analysis. Because they did not present the phase change, did not give the peak temperature of the phase change and hence did not store the high amount of enthalpy as shown in the Table 9. After performing number of cycles of dynamic as well as step method in the present analysis it can be said that the DSC could not be proven as a proper method for analyzing the salt hydrate samples. Probably this could be due to phase separation. Because these are the salt hydrates and salt hydrates usually present the phase separation due to the density difference of water and salt contents. Therefore, for such materials the method involving large sample size could be helpful to detect the actual thermal behaviour.

8 Conclusions

- *Paraffin samples (RT 20 and RT 27):*
- Due to the good thermal repeatability of RT 20 and RT 27 (Table 14), they are promising materials for the long term use in the associated application and for the builiding applications.
- All the sub-samples and their cycles of RT 20 and RT 27 presented almost similar behaviour, good heat storage capacity and similar melting and freezing temperatures.
- The standard deviation obtained for all the cycles of all the sub-samples of both RT 20 and RT 27 was lower than 0.02 °C for the temperature values and it was lower than 0.70 kJ/kg for melting enthalpy values.
- The values for the standard deviation prove that the precision of the results is well achieved and subsequently the repeatability of the results is assured.
- Finally, it could be conclude that the DSC is a proper method to analyze the paraffin samples, since the DSC provides high precision of the results.
- The thermal stability of these paraffin samples is quite good and the materials could be used for the long term applications.

- *Salt hydrate samples (SP 22 A17 and SP 25 A8):*
- Commercial data of the SP 22 A17 and SP 25 A8 show good thermal properties for the material but it has not been achieved by the present DSC analysis.
- It could be probably due to the very small sample size in the miligram range. Because the salt hydrates can present phase separation due to the different densities of salt and water components.
- Due to this reason, these samples should be analyzed using the method that allows large sample mass such as T-history method before using for any application.
- In the present analysis, DSC outputs did not present phase change of SP 22 A17 and SP 25 A8 and as a result they did not store large amount of energy. Finally, after performing number of analysis of SP 22 A17 and SP 25 A8 it could be concluded that the DSC is not a proper method for analyzing the salt hydrate samples (SP 22 A17 and SP 25 A8) due to the limitations for the sample size to be analyzed.

Table 14. Results of the analysis

Sample	Applied method	Commercial melting temperature (ºC) (Table 9)	Average measured temperature (ºC)	Standard deviation of measured melting temperature (ºC)	Commercial melting enthalpy (kJ/kg) (Table 9)	Average measured melting enthalpy (kJ/kg)	Standard deviation of measured melting enthalpy (kJ/kg)
RT 20	Dynamic	22	21.89	0.014	172	127.77	0.64
	Step		21.88	0		167.49	0.53
RT 27	Dynamic	27 (typical)	27.47	0.012	184	139.13	0.46
	Step		27.77	0.005		184.36	0.58
SP 22 A17	Dynamic	23 (typical)	No phase change	No phase change	150	No phase change	No phase change
	Step		As above	As above		As above	As above
SP 25 A8	Dynamic	26	As above	As above	180	As above	As above
	Step		As above	As above		As above	As above

Acknowledgments

I would like to acknowledge the help of the staff members of Universidad de Lleida for all their help.

... to Dr. Luisa F. Cabeza and Dr. Cristian Solé for their supervison.

... to the GREA staff of the Universidad de Lleida for their support.

9 References

1. http://organon.jimhufford.com/2010/06/energy-consumption-by-sector/

2. http://www.electricgreensolar.com/conserve.html

3. Ortiz M., Barsun H., He H., Vorobieff P., Mammoli A. "Modeling of a solar-assisted HVAC system with thermal storage". Energy and Buildings 42 (2010) 500–509.

4. http://en.wikipedia.org/wiki/Non-renewable_resource

5. http://en.wikipedia.org/wiki/Renewable_energy

6. http://en.wikipedia.org/wiki/World_energy_consumption

7. Tyagi V.V., Kaushik S.C., Tyagi S.K. , Akiyam T. a. "Development of phase change materials based microencapsulated technology for buildings: A review". Renewable and Sustainable Energy Reviews 15 (2011) 1373–1391.

8. http://epp.eurostat.ec.europa.eu/statistics_explained/index.php/Climate_change_-_driving_forces

9. Sharma A., Tyagi V. V., Chen C. R., Buddhi D. "Review on thermal energy storage with phase change materials and applications". Renewable and Sustainable Energy Reviews 13 (2009) 318-345.

10. Mehling H., Cabeza L. F., "Heat and cold storage with PCM – An up to date introduction into basics and applications" (Springer-Verlag Berlin Heidelberg, Germany, 2008.

11. Zalba B, Marín J. M., Cabeza L. F., Mehling H. "Review on thermal energy storage with phase change: materials, heat transfer analysis and applications". Applied Thermal Engineering 23 (2003) 251-283.

12. ErcanAtaer O.. Storage of thermal energy, ©Encyclopedia of Life Support Systems (EOLSS).

13. S.M. Hansain. "Review on Sustainable Thermal Energy Storage Technologies , Part I: Heat Storage Materials and Technologies". Energy Convers. Mgmt Vol. 39, No. 11, pp. 1127±1138, 1998.

14. Dincer I. "Thermal energy storage systems as a key technology in energy conservation". International Journal of Energy Research. 2002.

15. Survey of Thermal Storage for Parabolic Trough Power Plants Period of Performance: September 13, 1999.June 12, 2000.

16. Athientis A. K., Liu C., Hawes D., Banu D., Feldman D. "Investigation of the thermal performance of a passive solar test-room with latent heat storage wall". Building and Environment, 32 (1997), pp. 405-410.

17. Esen, M., Durmu, A., Durmu, A. "Geometric design of solar-aided latent heat store depending on various parameters and phase change materials". Solar Energy 1998, 62(1), 19-28.

18. Cabeza L. F. "Technologies overview. Phase Change Materials". Effstock 2009, Stockholm (Sweden), June, 14th-17th (power point presentation).

19. Streicher W., Cabeza L., Heinz A. Inventory of PCM - A report of IEA Solar Heating and Cooling Programme – Task 32 – "Advanced Storage Concepts for Solar and Low Energy Buildings". Report C2 of Subtask C" – February 2005.

20. Yilmaz S., Sheth K. F., Martorell I., Paksoy O. H., Cabeza L. F. "Salt-water solutions as PCM for cooling applications". EuroSun 2010, International Conference on Solar Heating, Cooling and Buildings. Graz, Austria.

21. Cabeza L. F., Roca J., Nogués M., Mehling H. and Hiebler S. – "Immersion corrosion tests on metal-salt hydrate pairs used for latent heat storage in the 48-58 ºC temperature range". Material and corrosion 53, 902-907 (2002).

22. Cabeza L. F., Illa J., Roca J., Badia F., Mehling H., Hiebler S. and Ziegler F. – "Middle term immersion corrosion tests on metal-salt hydrate pairs used for latent heat storage in the 32-36 ºC temperature range". Material and corrosion 52, 748-754 (2001).

23. Cabeza L. F., Badia F., Illa J., Roca J. "Corrosion experiments on salt hydrates used as phase change materials in cold storage". IEA, ECES IA Annex 17, Advanced Thermal Engineering Storage Techniques – Feasibility Studies and Demonstration Projects Planning Workshop, 5 6 April 2001, Lleida, Spain.

24. Castellón C., Martorell I., Cabeza L. F., Fernández I. A., and Manich A. M. "Compatibility of plastic with phase change materials (PCM)". Int. J. Energy Res. 2011; 35:765–771.

25. Kuznik F., David D., Johannes K., Roux J. J. "A review on phase change materials integrated in building walls". Renewable and Sustainable Energy Reviews 15 (2011) 379–391.

26. Farid M. M., Khudair A. M., Razak S. A. K., Al-Hallaj S. "A review on phase change energy storage: materials and applications". Energy Conversion and Management 45 (2004) 1597-1615.

27. Fellchenfeld H. and Sarlg S. "Calcium Chloride Hexahydrate: A Phase-Changing Material for Energy Storage". Ind. Eng. Chem. Prod. Res. Dev. 1985, 24, 130-133.

28. Cabeza L. F., Svensson G., Hiebler S., Mehling H. "Thermal performance of sodium acetate trihydrate thickened with different materials as phase change energy storage material". Applied Thermal Engineering 23 (2003) 1697–1704.

29. Biswas D. R. "Thermal energy storage using sodium sulphate decahydrate and water". Solar energy 1977; 19:99-100.

30. Zafer U. "Phase Change Materials - Eutectic Thermal Energy Storage Products". http://ezinearticles.com/?Phase-Change-Materials---Eutectic-Thermal-Energy-Storage-Products&id=1968752.

31. Rousse D. R., Salah N. B. and Lassue S. "An Overview of Phase Change Materials and their Implication on Power Demand". IEEE Electrical Power & Energy Conference. 978-1, 2009.

32. Farid M. M. and Chen X. D. "Domestic electrical space heating with heat storage". Proceedings of the Institution of Mechanical Engineers, Part A: Journal of Power and Energy. March 1, 1999 213: 83-92.

33. Yamaha M. "A study on a heat exchanging ventilation system for residential house using phase change material". IEA, ECES IA Annex 17, Advanced Thermal Energy Storage Techniques- Feasbility Studies and Demonstration Projects Planning Workshop, 5 – 6 April 2001, Lleida, Spain.

34. Hauer A., Mehling H., Schossig P., Yamaha M., Cabeza L. F., Martin V., Setterwall F. International Energy Agency. Implementing Agreement on Energy Conservation through Energy Storage, Annex 17. "Advanced Thermal Energy Storage through Phase Change Materials and Chemical Reactions – Feasibility Studies and Demonstration projects", Final Report.

35. http://en.wikipedia.org/wiki/Thermal_analysis

36. Klančnik G., Medved J., Mrvar P. "Differential thermal analysis (DTA) and differential scanning calorimetry (DSC) as a method of material investigation". RMZ – Materials and Geoenvironment, Vol. 57, No. 1, pp. 127–142, 2010.

37. Feldman D., Banu D., Hawes D.W. "Development and application of organic phase change mixtures in thermal storage gypsum wallboard". Solar Energy Materials and Solar Cells, 1995, v. 36, 147–157.

38. Hawlader M.N.A., Uddin M.S., Khin M. M. "Microencapsulated PCM thermal-energy storage system". Applied Energy, 2003. Vol. 74, 195–202.

39. Günther E., Hiebler S., Mehling H., Redlich R. "Enthalpy of phase change materials as a function of temperature: Required accuracy and suitable measurement methods". Int J Thermophys (2009) 30: 1257-1269. DOI 10.1007/s 10765-009-0641-z.

40. Castellón C., Günther E., Mehling H., Hiebler S., and Cabeza L. F.. "Determination of the enthalpy of PCM as a function of temperature using a heat-flux DSC – A study of different measurement procedures and their accuracy". Int. J. Energy Res. 2008; 32:1258–1265. DOI: 10.1002/er.1443.

41. Yinping Z., Yi J. and Yi J. "A simple method, the T-history method, of determining the heat of fusion, specific heat and thermal conductivity of phase-change materials". Meas. Sci. Technol. 10 (1999) 201–205.

42. Marín J. M., Zalba B., Cabeza L. F. and Mehling H. "Determination of enthalpy–temperature curves of phase change materials with the temperature-history method: improvement to temperature dependent properties". Meas. Sci. Technol. 14 (2003) 184-489.

43. Hong H., Kang C., Peck J. H. "Measurement methods of latent heat for PCM with low melting temperature in closed tube". International journal of Air-conditioning and Refrigeration. Vol. 12, No. 4 (200), pp. 206-213.

44. Park C. H., Choi J. H. and Hong H. "Considertation on the T-history method for measuring heat of fusion of phase change materials". Korean J. Air-Conditioning and Refrigeration Eng., 2001. Vol.13, No.12, pp. 1223-1229.

45. Park C. H., Peck J. H., Kang C. and Hong H. "Accuracy improvement for measurement of heat of fusion by T-history method". Korean J. Air-Conditioning and Refrigeration Eng., 2003. Vol.15, No.8, pp. 652-660.

46. Saito A., Okawa S., Iwamoto R. and Shintani T. "On the heat transfer characteristics of the thermal energy storage capsule in the heat removal process using an inorganic hydrate." Trans, of JSME, 1996. Vol.62, pp.4212-4219.

47. http://en.wikipedia.org/wiki/Differential_scanning_calorimetry

48. Höhne G. W. H., Hemminger W. F., Flammersheim H. J. Handbook of "Differential Scanning Calorimetry" second edition. Springer – Verlag Berlin Heidelberg Newyork, Berlin, Germany, 2003.

49. Sheth K. F., Solé C., Cabeza L. F., "GREA report – Sample from Task/Annex 4224, Results of Octadecane", 24/12/2010.

50. http://www.rubitherm.com/english/index.htm

51. Fieback K., Lindenberg G. 8th WorkShop and Experts Meeting of Annex 2005 - 04 - 18 - 20. "Advanced Thermal Energy Storage through Phase Change Materials and Chemical Reactions - Feasibility Studies and Demonstration projects".